Instituto de Física Interdisciplinar y Sistemas Complejos

TESI DOCTORAL

Coevolution and local versus global interactions in collective dynamics of opinion formation, cultural dissemination and social learning

Tesi presentada per Juan Carlos González Avella, al Departament de Física de la Universitat de les Illes Balears, per optar al grau de Doctor en Física

Juan Carlos González Avella

Palma de Mallorca, June 2010

Coevolution and local versus global interactions in collective dynamics of opinion formation, cultural dissemination and social learning

Juan Carlos González Avella
Instituto de Fisica Interdisciplinar y Sistemas Complejos
IFISC (UIB-CSIC)

PhD Thesis

Supervisors: Prof. Maxi San Miguel and Dr. Victor M. Eguíluz

Univertsitat de les Illes Balears
Palma de Mallorca

This document was typeset with LaTeX 2_ε

Maxi San Miguel, Catedràtic de la Universitat de les Illes Balears, i Victor M. Eguíluz, Científico Titular del CSIC (Consejo Superior de Investigaciones Científicas)

CERTIFICAN

que aquesta tesi doctoral ha estat realitzada pel Sr. *Juan Carlos González Avella* sota la seva direcció a l'Institut de Fisica Interdisciplinària i Sistemes Complexos; IFISC (UIB-CSIC) i, per a donar-ne constància, firmen la mateixa.

Palma de Mallorca, 25 de Juny del 2010

Maxi San Miguel Victor M. Eguíluz

"En el sentido místico de la creación que nos rodea, en la expresión del arte, en el anhelo hacia Dios, el alma crece en altura y encuentra la satisfacción de algo implantado en su naturaleza... La búsqueda de la ciencia (también) nace de un esfuerzo que la mente está impelida a seguir, un cuestionamiento que puede ser suprimido. Ya por la búsqueda intelectual de la ciencia o por la búsqueda mística del espíritu, la luz llama con señas y el propósito que brota de nuestra naturaleza responde".

Sir. Arthur Eddington

Si hay algo que he aprendido, es que la piedad es más inteligente que el odio, que la misericordia es preferible aún a la justicia misma, que si uno va por el mundo con una mirada amistosa, uno hace buenos amigos.
Philip Gibbs.

Acknowledgments

Al finalizar mi camino y alcanzar una nueva meta, vuelvo mi mirada hacia atrás y veo tantos rostros queridos, rostros que de una u otra forma han dejado huellas en mi, huellas que me han hecho sentir que mis sueños alcanzados no son sólos míos; sino de todos aquellos que me acompañaron en mi transitar. Hoy quiero agradecer a todos aquellos que han estado a mi lado, a aquellos que me animaron y me apoyaron en todo.

En primer lugar quiero agradecer a mis directores de tesis, *Prof. Maxi San Miguel y al Dr. Victor M. Eguíluz*, por haberme dado la oportunidad de realizar esta tesis, por confiar en mi, por motivarme a explorar nuevas líneas de investigación y asumir juntos retos intelectuales durante este tiempo. Quiero agradecerles el tiempo y la dedicación puesto en mí dentro y fuera del ámbito académico y sobre todo por su amistad. Especialmente quiero agradecer a Maxi, por sus consejos y atención en momentos difíciles, especialmente en la parte final en la realización de esta tesis, Gracias.

Prof. Fernando Vega-Redondo y Prof. Matteo Marsili, por haberme dado la oportunidad de visitarlos en sus respectivos grupos de investigación, por su atención y amistad.

Prof. Mario Cosenza, por sus consejos apoyo en momentos y situaciones difíciles y desinteresada amistad.

Quiero agradecer a todos los investigadores del IFISC, por hacer posible un ambiente de trabajo excelente, por compartir aciertos y desaciertos, dentro y fuera del ámbito académico. En particular quiero agradecer a mis compañeros y colegas, Luis Fernández Lafuerza, Juan Fernández Gracia, Guadalupe C. Garcéa, Ismael Hernández, Niko Komin, Leonardo Lyra Gollo, Maria Moreno, Romain Modeste Nguimdo, Antonio Pérez Serrano, Flora S. Bacelar, todos ellos por ser compañēros de viajes durante todo este tiempo.

A Xavi Castelló, Mi compañero de viaje desde el inicio en la conquista de esta meta, nunca tendré palabra alguna que describa la inmensa alegría de haber sido tu compañēro en esta etapa de la vida, donde compartimos directores de tesis, congresos, penas, alegrías. Gracias.

Federico Vázquez, de quien aprendí valiosas cosas.

Roberta, Damiá, Adrian, Laura, Alejandro y Lucia, por sus amistad apoyo y confianza.

Los informáticos, Ruben, Edu y Maria Antonia, sin ellos este trabajo no sería posible.

A *Rosa,* Amiga incondicional, gracias por todo cuanto me has brindado.

Mamá: Mujer hacedora de sueños. A ti agradezco que con tu dedicación, ternura, sacrificio y devoción, me has permitido que hoy se cumpla una de mis metas. A ti que guardaste tus ilusiones y sueños dentro de tu corazón, me regocijo en la alegría de llamarte madre y decirte que este triunfo es tuyo como mío, pues fuiste, eres y serás motivo de inspiración para ser mejor cada día y conquistar cada uno de mis sueños, pues veo en ti la fuerza de la entrega y el don del sacrificio, gracias *Vieja*.

Nona (Mamá Rosa): De quien aprendí la constancia, de quien agradezco sus sabios consejos y la palabra de aliento que siempre me permite caminar erguido y con la mirada en alto, quien con su propia vida me enseño que los logros se consiguen con trabajo. Gracias por darme cuanto te fue posible cuando estabas aquí.

Papá: Gracias por tu confianza.

Tía Ana: Toda palabra, toda frase, queda corta para agradecer todo el amor y el calor de una segunda madre que me cobijó para hoy hacer realidad este triunfo.

A mis hermanos y primos: Nano, Luis, Diego, Victor, Yanuilly, Ronald y Beyli, a quienes vi nacer, crecer, y han compartido conmigo mis inquietudes, logros, fracasos y esperanzas, siempre dándome ánimo en la distancia en todos mis proyecto. A ellos bendigo por estar siempre presentes a pesar de la distancia.

A Mercedes: de quien aprendí la superación.

Isabel y mis peques: Cesar y Ana: Simplemente no hay palabras para expresar lo que significa su apoyo y presencia en mi vida, Gracias

A *Joan Bauza* (Juanito), quien me ha brindado el calor de un hermano cuando he estado lejos de mi hogar, apoyo desinteresado, cualidad que demuestra su infinita calidad humana.

A *la Familia Bauza Santa Maria*: por adoptarme y permitirme ser parte de ellos.

Gabi: por estar cuando te necesitaba, por tu apoyo y confianza, gracias.

Andrea, Aunque llegaste al final de mi caminar en la conquista de éste, mi sueño, sentí tu apoyo como si lo hicieras desde el principio, tu lugar en mi, y mi lugar en ti, es y será fuente inagotable para mi motivación en seguir adelante, siempre me sentiré afortunado por haberme cruzado con vos. Gracias mi niña de ojos aguarapados por formar parte de todo.

Resumen

Fenómenos tales como sincronización, oscilaciones, formación de patrones, crecimientos de fases, segregación y diferenciación, consenso, entre otros, son ejemplos de comportamientos colectivos que ocurren en una variedad de contextos, tales como sistemas físicos, químicos, biologicos, e incluso en sistemas sociales y económicos [1–8]. Estos efectos son el resultado de las interacciones entre los elementos que constituyen el sistema. El concepto de sistemas complejos se aplica a este conjunto de elementos cuyos comportamientos o estructuras globales no son susceptibles de ser derivados trivialmente a partir del conocimiento del comportamiento de los elementos constituyentes. El estudio de comportamientos colectivos en términos de una descripción macroscópica basadas en interacciones locales, es un tema bien estudiado por la Física Estadística. Debido al éxito de esta disciplina al establecer una conexión entre los comportamientos a nivel micro y macro, los fenómenos colectivos en sistemas sociales se empiezan a estudiar cada vez más a partir de modelos microscópicos basados en agentes que interaccionan entre ellos siguiendo los métodos y conceptos de la Física Estadística. En problemas de dinámica social, los agentes se consideran nodos de una red donde cambian su estado (opción social) en función de unas reglas de interacción local con sus vecinos en la red.

En esta tesis abordamos diferentes aspectos del problema de formación de opinión y la emergencia del consenso versus polarización en sistemas sociales desde las perspectivas de la Física Estadística y de los Sistemas Complejos. Para ello consideramos diferentes mecanismos que capturan procesos básicos para la interacción local, basados en distintas reglas sociales. Adicionalmente, y como aporte al estudio del consenso social, incluimos dos nuevos ingredientes que forman el núcleo principal de esta tesis: la competencia entre interacciones locales versus globales, y la co-evolución entre la estructura de la red y la dinámica de

los nodos. En este trabajo, las interacciones locales se refieren a interacciones entre primeros vecinos (entorno local), mientras que las interacciones globales tienen en cuenta las interacciones con todos los elementos del sistema (entorno global) y/o con campos exógenos al sistema.

Los efectos de la competencia entre las interacciones locales y globales son analizados en el contexto de la teoría del aprendizaje social (todos los agentes del sistema aprenden de una señal externa) usando una variación del modelo de *umbral* introducido por Granovetter [9], en el *modelo de confianza limitada* para la formación de opinión propuesto por Deffuant et al. [10] y en el modelo de *diseminación cultural* introducido por Axelrod [11]. Mediante este enfoque, se analiza el mecanismo del aprendizaje social en la dinámica de umbrales bajo la influencia de una señal externa que cambia aleatoriamente en el tiempo. Encontramos que, dependiendo de la intensidad de la señal y del umbral para el cambio de opinión de los individuos, el sistema es capaz de aprender de la señal externa. También hemos estudiado los efectos de los medios de comunicación de masas en los modelos Deffuant y de Axelrod [12–15]. En este análisis hemos explorado diferentes formas de medios de comunicación de masas, modelados como distintos tipos de campos que interactúan con el sistema. Hemos considerado un campo externo, un campo global y un campo local. Dentro del contexto de las ciencias sociales, el campo externo se interpreta como una propaganda que tiene como objetivo imponer una opinión o un estado cultural específico en el sistema, mientras que un campo global puede ser interpretado como una moda global que refleja la opinión o la tendencia global del sistema. La tendencia de una opinión o un estado local es modelada como un campo local. En contra de lo que se espera intuitivamente, se encuentra que la interacción con un campo fuerte desordena el sistema, mientras que la interacción con campos débiles es capaz de ordenar el sistema en dirección del estado del campo. Mostramos que este efecto es independiente de la naturaleza externa o endógena del campo; sin embargo los resultados muestran que campos locales son más eficientes en promover el consenso que campos globales [12]. Para el caso de interacción con un campo externo, mostramos que el sistema para ciertos valores de parámetro, puede ordenarse en un estado distinto al que trata de imponer el campo. Esto ocurre cuando se incluyen interacciones de largo alcance en el sistema. Este efecto se observa en redes completamente conectadas, en redes de pequeño mundo y en redes libre de escala [13].

En la parte final de esta tesis analizamos el paradigma de la co-evolución en dos modelos distintos [16, 17]. Investigamos este problema en el modelo de Axelrod, y en un modelo donde combinamos una dinámica de umbrales con un mecanismo basado en la regla de la mayoría para la dinámica de los nodos. Independientemente de las reglas de evolución en estos modelos, encontramos

que para ciertos valores de parámetros, ambos sistemas muestran una transición hacia un estado de fragmentación donde el sistema se rompe en distintos grupos, y en cada uno de estos grupos se alcanza el consenso. Adicionalmente, mostramos que la transición ocurre cuando las escalas de tiempo que gobiernan, tanto la dinámica de la red como la dinámica de los nodos, son del mismo orden [17]. En particular mostramos que en el modelo de Axelrod co-evolutivo la fase de fragmentación es estable frente a la presencia de una deriva cultural que es modelado como ruido aplicado sobre el sistema [16].

Esta tesis quiere contribuir a la comprensión de los mecanismos subyacentes en problemas de consenso social y formación de opinión en donde la competición entre interacciones locales y globales está presentes, estudiando los fenómenos colectivos emergentes en distinto modelos de agentes en interacción en los que las dinámicas de ordenamiento, la naturaleza de la red son analizadas en detalle. Adicionalmente nuestros resultados en los estudios de la dinámica co-evolutiva de grupos culturales aportan detalles que ayudan al entendimiento al problema de la segregación y a la formación de comunidades.

Contents

Chapter 1

Introduction

1.1 Complexity and Social Sciences

The concept of Complex Systems has evolved from Chaos, Statistical Physics and other disciplines, and it has become a new paradigm for the search of mechanisms and an unified interpretation of the processes of emergence of structures, organization and functionality in a variety of natural and artificial phenomena in different contexts [1–8]. The study of Complex Systems has become a problem of enormous common interest for scientists and professionals from various fields, including the Social Sciences, leading to an intense process of interdisciplinary and unusual collaborations that extend and overlap the frontiers of traditional Science [18–26]. The use of concepts and techniques emerging from the study of Complex Systems and Statistical Physics has proven capable of contributing to the understanding of problems beyond the traditional boundaries of Physics.

Phenomena such as the spontaneous formation of structures, self-organization, spatial patterns, synchronization and collective oscillations, spiral waves, segregation and differentiation, formation and growth of domains, consensus phenomena [1–8, 11, 27–29] are examples of emerging processes that occur in various contexts such as physical, chemical, biological, social and economic systems, etc. These processes are the result of interactions and synergetic cooperation among the elements of a system. The general concept of Complex System has been applied to sets of elements capable of generating global structures or functions that are absent at the local level. Understanding the complex collective behavior of many particles systems, in terms of macroscopic descriptions based on local interaction rules of evolution leading to the emergence of global phenomena is

at the core of Statistical Physics and it is relevant in Social Sciences. An example of this micro-macro paradigm that shows a close relationship between both fields, Statistical Physics and Social Science, is Schelling's model of residential segregation, mathematically equivalent to the zero-temperature spin-exchange Kinetic Ising model with vacancies [30, 31].

Within this framework of the applications of concepts of Complex Systems to Social Science, there is a large number of physicists, economists, sociologists and computer scientist who are studying social systems and characterizing mechanisms involved in the processes of opinion formation, cultural dissemination, spread of disease, formation of social networks of interaction. This has led to the establishment of links between various disciplines and to an increasing interdisciplinary collaboration between different areas of knowledge [16, 19, 20, 23–26, 32–41].

It may seem unconventional that physicists study dynamical models of social systems. However, the attempt to explain social phenomena as any other physical phenomena is not new. These ideas, somehow, were anticipated by several social scientists of the nineteenth century. Auguste Comte, considered as the father of Sociology, was heavily influenced by Newtonian and Galilean Mechanics. He thought that Physics could apply to all natural phenomena, including the social phenomena. In his famous classification of sciences, Comte assumed that all scientific disciplines are eventually some kind of applications or branches of Physics. In this classification, Comte distinguishes differences in Physics applications, separating them into two main areas: Inorganic Physics and Organic Physics. This separation also contains a list of different disciplines, such as, Celestial Physical (Astronomy), Terrestrial Physics (Geology); Physiological Physics (Biology), etc. In this scheme, there was room for Social Physics, which would be devoted to studying positively the social phenomena. Comte proposed to develop this science in his famous treaty "Cours de Philosophie Positive" [42].

A typical social system is composed of a number of individuals that interact among them, showing nontrivial collective behavior. The consideration of these phenomena is the key for a qualitative and quantitative study from the point of view of Statistical Physics and Complex Systems [20, 43]. In particular, the paradigm of Complex Systems in the context of social systems means that collective social structures emerge from the interactions among individuals. In other words, we assume that many social phenomena are collective processes similar to those taking place in many nonequilibrium dynamical systems composed by many elements. In this regard, a variety of models have been proposed to explain the formation of structures from the interactions between agents of social systems. Many of these models address the question of the emergence of social consensus: the aim is to establish when the dynamics of a set of interacting agents

that can choose among several options, reaches to a consensus in one of these options, or when a state coexistence of several options prevails (polarization) [41]. The parameters of these models drive transitions between consensus and polarization. This change in the global state of the system between consensus and polarization could be seen as the analogous an order-disorder transition in Statistics Physics.

In this context, different models considered in the last few years account for different mechanisms of interaction that capture the essence of various social behaviors through simple interaction rules:

- Imitation (voter model [44]).
- Social pressure (Spin Flip Kinetic Ising models [45])
- Homophily (Axelrod model for cultural dissemination [11])
- Majority convinces (Sznajd model [46])
- Threshold model (Granovetter model [9]) or complex contagions [47]
- Bounded confidence (Deffuant model [10] and Hegselmann and Krause [48])
- Semiotic dynamics Naming Game for the emergence of a shared language [49–51])
- Interaction through small groups (Galam model [52])
- Cost-benefit optimization in the framework of game theory [53–56]
- Imitation, prestige and volatility in language competition [50, 57–61]

The emergence of consensus or polarization depends on the mechanism of interaction and on a second ingredient, namely the network of interactions that defines who interacts with whom. These networks of interaction can be seen as the skeleton a Complex Social System. In section 1.2 we review the main concepts and basic models of networks that we use throughout the thesis.

In this thesis, we address different aspects of the consensus problem considering different interaction mechanism and studying the effects of different topologies of the interaction networks. The two key new issues that we introduce in this work are the competition between local and global interaction (section 1.3) and the concept of co-evolution dynamics of the states of the agents and network of interaction (section 1.4).

1.2 Complex Networks

The study of the interrelations among interactive elements has revealed the existence of underlying networks of connections in many systems [62–66]. It has been found that systems as diverse as the World Wide Web, Internet, telecommunication networks, dynamical social groups, economic corporations, metabolic flows in cells, neurons in the brain, etc., show common network structures and share similar properties of self-organization. The topological structure of the interaction network can be considered as an esential ingredient of a Complex System. In this regard, the interaction in complex networks is a recent new paradigm in Statistical Physics. [67].

The approach of Statistical Physics in the study of interaction networks has revealed the ubiquity of various striking characteristics, such as the small-world effect: although each node has a number of neighbors much smaller with respect to the total number of nodes, only a small number of hops suffices to go from any node to any other on the network. This has prompted the investigation of the effect of various interaction topologies on the behavior of agents connected according to these topologies, highlighting the relevance of small-world and heterogeneous structures [68–70].

More precisely, a network is a set of elements, which we will call *vertices* or *nodes*, with connections among them, called, *edges* or *link*s. Complex networks research can be conceptualized as lying at the intersection between graph theory * and Statistical Mechanics, which endows it with a truly multidisciplinary nature. While its origin can be traced back to the pioneering works on percolation and random graphs by Flory [71], Rapoport [72], and Erdos and Renyi [73], research in complex networks from the view point of physics became a focus of attention only recently. The main reason for this was the discovery that real networks have characteristics which are not explained by random connectivity. Instead, networks derived from real data may involve community structure, power law degree distributions and hubs, among other structural features. Three particular developments have contributed particularly to the ongoing related developments: Watts and Strogatz's investigation of small-world networks [63], Barabási and Albert's characterization of scale-free models [74], and Girvan and Newman's identification of the community structures present in many networks [75]. The introduction of the models by Watts-Strogatz, and Barabasi-Albert to explain and study the basic features observed in real networks, have triggered a revolution in the field of Statistical Physics, with the number of contributions to the field

*Term used by mathematicians

constantly increasing until today. Physicists became interested in the formation, structure and evolution of complex networks, as well as in the topological effects on social interaction problems, such as opinion dynamics, cultural diffusion or language competition [20]. The study of complex networks has attracted the attention of the general public during these years, and several popular science books have been published on the topic[64, 76].

1.2.1 Basic concepts

In mathematical terms a network is represented by a graph. A graph is a pair of sets $G = \{P, E\}$ where P is a set of N nodes (or vertices) $P_1, P_2, ..., P_N$ and E is a set of edges (links or ties) that connect two elements of P. Networks can be directed or undirected. In directed networks [77, 78], the interaction from node i to node j does not imply an interaction from j to i. On the contrary, when the interactions are symmetrical, we say that the network is undirected. Moreover, a network can also be weighted [79, 80]. A weight is defined as a scalar that represents the strength of the interaction between two nodes. In an unweighted network, instead, all the edges have the same weight (generally set to 1).

In this Section, we define basic concepts that characterize complex networks

Adjacency matrix

An adjacency matrix represens which vertices of a graph are adjacent to which other vertices. Specifically, the adjacency matrix of a finite network G on N vertices is the $N \times N$ matrix where the nondiagonal entry a_{ij} is the number of edges from node i to node j, and the diagonal entry a_{ii}, depending on the convention, is either once or twice the number of edges (loops) from vertex i to itself. Undirected graphs often use the former convention of counting loops twice, whereas directed graphs typically use the latter convention. There exists a unique adjacency matrix for each graph (up to permuting rows and columns), and it is not the adjacency matrix of any other graph. In the special case of a finite graph, the adjacency matrix is a (0,1)-matrix with zeros on its diagonal. If the graph is undirected, the adjacency matrix is symmetric. The relationship between a graph and the eigenvalues and eigenvectors of its adjacency matrix is studied in spectral graph theory.

Degree and degree distribution

The degree k_i of a node is the number of links adjacent to a node i, that is the total number of nearest neighbors of a node i in a network.

The degree distribution $P(k)$ is the average fraction of nodes or vertices of degree k: $P(k) = \langle N(k) \rangle / N$. Here, $N(k)$ is the number of nodes of degree k in a particular graph of the statistical ensemble. The averaging is over the entire statistical ensemble. Some networks can be degree-homogeneous, where each node i has the same number of connections, such as lattice networks. While, other networks might have certain degree of heterogeneity in the connections of the nodes. For example, in a random network, each node is connected (or not) with probability p (or $1 - p$). In this case the $P(k)$ is a binomial distribution. Other example are networks where the degree distribution follow a power law: $P(k) \sim k^{-\gamma}$, where γ is a constant. Such networks are called scale-free networks and have attracted particular attention for their structural properties.

Clustering coefficient

In graph theory, a clustering coefficient is a measure of the extent to which nodes in a graph tend to cluster together. Evidence suggests that in most real-world networks, and in particular social networks, nodes tend to create tightly knit groups characterized by a relatively high density of ties. In real-world networks, this likelihood tends to be greater than the average probability of a link randomly established between two nodes [63, 81].

The definition for clustering coefficient quantifies the local cliquishness of its closer neighborhood, and it is know as local clustering coefficient C_i:

$$C_i = \frac{2\varepsilon}{k_i(1 - k_i)}, \tag{1.1}$$

where k_i is the degree of node i and ε is the number of links between its k_i neighbors. From this definition, the clustering coefficient of the whole network is defined as the average over all nodes C_i:

$$C \equiv \frac{1}{N} \sum_{i=1}^{N} C_i \tag{1.2}$$

where N is the total of nodes in the system. In a social network, it can be interpreted as a measure of the probability that the friends of a given agent are at the same time friend of each other.

Average path length

The average path length l is the average number of steps along the shortest paths for all possible pairs of network nodes. It is a measure of the efficiency of information or mass transport on a network. Average path length is one of the three main measures of network topology, along with its clustering coefficient and its degree distribution. The average path length depends on the system size. Regular d-dimensional lattice display an average path length which scales with system size as $l \sim N^{1/d}$, while, the Complex Networks are characterized by shorter path lengths, which scale as $l \sim \ln(N)$, where N is the system size.

Community structure

Although there is not an agreed common definition about what is a community in the field of complex networks theory, the most usuall one is the following: a set of nodes is a community if a network can have a non homogeneous structure formed by a group of vertices strongly connected among them but with few links connecting them to the rest of the network (see Figure 1.1). These networks have a modular (or community) structure [82]. Several other definitions can be found in the ref. [83]. A given community division of a network can be evaluated by computing its modularity, a measure introduced by Newman and Girvan [82].

The most interesting features that display the real social networks are: a) short average path length, b) large clustering coefficient and c) broad degree distributions.

1.2.2 Basic complex networks models

Modeling networks is an important tool to improve the understanding of real networks. In this section, we present a brief introduction of the three most important network models that we use on the course of this thesis: Erdös-Rényi random networks [73], Watts-Strogatz small world networks [63] and Barabśi-Albert scale free networks [74].

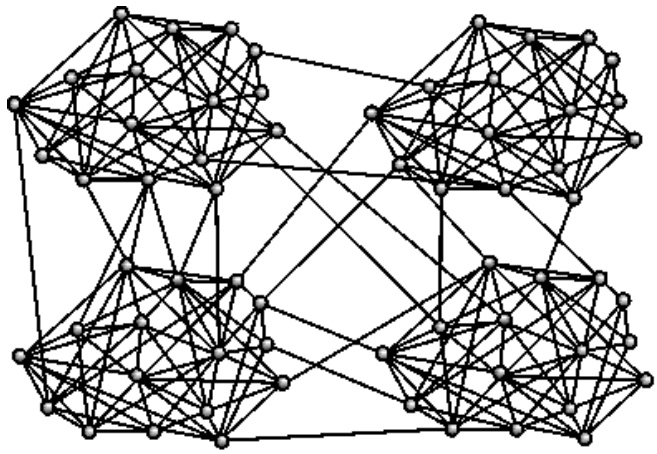

Figure 1.1: An example of a random network with community structure formed by 64 nodes dividend in 4 community. From [84]

Erdös-Reny random network

The random network, developed by Rapoport [72] and independently by Erdös and Reny [73], can be considered the most basic model of complex networks. In their 1959 paper [73], Erdös and Reny introduced a model to generate random graphs consisting of N vertices connected by m edges, which are chosen randomly from the $N(N-1)/2$ possibles edges. Another alternative model defines N vertices and a probability p of connecting each pair of vertices. The average degree of a node in a random networks is:

$$\langle k \rangle = p(N-1) = \frac{2m}{N}. \tag{1.3}$$

When dealing with the large network size limit ($N \to \infty$), $\langle k \rangle$ diverges if p is fixed. Instead, p is chosen as function of N to keep $\langle k \rangle$ fixed: $p = \langle k \rangle/(N-1)$. So, the probability of a randomly chosen node having degree k is binomial:

$$P(k) = \binom{N-1}{k} p^k (1-p)^{N-1-k} \tag{1.4}$$

For large N and $\langle k \rangle$ fixed, this distribution approaches Poisson distribution with mean value $\langle k \rangle$:

$$P(k) \cong \frac{\langle k \rangle^k e^{-\langle k \rangle}}{k!}, \tag{1.5}$$

which is sharply peaked at $\langle k \rangle$.

The small world model

Many real social networks are characterized by having a short average path length, like the random network, but with a large cluster coefficient, if it is compared with a random graph (see table 1.1). This characteristic is known as *small world* property. This concept originated from the famous experiment made by Milgram in 1967 [85], who found that two US citizens chosen at random were connected by an average of six acquaintances.

The small-world networks were identified as a class of random graphs by Duncan Watts and Steven Strogatz [86]. They noted that graphs could be classified according to two independent structural features, namely the clustering coefficient and average node-to-node distance, the latter also known as average shortest path length. Purely random graphs, built according to the Erdös-Rényi model, exhibit a small average shortest path length (varying typically as the logarithm of the number of nodes) along with a small clustering coefficient. Watts and Strogatz measured that in fact many real-world networks have a small average shortest path length, but also a clustering coefficient significantly higher than expected by random chance. Watts and Strogatz then proposed a novel graph model, currently named the Watts and Strogatz model, with (i) a small average shortest path length, and (ii) a large clustering coefficient.

To construct a small-word network, one starts with a regular lattice of N vertices in which each vertex is connected to k nearest neighbors in each direction, totalizing 2 connections, where $N \gg k \gg \log(N) \gg 1$. Next, each edge is randomly rewired with probability p. When $p = 0$ we have an ordered regular lattice with high number of loops but large distances and when $p \to 1$, the network becomes a random graph with short distances but few loops. In this way, changing the

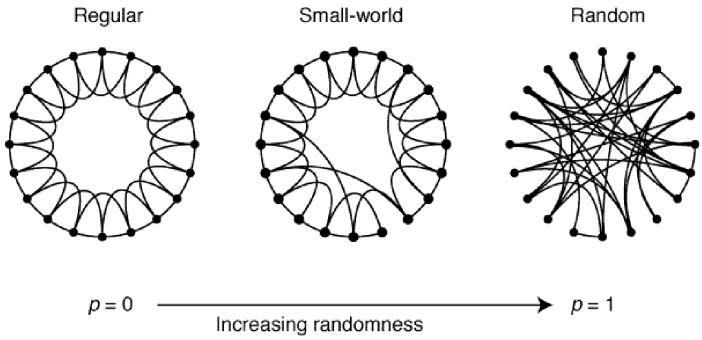

Figure 1.2: The Watts-Strogatz random rewiring procedure, which interpolates between a regular ring lattice and a random network keeping the number of nodes and links constant. $N = 20$ nodes, with four initial nearest neighbors. For $p = 0$ the original ring is unchanged; as p increases the network becomes increasingly disordered until for $p = 1$ a random. From [63]

parameter p, we observe a transition between a regular lattice and a random network as shown in figure 1.2. There exists a sizable region in between these two extremes for which the model has both short path lenghts and high clustering coefficient (see Figure 1.3)

Alternative procedures to generate small-world networks based on addition of edges instead of rewiring have been proposed [87, 88]. The degree distribution in Watts-Strogatz small world networks is similar to that of a random graph: it has a pronounced peak at $k = k_0$ and decays exponentially for large k. Thus the topology of the network is relatively homogeneous, with all nodes having approximately the same number of links [67].

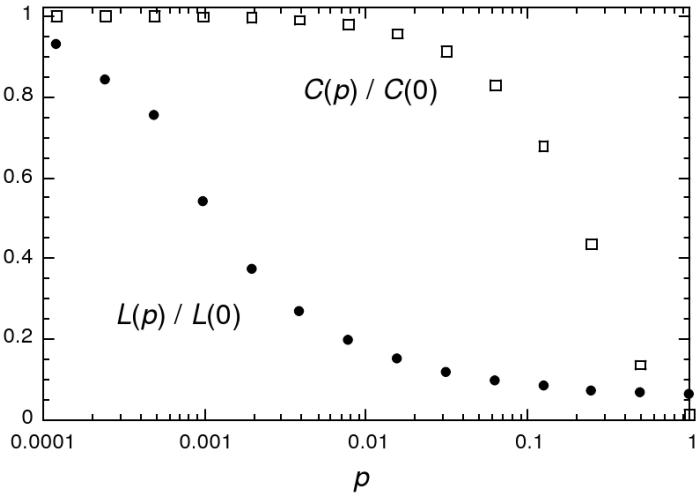

Figure 1.3: .Characteristic path length $l(p)$ and clustering coefficient $C(p)$ for the Watts-Strogatz model. Data are normalized by the values $l(0)$ and $C(0)$ for a regular lattice. Averages over 20 random realizations of the rewiring process; $N = 1000$ nodes, and an average degree $\langle k \rangle = 10$. From [63].

Barabasi-Albert scale free networks

As we mentioned above, many real networks display small network properties. However, empirical results demonstrate that many large networks are also scale-free, that is, their degree distribution $P(k)$ follows a power law for large k [65, 67]. Furthermore, even for those networks for which $P(k)$ has an exponential tail, the degree distribution significantly deviates from a Poisson distribution. In this case, a random graph or small-world model can not reproduce these features. The origin of the power law in networks was first addressed in a seminal paper by Barabási and Albert [74], where they showed that the degree distribution of many real systems are characterized by an uneven distribution of connectedness. In these networks, the nodes have a random pattern in the connections, some nodes are highly connected while others have few connections (see fig. 1.4-a). In this direction, they propose a simple model with two ingredients:

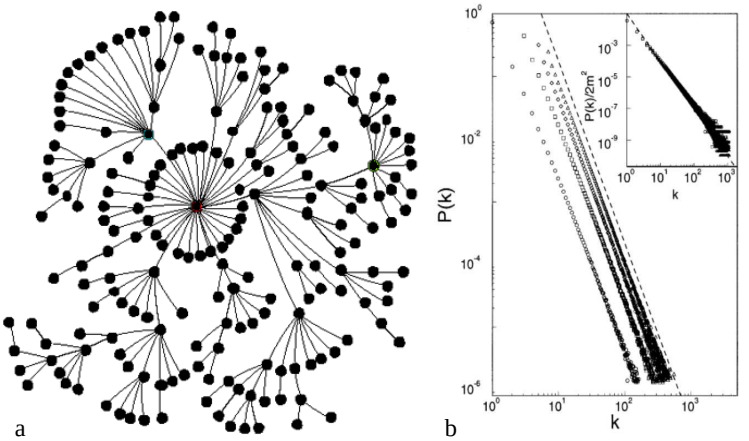

Figure 1.4: (a) An example of Scale-free networks of Barabási-Albert. (b) Degree distribution for the BA-network. $N = m_0 + t = 3^5$; with $m_0 = m = 1$ (circle), $m_0 = m = 3$ (square), $m_0 = m = 5$ (diamond), $m_0 = m = 7$ (triangle). The slope of the dashed line is $\gamma = 2;9$. Inset: rescaled distribution with m, $P(k)/2m^2$ for the same parameter values. The slope of the dashed line is $\gamma = 3$ From [67].

- Growth: Starting with a small number N_0 of nodes all conected among them, at every time step, a new node is added with $m(\leq N_0)$ edges that link the new node to m different nodes already present in the system.

- Preferential attachment: When choosing the nodes to which the new node connects, we assume that the probability P that a new node will be connected to node i depends on the degree k_i of node i, such that: $\Pi(k_i) = \frac{k_i}{\sum_j k_j}$. After t times steps this procedure results in a network with $N = t + N_0$ and $mt + \frac{N_0(N_0-1)}{2}$ edges. Numerical simulations show that this network evolves into a scale invariant form with the probability that a node has k links following a power law $P(k) \sim k^{-\gamma}$, with $\gamma \approx 3$ (see fig. 1.4).

Dynamical properties of this model can be addressed using various analytic approaches: The continuum theory [89] master-equation approach [90] and the rate-equation approach [91]. All these approach are studied and summarized in detail in ref. [67].

	Path Length (L)	Clustering (C)	Degree Dist. $P(k)$
Regular Network	$L \sim N^{1/d}$	$C \sim N^{0}$	$P(k) = \delta(k - z)$
Random E-R Network	$L \sim \ln(N)$	$C \sim N^{-1}$	Poisson
Samall-World Network	$L \sim \ln(N)$	$C \sim N^{0}$	Exponential
B-A Scale-free Network	$L \sim \frac{\ln(N)}{\ln(\ln(N))}$	$C \sim \frac{ln(N)^2}{N}$	$P(k) \sim k^{-3}$

Table 1.1: Complex Networks Characteristics. Here N is the number of nodes.

To finish this brief introduction about of the paradigmatic models for complex networks, we summarize in table 1.1 the most important characteristics of these networks:

1.2.3 Social Networks

A social network is a set of individuals (or organizations) called "nodes," which are tied (connected) by one or more specific types of interdependency, such as friendship, kinship, common interest, financial exchange, dislike, sexual relationships, or relationships of beliefs, knowledge or prestige. In the language of social network analysis, the individuals are called actors and the connection ties. Actors and ties can be defined in different ways depending on the questions of interest.

Social network analysis has a history stretching back at least half century and has produced many results about of social influences, social groupings, disease propagation, communication of information. In this way, an intersting review of the historical development of social networks theory during the 20th century is presented by Borgatti et al. [92].

The Social Sciences have a long history in the study of real-world networks. Of particular interest among the early works on the subject are: friend-ship patterns within small groups [93]; the so-called women study [94], social networks of factory workers in the late 1930s in Chicago [95]; the mathematical models of Anatol Rapoport [72], who was one of the first theorists, to stress the importance of the degree distribution in networks; the studies of friendship networks of school children [96, 97]. Studies of business communities [98–100] and of patterns of sexual contacts [101–103].

In the sixties, Milgram published his famous experiment on the small world phenomena [85, 104]. The experiment proby the distribution of path lengths in

an acquaintance network by asking participants to pass a letter to one of their first-name acquaintances in an attempt to get it to an assigned target individual. Most of the letters in the experiment were lost, but about a quarter reached the target and passed on average through the hands of only about six people in doing so. This experiment was the origin of the popular concept of the six degrees of separation," although that phrase did not appear in Milgram's writing, being coined some decades later by Guare [105]. A brief but useful early review of Milgram's work and work stemming from it was given by Garfield [106].

In the last years, social networks have become the focus of considerable attention in the applied mathematics and statistical physiscs community [20, 64, 65, 76, 107]. Onnela et al. [108] studied a mobile telephone network with more than 4 million users. They constructed social links between two users when they found a reciprocal call between two agents, and the strength of the social tie was defined as the aggregated duration of calls they shared. It is important to stress that they could confirm Granovetter's theory of the strength of weak ties [109]. Strong ties are found within communities, while weak ones tend to connect different clusters. They found that a successive removal of the weak ties results in a phase transition-like network collapse, while the same removal process starting by the strong ties has little impact in the overall structure of the network. In this regared, an interesting analysis of real social data is made by Leskovec and Horvitz [110] . They presented a study of anonymized data capturing a month of high-level communication activities within the whole of the Microsoft Messenger instant-messaging system. They examined characteristics and patterns that emerge from the collective dynamics of large numbers of people, rather than the actions and characteristics of individuals. This dataset contains summary properties of 30 billion conversations among 240 million people. From the data, they construct a communication graph with 180 million nodes and 1.3 billion undirected edges, creating the largest social network constructed and analyzed to date. In this work they report on multiple aspects of the dataset finding that the graph is well-connected and robust to node removal. They confirmed "six degrees of separation" finding that the average path length among Messenger users is 6.6. Also, they found that people tend to communicate more with each other when they have similar age, language, and location, and that cross-gender conversations are both more frequent and of longer duration than conversations with the same gender.

Other studies of real social networks deal with social phenomena such as author collaboration networks [111], sexual contacts [103] or citation networks [112].

1.3 Local and global interactions

There is a variety of processes occurring in spatiotemporal dynamical systems where both, spatially local and global interactions contribute in different and competing ways to the emergence of collective behavior. Some examples include Turing patterns [113] (with slow and fast diffusion), Ginzburg-Landau dynamics [5], surface chemical reactions [114], sand dunes (with the motions of wind and of sand) [115], and pattern formation in some biological systems [4]. Recently, the collective behavior of dynamical elements subject to both local and global interactions has been experimentally investigated in arrays of chaotic electrochemical cells [116].

Local interactions mean that individual elements of the system interact with each other within a local environment, where the local environment is much smaller than the size of the system. In other words, each element only interacts with an immediate neighborhood. On the other hand, in global interactions each individual element experiences the influence of a common environment acting on the entire system. Mean field coupling and externally applied fields are examples of a global interaction.

Systems where the evolution of the state of any element depends only on the interactions with other elements in the system are called *autonomous dynamical systems*. If the elements in a system interact with an external field, the term *forced or driven system* is employed. Mean field coupling is an example of a global interaction in an autonomous system, while an external field gives a global in a forced system. The phenomena of pattern formation and collective behavior induced by external forcing on spatiotemporal systems, such as chemical reactions [27, 28] or granular media [29], have also been considered. The analogy between external forcing and global coupling in spatiotemporal dynamical systems has recently been explored in the framework of coupled map lattice models [117–119]. It has been found that, under some circumstances, the collective behavior of an autonomous spatiotemporal system with local and global interactions is equivalent to that of a driven spatiotemporal system possessing similar local couplings as in the autonomous system.

The addition of a global interaction to a locally coupled system is known to be able to induce phenomena not present in that system, such as chaotic synchronization and new spatial patterns. However, the classification and description of generic effects produced by external fields or global coupling in a nonequilibrium system of locally interacting units is still an open general question. The common wisdom for equilibrium systems is that under a strong enough external

field, local interactions become negligible, and the system orders following the external field. For nonequilibrium nonpotential dynamics [120] this is not necessarily the case, and nontrivial effects might arise depending on the dynamical rules. Moreover, it has shown that the addition of a global interaction in the autonomous system allows for chaotic synchronization that is not possible in a large coupled map system possessing only local interactions. [117, 118]

This problem of the competition between local and global interaction is, in particular, relevant for recent studies of social phenomena in the general framework of Complex Systems. The aim is to understand how collective behaviors arise in social systems. Several mathematical models, many of them based on discrete-time and discrete-space dynamical systems, have been proposed to describe a variety of phenomena occurring in social dynamics where local and global interactions are present [35–41, 62]. However, a global picture of the results of the competition between the local interaction among the agents and the interaction through a global coupling field or an external field is missing.

In a general framework, we consider interaction fields that originate either externally (driven dynamics) or from the contributions of the elements in the system through a global or a local function of their internal variables (autonomous dynamics). In the context of Social Science an external interaction field is interpreted as a specific state or opinion being imposed on all elements by controlled mass media, while the presence of either a local or global interaction function describes a social system subject to endogenous cultural influences, or information feedback.

1.4 Co-evolution Dynamics

As we have mentioned above, the dynamics of collective phenomena in a system of interacting units depends on both the topology of network of interactions and the interaction rule among connected units. In this context, the effects of these two ingredients on the emergent phenomena in fixed networks have been extensively studied [20, 67].

However, many real-world systems observed in physics, chemistry, biology and Social Sciences can be regarded as dynamical networks of active elements where the coupling connections and the states of the elements evolve simultaneously. In this case the links that connect a pair of elements in a system can move or appear and disappear as the system evolves on many timescales. These modifications in the network's topology do not occur independently from the

nodes' states but as a feedback effect: the topology determines the evolution of the nodes' states, which in its turn determines how the topology can be modified [16, 17, 33, 55, 62, 66, 121–125]; i.e., the network becomes adaptive.

The feedback between the state variables and the topology of the network can give rise to a complicated mutual interaction between a time varying network topology and nodes's states. Systems that display this feedback loop between the topology and states are defined as co-evolutionary dynamical systems or adaptive networks [124].

One of the first works that implement co-evolutionary dynamics were introduced by Zimmerman et al. in the context of game theory [55, 62, 66, 125]. In these papers, the authors have shown that cooperation is favored in the prisoner's dilemma spatial game when agents can change their neighborhood. More precisely, links between cooperators are naturally maintained; in the case of a link between a cooperator and defector, the cooperator may want to break the interaction, but not the defector, so that these reactions are balanced, and for simplicity only links between defectors are assumed to be rewired, with a certain probability p at each time step. Defectors are thus effectively competitive, since they rewire links at random until they find a cooperative neighbor. A rich phenomenology follows from these dynamical rules, yielding a stationary state with a larger number of cooperators as soon as $p > 0$ (see figure 1.5), exploited by a smaller number of defectors, who have on average a larger payoff. Other interesting result is that a hierarchical interaction network is reached as a stationary network starting from a random network of interactions (see Figure 1.6). The network appears structured from a few highly connected elements easily identified through an imitation network. Such a network has the characteristics of a small world when a mechanism of local neighbor selection is introduced in the adaptive dynamics of the network. The hierarchical structure supports a stationary, highly cooperative state for general situations in which, for a fixed network, the system would not settle in a stationary state and in which the cooperation level would be much smaller. The stability of the network is very sensitive to changes in the state of the few highly connected nodes: external perturbations acting on these nodes trigger global avalanches, leading to transient dynamics in which the network completely reorganizes itself searching for a new, highly cooperative stationary state.

Others co-evolutionary dynamics in the context of game theory have been considered in references [126, 127]. These works introduce a model where the network growth co-evolves together with the dynamics, giving rise to cooperative scale-free networks. The authors find that the organization of cooperation is radically different from the case where the underlying network is static. They show that the general belief that hubs can only be occupied by cooperators does

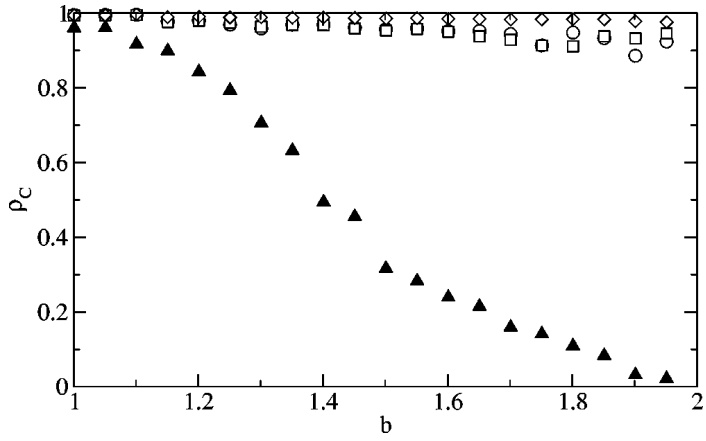

Figure 1.5: Average fraction of cooperators ρ_c in the steady state as function of the temptation to defect b, for various rewiring probabilities $p : p = 0$ (triangles), $p = 0.01$ (circles), $p = 0.1$ (squares) and $p = 1$ (diamonds) From [62].

not hold. Moreover, these scale-free networks support high levels of cooperation despite the presence of defector hubs.

In a variety of dynamical models where this type of co-evolution dynamics has been implemented recently a transition is often observed from a phase where all nodes are in the same state forming a single connected network to a phase where the network is fragmented into disconnected components, each composed by nodes in a common state. This network fragmentation transition observed in different co-evolutionary dynamics models is a generic result, and it is independent of link number conservation, rewiring rule and local interaction rule among elements of the system [124]. This behavior is related to the difference in time scales that govern the two dynamics: the state of the nodes and the network of interactions, which in many cases are controlled by some external parameter. In this direction, several works have been published. This is the point of view adopted in references [18, 121, 128]. In this approach, each node carries an internal variable that is updated through interactions with its neighbors. Each link between agents decays spontaneously at a certain rate λ, and new links are created at rate η only between agents whose internal variables are close enough.

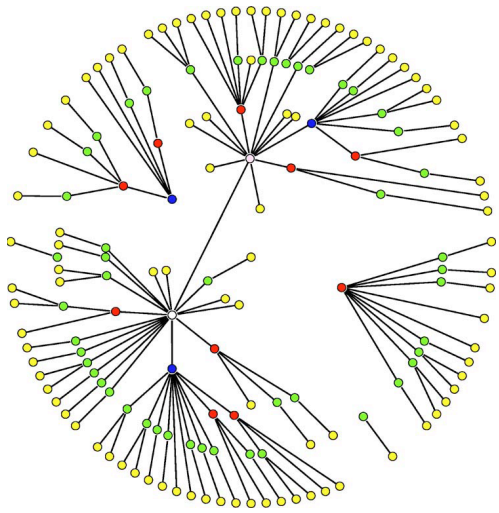

Figure 1.6: Partial view of a sample imitation network in steady state. From [62].

The topology thus has an impact on the evolution of the agents' states, which in turn determines how the topology can be modified. When the state update (rate ν) is fast with respect to the link's update process, the competition between link decay and creation rates leads to a phase transition from a very sparse phase in which the population is divided into many small clusters, to a denser globally connected network with large average degree. In this model the links are formed only if the state of nodes are within a threshold d. This transition, studied trough a mean-field approach in the limit $\nu \gg 1$, turns out to be sharp and displays hysteresis phenomena [121, 128].

References [33, 122, 123] consider the co-evolutionary voter model as the simplest model to study the network fragmentation transition. In this model, the interaction between two agents that do not share the same state can lead either to a local consensus via random imitation mechanism (one adopt the state of the other) with a probability p, or to breaking of the link if the agents fail to reach an agreement, with probability $1 - p$. This external parameter p controls the internal time scale of both dynamics in the system. In reference [123], this model is studied starting from a fully connected network and, depending on the model's parameters, the final state can be formed of one o more separated communities of agents sharing the same state. In order to mimic the introduc-

tion of new social relations, another hypothesis consists of considering that links do not disappear but are simply rewired by the agent who decides to change an interaction partner. Holme and Newman [33] uncover an interesting out-of-equilibrium phase transition in the co-evolution of the network of contacts of agents interacting through a Voter-like model with q opinions. In this model, starting from a random network of agents with randomly chosen opinions; an agents i is selected at each time step; then with probability p, i adopts the opinion of one randomly selected neighbor, and with propability $1 - p$ one of the links connecting i to a neighbor with different state is rewired towards another agent that shares the state of i. Here, the total number of links is conserved during the evolution. In this model, when p is smaller than a certain critical value p_c, the system evolves towards a set of small communities of agents sharing the same opinion. On the other hand, for larger values of p the states of the nodes in the system change faster than the topology, and consensus is obtained as a giant connected clusters of agents. In order to understand the nature of these transitions, a mean field approach of this model for two opinions ($q = 2$) has been discussed by Vazquez et al. [122]. In this approach the authors predict the a transition from active phase, where the links are continuously rewired (evolving network) and nodes flipp their states, to a frozen phase that correspond to a fixed network where connected nodes have the same state and no more evolution is possible. They show that the critical value p_c only depends on the average degree of the network, and the time scale to approach the final state diverges as $|p - p_c|^{-1}$ near p_c. In this paper, the authors found that for any value of p, due to fluctuations, a finite-size network eventually reaches an absorbing state composed by inert links (links between nodes in the same states) only. They studied the structure of the network in the final state by performing numerical simulations of the dynamics starting with a degree-regular random graph with connectivity $\langle k \rangle = 4$ and letting the system evolve until it was frozen. They observe that the largest component S in the final configuration is very close to the system size for values of p below a transition point p_c, indicating that the network forms a single component. Above p_c the network gets disconnected into two large components and a set of components of size much smaller than the system size. This result suggests that the active and frozen phases observed in infinite large systems correspond to the connected and disconnected phases, respectively, in finite systems.

While the co-evolution dynamics as a feedback process between node state and network topology is clearly a key issue for the understanding of many real systems, its study in the context of complex networks is still at an early stage. This problem highlights one of the fundamental questions in the network dynamics, namely whether dynamics controls the structure of a network , or the structure controls the node's dynamics.

1.5 Outline

In this thesis we address different aspects of the general problem of the emergence of consensus versus polarization in social dynamics. We have considered different mechanisms for the interaction, including two new ingredients that constitute the core of this thesis, namely the competition between local versus global interaction and co-evolutionary dynamics. The effects of the competition between local versus global interactions are studied in the framework of social learning (i.e., all the interacting elements in a social system should adopt the state of a signal) using a modification of the threshold model of interaction of Granovetter [9]. We also study the competition between local and global interaction in the context of the bounded confidence model of opinion formation introduced by Deffaunt et al. [10], and Axelrod's model [11]. These models are characterized by the existence of non-interacting states in their dynamics. The paradigm of co-evolution is analyzed in detail in the context of Axelrod's cultural model and also in the case of a model inspired in Granovetter's threshold model for local interaction that we introduce in the present work.

The presentation of this thesis is organized as follows: In Chapter 2 we discuss the concept of social learning. We introduce a threshold model for social learning subject to the influence of an external field that changes randomly over time. We perform a mean field analysis and numerical simulations for the model, and address the effect of the topology of the underlying network of interactions on the collective dynamics of the system.

In Chapter 3 we first review the bounded confidence model proposed by Deffuant et al. [10] for opinion formation. We study the collective behavior of this model subject to an external field and investigate the role of the network topology, specially the implications of the existence of long range interactions. When these interaction are present the system is known to be able to order spontaneously in a state different to the one selected by the field.

In Chapter 4 we consider Axelrod's model for the dissemination of culture [11]. We present general properties and the most important previous results on the model. In section 4.2, we study the effects of mass media, modeled as applied fields, on a social system based on Axelrod's model. We define different types of fields: a *constant external field*, a *global field*, and a *local field*. These fields represent influences of different types of mass media. The effects of these fields are analyzed in both the order and disorder phases of the system. We also study another mechanism of interaction with mass media fields, introduced by Shibanai et al. [129]: indirect mass media influence. It is defined as a global field acting as

a filter for the influence of the existing network of interactions on each agent. We also show that the system exhibit the same phenomenon of spontaneous ordering against the external field found in Deffuant's model in networks with long range interactions. Finally, we discuss the connection of our study with the site percolation problem in the limit in which the elements only interact with an external field. In section 4.3 we consider the issue of co-evolution dynamics in the context of Axelrod's model. We develop a model of cultural differentiation, where the network structure co-evolves with the cultural interactions between the agents and study the process of cultural group formation. The of the effect of cultural drift in Axelrod's model is re-examine from this co-evolution perspective.

In Chapter 5 we introduce a second co-evolutionary dynamic model, where the local interactions follow a majority rule in order to reach consensus. A fragmentation transition is obtained, similar to the one discussed in connection with group cultural differentiation in Axelrod's model

In Chapter 6 we present our conclusions and point to various directions for future research.

Chapter 2

Social learning

2.1 Introduction

The emergence of consensus is a paradigm of broad interest, recently addressed by Statistical Physics. The main question is to establish when the dynamics of a set of interacting agents that can choose among several opinions converge to a consensus on one of these opinions or, alternatively, when a state with several coexisting opinions (polarization) prevails. In the study of the consensus versus polarization problem, several models have been proposed to account for different mechanisms of local interaction [9–11, 44–53, 57, 58] (see Section 1.1). Recently, different models have incorporated some form of interaction with external influences in order to study how the emergence of consensus is affected by external signals [12–15, 130, 131]. In this Chapter we consider the problem of social learning from this point of view. Although social learning is a broad concept [132, 133] we refer to it in this thesis as the problem in which all agents in a system should adopt ("learning") the state of external signal as a consequence of their local interactions and their interaction with that signal. This situation gives a first example of one of the general question addressed in this thesis, namely the competition between local-local agent interaction with the global interactions of the agents with a field.

This problem of social learning has been a focus of much attention in Economics during the last decades. In a recent work, Golub and Jakson [134] study social learning in a setting where agents in a network receive independent noise signals at an initial time (as initial condition), and then they interact with each other. During the evolution of the system, complete learning occurs due solely to

interactions between the agents. The agents update their states by repeatedly taking weighted averages of their neighbors' opinions. The authors show that the states of all agents converge to the state of the external signal if and only if the interactions with the most influential agent vanish as the size of the society grows.

Partly motivated by the work in reference [134] and along similar lines, our aim in this Chapter is to revisit the issue of the evolution of social learning but using simple learning rules for the agents in a system that combine the external signal recived by each agent at each time step, with the observed behavior of their neighbors. Succinctly, we postulate any agent recurrently receives a noise signal that can take two values, and then he chooses to adjust (or not) its behavior after looking for confirmation of its state in the observed behavior of its neighbors. The key question is whether or not agents will eventually converge to the state of the external signal, that is considered as the best action. To address this question, we introduce a modification of the threshold model proposed by Granovetter [9].

2.2 The model

The system is composed of a set of N agents located at the nodes of a network. An agent i possesses k_i neighbors. At each time t, a randomly chosen agent chooses one of two alternative actions, action 1 or action -1. In terms of economic theory, these actions are not equivalent. One of them, say action 1, always induces a higher payoff (at least in expected terms), but the agents do not know this. Instead, we assume that, at each t, they receive a signal about the relative payoff of the two actions. This signal, which is independent of the agents, is only partially informative. Specifically, it provides the correct information (i.e., "action 1 is best") with probability $p > 1/2$, while it delivers the opposite information with probability $1 - p$. Each agent is assigned a fixed threshold parameter $0 < \tau < 1$ that determines the fraction of neighbors required to change the agent's action.

Let us assume that, for all times, the value of the external signal is $+1$ with probability p, while this value is -1 with probability $1 - p$. As initial conditions, agents with action 1 are uniformly distributed at random with probability p in the system, while agents with the action -1 are also uniformly distributed at random with probability $(1 - p)$ over the system. In other words, we posit that the probability distribution of state s_i of each i at the start of the process is the same probability distribution of the external signal.

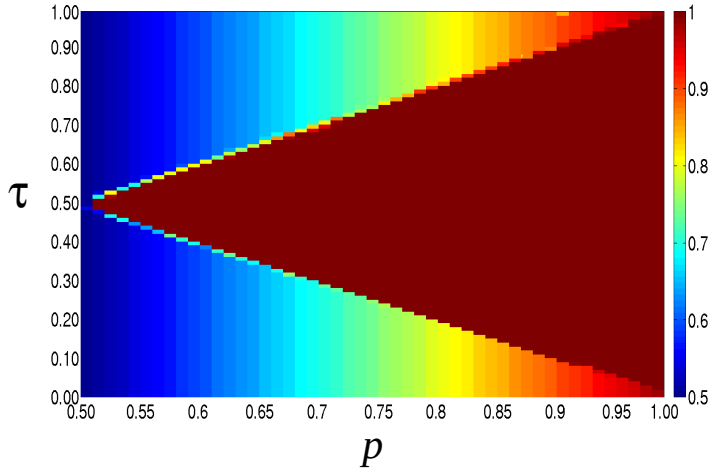

Figure 2.1: Phase diagram of the threshold model on a fully connected network. The colors represents the fraction of agents choosing action 1 (from red, $x = 1$ to blue, $x = 0.5$). System size composed by $N = 10^4$ agents; averaged over 100 realizations.

Thus, at each t, an agent i is randomly chosen and receives the external signal. If the action of the signal is equal to that of the selected agent, nothing happens. Otherwise, if the action of the signal is different from that of the selected agent, the agent evaluates the actions of its k_i neighbors. Let τ_i be the fraction of neighbors disagreeing with i. If $\tau_i > \tau$, node i adopts the action of the signal.

The central question addressed in this chapter can now be precisely formulated:

> What is the relationship between p (the quality of the signal) and τ (the threshold parameter for action change) that underlies the spread and consolidation of action 1?.

We investigate this question in what follows, for a range of different setups and relying on a variety of methodologies.

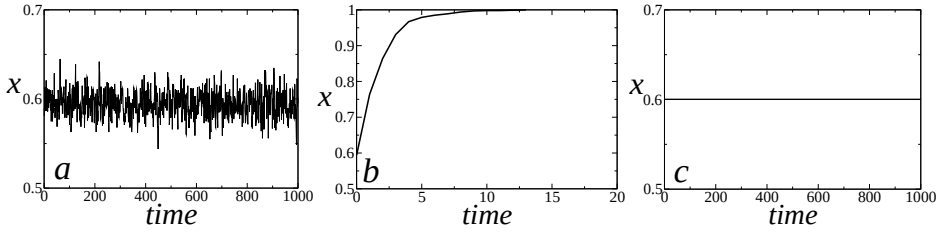

Figure 2.2: Time evolution of the fraction of agents choosing action 1 (x) in a typical realization with $p = 0.60$, and (a) $\tau = 0.20$; (b) $\tau = 0.50$; (c) $\tau = 0.80$.

2.3 Mean-field analysis

Let $x(t) \in [0, 1]$ stand for the fraction of agents choosing action 1 at time t. Then its (continuous-time) dynamics are given by:

$$\dot{x} = -(1-p)x\,\theta(1-x-\tau) + p(1-x)\,\theta(x-\tau) \tag{2.1}$$

where $\theta(z) = 1$ if $z \geq 0$ while $\theta(z) = 0$ if $z < 0$. In this equation, the first term accounts for the number of agents initially with the right signal (x) who receive the wrong signal (with probability $1-p$) and adopt it, as the fraction of agents also adopting it is larger than the threshold ($1 - x > \tau$). The second accounts for the opposite process, whereby agents who receive the correct signal (with probability p) switch to the correct action when the population supports it ($x > \tau$).

We assume that, at time $t = 0$, each agent receives a signal $\alpha_i(0)$ and adopts the corresponding action $a_i(0) = \alpha_i(0)$. Hence the initial condition for the dynamics above is $x(0) = p$.

It is useful to divide the analysis into two cases:

Case I: $\tau > 1/2$

In this case, it is straightforward to check that

$$\begin{array}{rcl} x < 1-\tau & \Longrightarrow & \dot{x} = -(1-p)x < 0 \\ 1-\tau < x < \tau & \Longrightarrow & \dot{x} = 0 \\ x > \tau & \Longrightarrow & \dot{x} = p(1-x) > 0 \end{array}$$

So, it follows that correct social learning occurs iff $p > \tau$.

Case II: $\tau < 1/2$

In this case, we find:

$$\begin{array}{rcl} x < \tau & \Longrightarrow & \dot{x} = -(1-p)x < 0 \\ \tau < x < 1-\tau & \Longrightarrow & \dot{x} = p - x \\ x > 1-\tau & \Longrightarrow & \dot{x} = p(1-x) > 0 \end{array}$$

And, therefore, correct social learning occurs iff $p > 1 - \tau$

Combining both cases simply stating that mean-field analysis predicts that correct social learning, $x_\infty = x(t \to \infty) = 1$ occurs if, and only if,

$$\tau \in (1-p, p)\,, \tag{2.2}$$

that is, the threshold τ is within an intermediate region whose size grows with the probability p, which determines the informativeness of the signal. However, there are other two phases: if $\tau \in (0, 1-p)$, the system reaches the stationary solution $x_\infty = p$; while if $\tau \in (p, 1)$, the system stays ($\dot{x} = 0$) in the initial condition $x_\infty = x = x(t=0) = p$.

2.4 Numerical simulations

Next, we explore whether the insights obtained from the mean-field model carry over to setups where agents are genuinely connected through a social network. First, we consider the benchmark case of global interaction (i.e., a completely connected network). Then, we turn to the case of local interaction and focus on three paradigmatic network setups: lattice networks, Erdös-Renyi (Poisson) networks, and Barabási-Albert (scale-free) networks.

2.4.1 Global interaction

The results obtained on the completely connected network (i.e., the network where every pair of nodes is linked) are in line with the mean-field theory presented in the previous section. The essential conclusions can be summarized through the phase diagram in the (p, τ)-space of parameters depicted in Figure 2.1. Here we represent the fraction of agents choosing action 1 in the steady state for each parameter configuration, with the red color standing for a homogeneous situation with $x = 1$ (i.e., all agents choosing action 1) while the blue

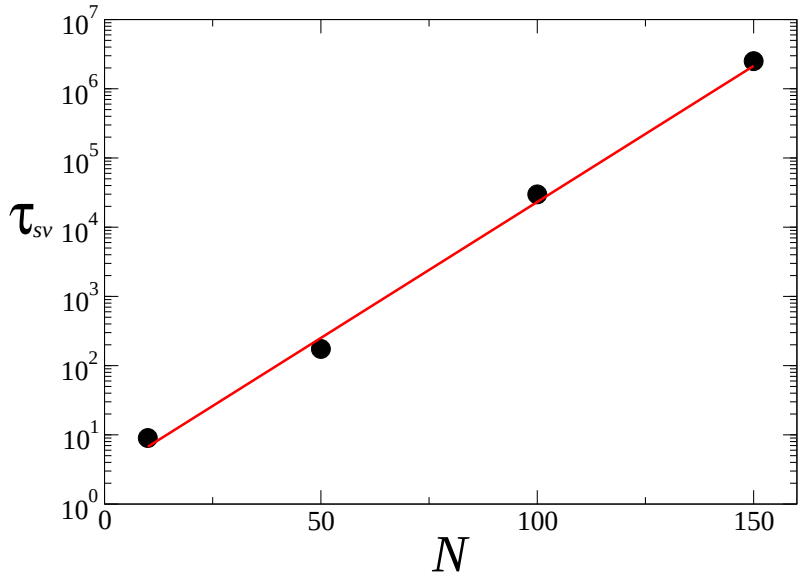

Figure 2.3: The average time of surviving runs τ_{sv} for different system sizes N for $p = 0.60$ and $\tau = 0.20$. The continuous line corresponds to an exponential fit of the form $\tau_{sv} \sim \exp(\alpha N)$.

color codes for situation where $x = 0.5$ and therefore the two actions are equally present in the population. Intermediate situations appear as a continuous color grading between these two polar configurations.

We observe, therefore, that depending on the quality of the external signal p and the threshold τ, the system reaches configurations where either complete learning occurs ($x = 1$) or not ($x = p$). Indeed, the observed asymptotic behavior is exactly as predicted by the mean-field analysis and displays the following three phases:

- Phase I: $\tau < 1 - p$. The system reaches a stationary aggregate configuration where the state of the nodes is continuously changing but the average fraction of those choosing action 1 gravitates around the frequency $x = p$, with some fluctuations (see Figure 2.2*a*). The magnitude of these fluctuations decreases with system size N.
- Phase II: $1 - p < \tau < p$. The system reaches the absorbing state $x = 1$ where everyone adopts action 1. This is a situation where the whole population eventually learns that the correct choice is action 1 (see Figure 2.2*b*)..

- Phase III: $\tau > p$. The system freezes in the initial state, so the fraction $x = p$ of agents choosing the correct action coincides with the fraction of those that received the corresponding signal at the start of the process (see Figure 2.2*c*).

It is worth noting that, while in Phase I the mean-field theory predicts $x = p$, any finite-size system must eventually reach an absorbing homogenous state due to fluctuations. Thus, to understand the nature of the dynamics, we determine the average time τ_{sv} that the system requires to reach such an absorbing state. As shown in Figure 2.3, τ_{sv} grows exponentially with N. This means that τ_{sv} grows very fast with system size, and thus the coexistence predicted by the mean-field theory in Phase I can be regarded as a good account of the situation even when N is just moderately large.

2.4.2 Lattice networks

Assume that all nodes are placed on a *two dimensional square-lattice with periodic boundary conditions* and von Newmann neighborhood ($k = 8$).

The behavior of the system is qualitatively similar to the case of a fully connected network. Again we find three phases: two of them in which both actions coexist and their respective frequencies p and $1 - p$ are given by the signal probabilities (one phase is frozen, while the other continuously fluctuates), and another one where the whole population converges to action 1. A global picture of the situation for the entire range of parameter values is shown in Figure 2.4, with the black diagonal lines in it defining the boundaries of the full-convergence region derived from the mean-field theory. Comparing it with Figure 2.1, we observe that the region in the (p, τ)-space where behavioral convergence obtains in the lattice network is broader in the lattice network than in the completely connected network. This indicates that restricted (or local) interaction facilitate social learning, in the sense of enlarging the range of conditions under which the behavior of the population converges to action 1.

As a useful complement to the previous discussion, Figure 2.5 illustrates the evolution of the spatial configuration for a typical simulation of the model in a lattice network, with different values of τ and $p = 0.6$. Panels *a*, *b* and *c* show the configurations of the system for a low value of $\tau = 1/8$ at three different time steps: $t = 0$, 1000 and 2000 respectively. The evolution of the system displays a configuration analogous to the initial condition, both actions coexisting and evenly spreading throughout the network. This is a situation that leads to dynamics of the sort encountered in *Phase I* above. In contrast, Panels g, h and i correspond to a context with a high $\tau = 7/8$, which induces the same performance

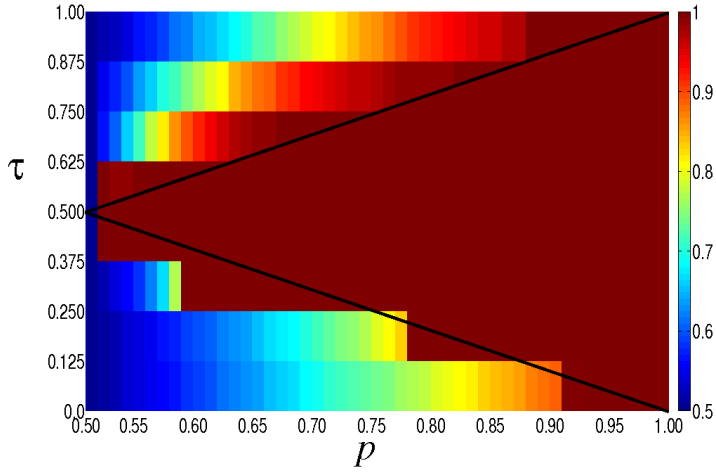

Figure 2.4: Phase diagram of the threshold model on a two-dimensional square-lattice with $k = 8$. The colors represents the fraction of agents choosing action 1 (from red, $x = 1$, to blue, $x = 0.5$). System size $N = 10^4$; average over 100 realizations).

as in *Phase III*. It is worth emphasizing that although Panels a, b and c display a similar spatial pattern, they reflect very different dynamics, i.e., in continuous turnover in the first case, while static (frozen initial conditions) in the second case. Finally, Panels d, e and f illustrate the dynamics for an intermediate value of $\tau = 1/2$, which leads to a dynamic behavior of the kind displayed in *Phase II*. Specifically, these panels present the spatial configurations observed at three different time steps: $t = 0$, 16 and 21. They show that the system evolves, very quickly, toward a state where all agents converge to action 1.

2.4.3 Erdös-Renyi and scale-free networks

A lattice network is the simplest possible context where local interaction can be studied. It is, in particular, a regular network where every agent faces exactly symmetric conditions. It is therefore interesting to explore whether any deviation from this rigid framework can affect our former conclusions. This we do here by focusing on two of the canonical models proposed in the network literature: the classical model of Erdös and Rényi (ER) [73] and the more recent scale-free model introduced by Barabási and Albert (BA) [74]. Both of them deviate from the

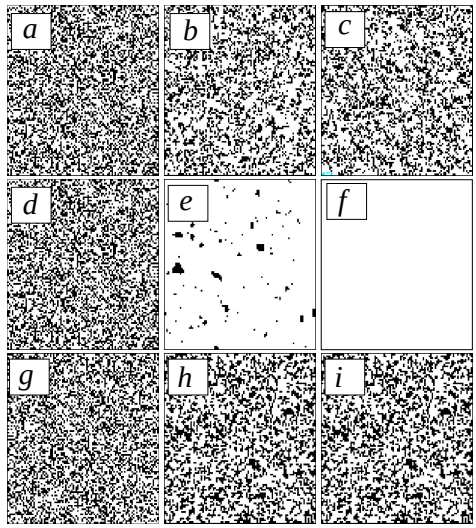

Figure 2.5: Time evolution of the threshold model on a two-dimensional lattice with $k = 8$ for different values of τ and $p = 0.60$. Panels a, b, c: $\tau = \frac{1}{8}$ and time steps (a) $t = 0$, (b) 1000 and (c) 2000. Panels d, e, f: $\tau = \frac{1}{2}$ and time steps (d) $t = 0$, (e) 16 and (f) $t_3 = 21$. Panels g, h, i: $\tau = \frac{7}{8}$ and time steps (g) $t = 0$, (h) 1000 and (i) 2000. Black color represents an agent using action -1, while white color represents action $+1$. The system size is $N = 10^4$ and each time step corresponds to N iterations of the dynamics.

regularity displayed by the lattice network, by contemplating a non-degenerate distribution of node degrees.

The ER random graph is characterized by a parameter μ, which is the connection probability of agents. It is assumed, specifically, that each possible link is established in a stochastically independent manner with probability μ. Consequently, for any given node, its degree distribution $P \equiv \{P(k)\}$ determining the probability that its degree is k is Binomial, i.e., $P(k) = \binom{N-1}{k}\mu^k(1-\mu)^{N-1-k}$, with an expected degree given by $\langle k\rangle = \mu(N-1)$. In the simulations reported below, we have focused on networks with $\langle k\rangle = 8$ and $N = 10^4$.

On the other hand, to build a BA network, we follow the procedure described in Ref. [74]. At each time step, a new node is added to the network, establishing m links to existing nodes. The newcomer selects its neighbors randomly, the probability of attaching to each of the existing modes being proportional to the latters' degree k. It is well known that this procedure generates networks whose degree distribution follows a power law of the for $P(k) \simeq 2m^2k^{-\gamma}$, with

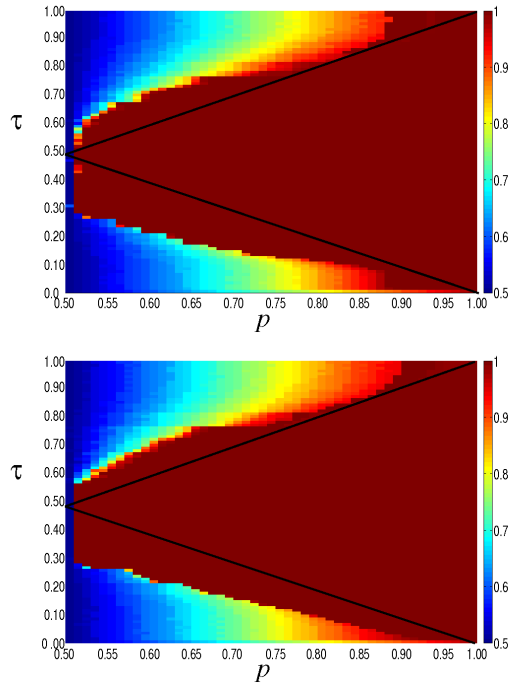

Figure 2.6: Phase diagram of the threshold model in a (Top) ER network and in a (Bottom) scale-free network with average degree $\langle k \rangle = 8$. The colors represents the fraction of agents choosing action 1 (from red, $x = 1$, to blue $x = 0.5$). System size $N = 10^4$, average over 100 realizations.

$\gamma \approx 3$. An interesting contrast between the Binomial distribution obtained in ER networks and the present one is that while the former associates an exponentially decaying probability to high-degree nodes, the latter displays “fat tails", i.e., associates significant probability to high-degree nodes. For our simulations, we have constructed BA networks using the aforementioned procedure with value of $m = 4$, leading to an average degree $\langle k \rangle = 2m = 8$.

The results are illustrated in Figure 2.6. For these two alternative network topologies, the system displays qualitatively the same behavior observed for lattice network. That is, there are three phases corresponding to three distinct kinds of dynamic performance: convergence to action 1, frozen behavior, persistent turnover. In contrast with the predictions of the mean-field model, the convergence region (which we labeled as Phase II) is larger than predicted by

the mean field theory. As mentioned above, this suggests that local (i.e. limited) connectivity facilitates social learning.

Why does limited connectivity extend the learning region? To see why this happens, let us first try to understand its effect on the likelihood that, at some random initial conditions, any given node faces a set of neighbors who favors a change of actions. This, of course, is just equal to the probability that the fraction of neighbors who display opposite behavior is higher than τ, the required threshold for change. Thus, more generally, let us focus on the conditional distributions $\phi_+(\nu)$ and $\phi_-(\nu)$ that specify, for an agent displaying actions 1 and -1 respectively, the probability of finding a fraction ν of neighbors who adopt actions -1 and 1, respectively. Of course, these distributions must depend on the degree distribution of the network and, in particular, on its average degree. Intuitively, when the average degree of the network is large relative to population size those distributions must be highly concentrated around p and $1-p$ respectively, while in the opposite case they will tend to be quite disperse.

Now, let us see what are the implications of each case. In the first one, when the distributions ϕ_+ and ϕ_- are highly concentrated, the situation is essentially as captured by the mean-field approach, and thus the induced dynamics must be well described by this approach (in particular, as it concerns the size of the convergence region). In contrast, when those distributions are disperse, a significant deviation from the mean-field theory is introduced. In fact, the nature of this deviation is different depending on the level of the threshold τ. If it is low, and thus action turnover high, it mitigates such turnover by increasing the probability that the fraction of neighbors with opposite behavior lie below τ. Instead, if τ is high and action change is difficult, it renders it easier by increasing the probability that the fraction of neighbors with opposite behavior lies above τ. Thus, in both cases it works against the forces that hamper social learning and thus improves the chances that it occurs.

The above considerations are illustrated in Figure 2.7 for a lattice network. There we plot the distributions $\phi_+(\nu)$ for different levels of connectivity k and parameter values $p = 0.60$ and $\tau = 0.30$ (recall that these values correspond to Phase I in a fully connected network). Consider first the situation that arises for values of $k = 8,\ 24,\ 56$ – i.e. low connectivity relative to the size of the system. Then we find that, among the nodes that are adopting action 1, ϕ_+ attributes a significant probability mass to those agents whose fraction of neighbors ν choosing action -1 is below the threshold required to change (as marked by the vertical dashed line). Such nodes, therefore, will not change their action. And, as explained, this has the beneficial effect of limiting the extent of action turnover as compared with the mean-field (or complete-network) setup. On the other hand, the inset of Figure 2.7 shows that, among the nodes that are adopting action -1, the

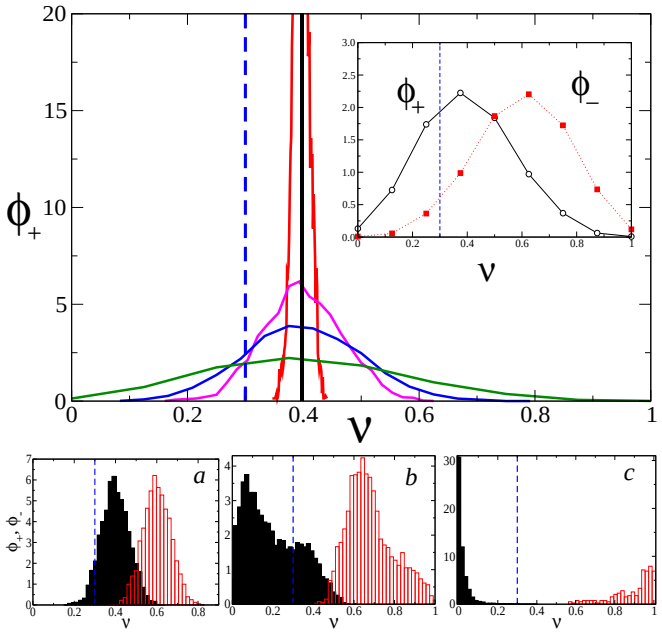

Figure 2.7: (Top row) The initial probability density ϕ_+ that a node using action 1 has a fraction of neighbor nodes with action -1, computed on a two-dimensional lattice for $k = 8, 24, 56, 828$ and a completely connected network. System size is $N = 10^4$, $p = 0.60$, and $\tau = 0.30$. Inset: ϕ_+ (black, continuous) and ϕ_- (red, dotted)$k = 8$. (Bottom row) Time evolution of the probability densities ϕ_+ (black) and ϕ_- (red) in a two-dimensional lattice with $k = 56$ for (a) $t = 0$, (b) 5 and (c) 10. The dashed line indicates the threshold $\tau = 0.3$.

distribution ϕ_- associates a large probability mass to those agents whose fraction of neighbors ν choosing the opposite action is above τ. This ensures that there is a large enough flow from action -1 to action 1. In conjunction, the former two considerations lead to a situation that allows, first, for some limited nucleation around action 1 to take place, followed by the ensuing spread of this action across the whole system.

Let us now contrast the previous considerations with those arising when k is large – in particular, focus on the case $k = 828$ depicted in Figure 2.7. In this case, the corresponding distribution ϕ_+ is highly concentrated around $\nu = p$, essentially all its probability mass associated to values that lie above $\tau = 0.30$. This means that the induced dynamics must be similar to that resulting from the

mean-field or complete-network setups, with too-fast turnover in action choice preventing the attainment of social learning. Clearly, social learning would also fail to occur for such high value of k if the threshold τ were large. In this case, however, the problem would be that the highly concentrated distributions ϕ_+ and ϕ_- would have most of their probability mass lying below the threshold. This, in turn, would lead to the freezing of the initial conditions, again just as found for the mean-field or complete-network setups.

2.5 Summary

In this chapter we have studied a simple threshold dynamics for social learning, in order to understand the relationship that exist between the quality of the signal and the threshold for action change. Agents recurrently receive an external signal on the relative merits of two actions. But they switch to the action supported to the signal only if they find support for it among their peers - specifically, the fraction of these choosing that action must lie above a certain threshold.

Depending on the quality of the signal and the level of the threshold, social learning of the correct action occurs. This requires that the threshold be neither too low nor too high. For, in the first case, the social dynamics enters into a process of continuous action turnover, while in the second, it freezes at the configuration shaped at the beginning of the process.

Finally, we have also analyzed the model via numerical simulations on different complex networks. We found that limited connectivity due the structure of the network interaction enhances social learning. This occurs because genuinely local interaction favors a process of spatial nucleation and consolidation around the correct action, which can then spread to the whole population.

Chapter 3

Bounded confidence model: Deffuant's model

3.1 Introduction

The study of opinion formation includes a wide class of different models differing in heuristics, formalization as well as in the phenomena of interest. One generally considers a set of agents where each holds an opinion from a certain opinion space. An agent may change her opinion depending on certain dynamical rules. In the physics literature discrete opinion spaces (classically binary opinions)[46, 52, 68, 135] have dominated research due to their analogy with spin systems. In this framework, several models about opinion formation, are based on binary opinions. Social actors update their opinion as a result of social influence, often according to some version of a majority rule. Sometimes these models have been extended to more than two options, which are ordered and thus get closer to continuous opinion dynamics. [136, 137]. One issue of interest concerns the importance of the binary assumption:

what would happen if opinion were a continuous variable such as the worthiness of a choice (a utility in economics), or some belief about the adjustment of a control parameter?

The rationale for binary versus continuous opinions might be related to the kind of information used by agents to validate their own choice. The bounded confidence model of continuous opinion dynamics proposed by Deffuant et al. [10], provides a scenario to answer this question. In this model, the agents can influence each other's opinion when they are already close enough. A tolerance

threshold d is defined, such that agents with difference in opinion larger than the threshold can not interact. Several variants of the model have been proposed in [10, 48, 138]. In these models, the only restriction on the interaction is the threshold condition and interactions among any pair of agents may occur. A related model of bounded confidence is the Hegselmann-Kraus model [48]. In this model, the interaction is not between pair of agents as in Deffuant's model. On the contrary, an agent i, with opinion $x_i \in [0,1]$ interacts with all agents whose opinion lie in the range $[x_i - d, x_i + d]$. All the agents in this interaction range adopt a common opinion. Qualitative results are the same in both models [139].

The model propose by Deffuant et al. considers a population of N agents in an interaction network where the state of agents or node i is given at time t by a real number $C_i^t \in [0,1]$ that respresents the opinion of an individual. The opinion is the individual's position on a given subject. This picture could apply to many different fields such as politics, marketing, religion, etc.

The dynamics is given by the following rules:

We start from a uniform, random initial distribution of the states of the particles. At each time step, a particle i is randomly chosen, then a nearest neighbor j in the network is selected at random:

If their difference in opinion is smaller than the threshold d, their opinion tends to converge. Otherwise, their opinion remains unaltered. Specifically:

1. If $|C_i^t - C_j^t| \leq d$ then

   $C_i^{t+1} = C_i^t + \mu\left[C_j^t - C_i^t\right];$

   $C_j^{t+1} = C_j^t + \mu\left[C_i^t - C_j^t\right];$

2. otherwise, if $|C_i^t - C_j^t| > d$ then

   $C_i^{t+1} = C_i^t;$

   $C_j^{t+1} = C_j^t;$

where μ is the convergence parameter whose value may range from 0 to 1.

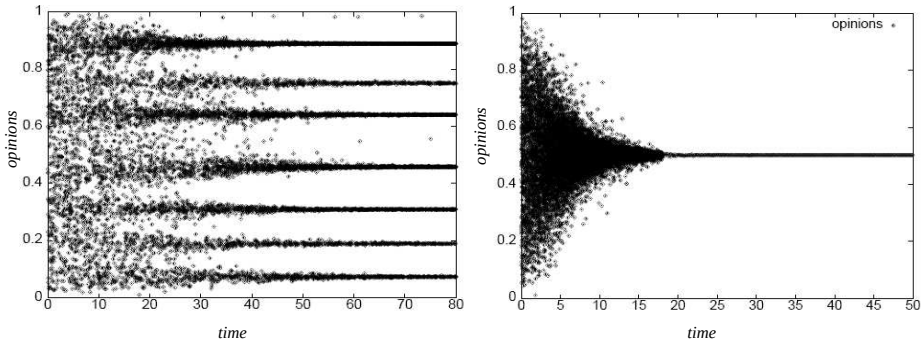

Figure 3.1: Time chart of opinions. Left: $d = 0.07$, $\mu = 0.5$ and $N = 2000$. Right: $d = 0.5$, $\mu = 0.5$ and $N = 2000$. One time unit corresponds to sampling a pair of agents. (From [10])

3.2 Summary of previous results

First we consider a basic model in which the threshold d is taken as constant in time and across the whole population and each individual interacts with the rest of the agents (all to all interactions). For this case, the main result is that, depending on the value d, the process may lead to a consensus among the individuals or to a fragmentation in N_c clusters of opinions. In other words, numerical simulations and different theoretical analysis show that there is a critical threshold d_c, where a nonequilibrium transition occurs between a state of consensus, and a disordered state, where many opinions coexist [10, 140], as shown in figure 3.1. In this Figure the time evolution of the opinions is plotted, starting from uniform distribution opinions for two values of d. The first one is for $d < d_c$ and the second one is for $d > d_c$. For low threshold values, several clusters can be observed (see Fig 3.1-left). Consensus is not achieved when threshold is below a critical values ($d < d_c$). For large threshold values ($d = 0.3 > d_c$) only one cluster is observed for long times at the average initial opinion (see Fig 3.1-right).

In ref [141], D. Nau reports that the evolution of opinions may be mathematically predicted in the limiting case of small values of d. Within this framework, a master equation for the distribution $P(x,t)$, where x are the opinios, i.e. the fraction of agents that have opinions in the range $[x, x + dx]$ can be derived. This

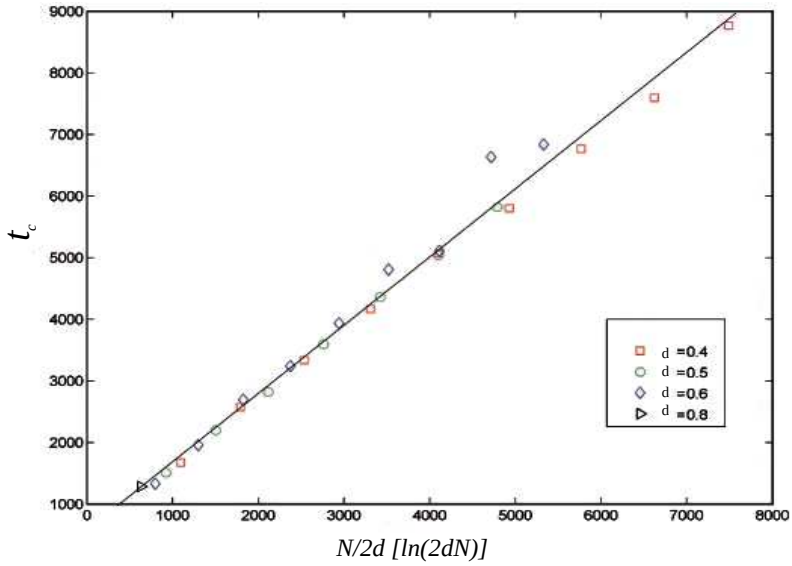

Figure 3.2: The relaxation time t_c as a function $\frac{N}{2d}\ln(2dN)$. Symbols refer to numerical simulations carried out for different values of d, see the legend. As predicted by the proposed theory, a very good linear correlation is observed. The numerical relaxation time is measured by performing the histogram of the opinion distribution at every time step. The convergence is assumed to be reached when all the bins are zero but one. The slope of the continuous curve depends on the chosen binning size.(From [142])

allows to implement a very efficient numerical integration scheme [138]. It has been found that the number of clusters is given by $N_c \approx Integer(\frac{1}{2d})$[10, 138]. This result agrees with the number of clusters observed in Figure 3.1.

Moreover, it has been shown that the parameter μ only influences the relaxation time, i.e., time required for the system to reach the equilibrium, and that the critical value of d is independent of μ [10, 139]. In ref. [142] Carletti et al. provide an analytical estimate of the characteristic relaxation time, hereafter termed t_c, for $\mu = 1/2$ and different values of d:

$$t_c \approx \frac{N}{2d}\frac{\ln(2dN)}{ln(2)}. \tag{3.1}$$

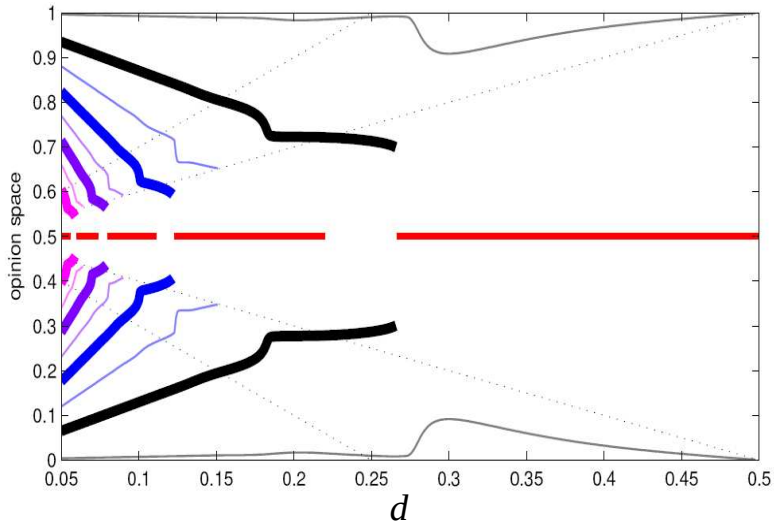

Figure 3.3: Bifurcation diagram for the bounded confidence model (Deffuant's model [10])(From [139])

The functional dependence on N and d is in agreement with the results of numerical simulations, as clearly displayed in figure 3.2.

In ref. [139], Lorenz studied the basic bifurcation diagram (*BD*) * that characterizes the dynamic of the system. This *BD*, shows the location of clusters in the opinion space versus the values of the bound of confidence d. Here, it is easy to determine the attractive cluster patterns for each value of d and observe the transition where a single cluster appears at a critical value of d. Figure 3.3 shows the *BD* with uniform initial density in the opinion space $[0, 1]$ In this figure we observe that for $d > 0.5$ only one big central cluster evolves. As d decreases bifurcations and nucleations of clusters occur: First, the nucleation of two minor extremal clusters, then the bifurcation of the central cluster into two major clusters, and third the rebirth of the central cluster. For details see refs. [143] and [138]. This bifurcation pattern is then repeated in shorter $d-$*intervals*. The length of these intervals seems to scale with $1/d$. This can be better seen in the bifurcation diagram of ref. [138], where numerical analisys indicates that the bifurcation pattern seems to repeat itself on intervals that converge towards a length of about 2.155. This result resembles the rough $1/2d$-rule reported in

*For computational details see ref. [143]

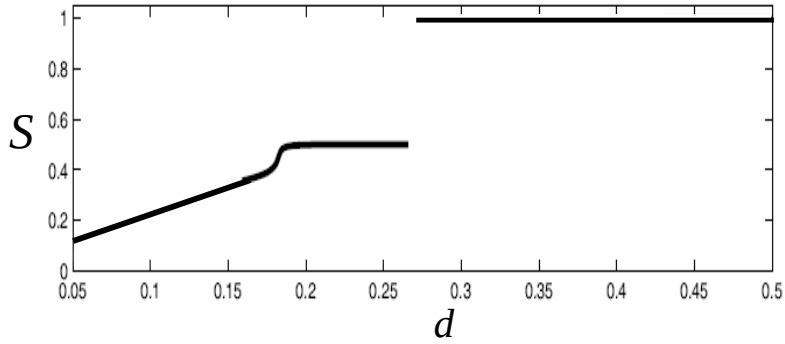

Figure 3.4: S vs. d (From [139])

refs. [10] and [140] from agent-based simulation, which says that the number of major clusters after cluster formation is roughly determined as the integer part of $1/2d$.

In references [10, 138–140, 142, 144] the average size of the largest domain S is introduced as order parameter to characterize the ordering properties of the system. Figure 3.4 shows that for $d > d_c$, $S = 1$ indicating that the system will only get a cluster, while for $d < d_c$ several groups coexist (S decreases). Note that when d decreases, S decreases linearly. This behavior is associated with the multiple bifurcation of the big cluster when d decreases [143].

When heterogeneity of thresholds is introduced (population where each individual has a different thresholds d_i), some new features appear, as reported in ref. [10]. To simplify the analisys, Deffuant et al. consider a population with two values of threshold confidence d_1 and d_2. They studied a set of 192 agents with $d_1 = 0.2$ (closed-minded agents) and eight agents with $d_2 = 0.4$ (open-minded agents). They found that in the short run, the cluster pattern of the closed-minded (two big clusters) dominated while in the long run, one of the open-minded (consensus) takes over. This behavior is generic for heterogeneous thresholds. In this case, the number of clusters also obeys a generalized $N_c \approx 1/2d$ rule: 1) on the long run clustering depends on the higher threshold. 2) on the short run clustering depends on the lower threshold. 3) the transition time between the two dynamics is proportional to the total number of agents and to the ratio of narrow minded to open minded agents. Considering situations of two groups of agents with different confidence level (see ref. [143]) it has been shown that consensus can be achieved by mixing closed- and open-minded agents even if

both bounds of confidence are far below the critical value of the consensus transition (e.g., $d_1 = 0.11$ and $d_2 = 0.22$). But on the other hand drifting of clusters of open-minded towards clusters of closed-minded agents becomes a generic feature of dynamics which can amplify some asymmetric disturbances in the initial profile. So in the end a final consensual cluster may lie very far from the initial average opinion.

The influence of noise has been considered in ref. [145] . Here the free will is introduced in the form of noisy perturbations: individuals are given the opportunity to change their opinion, with a given probability, to a randomly selected opinion inside the whole opinion space. In this paper, the main result is that the noise is able to induce an order-disorder transition. In the disordered state the opinion distribution tends to be uniform, while for the ordered state a set of well defined opinion clusters are formed, although with some opinion spread inside them. The master equation and approximate conditions for the transition between opinion clusters and the disordered state are derived in this work.

Deffuant's model has been studied on different static networks. Ref. [146] considers networks with scale-free distribution a la Barabasi-Albert, random graphs a la Erdos-Reenyi, and square lattices. Evidence is given in [146], that for large enough networks, consensus is always reached for $d > 0.5$, which was later proven in ref. [13, 145, 147] where it is concluded that restricting influence by a netwok topology does not drastically change the behavior of these model as compared to the case of all to all interaction.

In ref. [148] the model was again considered on a Barabasi-Albert graph, finding that the number of final clusters scales with the number of agents and not only with $1/d$. The extremism version of the model proposed in ref. [149] has been considered on small world graphs a la Watts-Strogatz. In this paper, they found that a drift to one extreme only appears beyond a critical level of random rewiring of the regular network.

3.3 Bounded confidence model with external field

In this chapter we study the effects of external influences on social dynamics for opinion formation in the context of Deffuant's model. The main question addressed here is the competition between collective social self-organization versus external mass-media or a propaganda message. In this case, we model mass media as an interaction field applied to the system that originates externally.

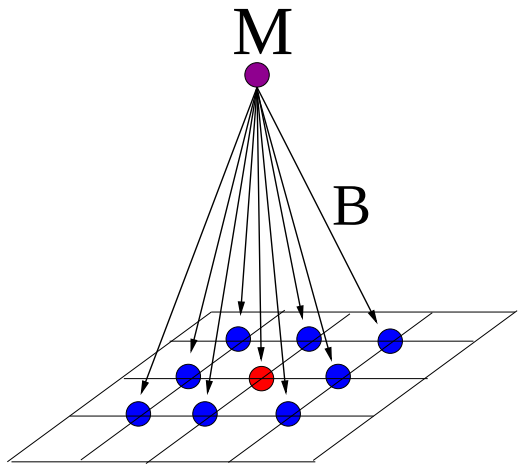

Figure 3.5: Diagram representing the external mass-media influence.

We consider that both, agent-agent interactions and agent-field interactions, depend on the distance between the respective states based on the dynamics of bounded confidence [10]. Collective social self-organization arises from the local interaction among agents, while mass media or the external message constitutes a global interaction.

From the point of view of common wisdom on physical interactions, our results in this model challenge the expected effect of an external: We find collective ordering in a state different from the one imposed by an external forcing field. The external field might break the symmetry in a given direction, but the system orders, breaking the symmetry in a different direction.

A subsidiary question addressed in this section is the dependence of this phenomenon of self-organization in a state different of the one selected by the external field on the topology of the network of interactions. We show that the phenomenon is not found for particles interacting with its nearest neighbors in a regular lattice, but occurs in a globally coupled system, in a small-world network, and in random and scale-free networks: it emerges as long range links in the network are introduced [63].

To study this problem we consider a population of N particles in an interaction network where the state of particle i is given at time t by a real number $C_i^t \in [0, 1]$. We introduce an external field $M \in [0, 1]$ that can interact with any of the particles

in the system. The strength of the field is described by a parameter $B \in [0,1]$ that measures the probability for the particle-field interactions.

We start from a uniform, random initial distribution of the states of the particles. We adopt the dynamical model discussed in 3.1 as follows:

At each time step, a particle i is randomly chosen;

1. with probability B, particle i interacts with the field M: if $|C_i^t - M| < d$, then

$$C_i^{t+1} = \frac{1}{2}(M + C_i^t)\,; \tag{3.2}$$

   if $|C_i^t - M| \geq d$ the state of particle i does not change.

2. otherwise, a nearest neighbor j in the network is selected at random: if $|C_i^t - C_j^t| < d$ then:

$$C_i^{t+1} = C_j^{t+1} = \frac{1}{2}(C_j^t + C_i^t)\,; \tag{3.3}$$

   if $|C_i^t - C_j^t| \geq d$ the state of particle i does not change.

The parameter d defines a threshold distance for interaction, while the strength of the field, represented by the parameter $B \in [0,1]$ measures the relative intensity of the mass media message with respect to the local interactions, or the probability that this message has to attract the attention of the agents in the system. This parameter B represents enhancing factors of the transmitted message that can be varied externally, such as its amplitude, frequency, attractiveness, etc. It is assumed that B is uniform, i.e., the mass media message reaches all the agents with the same intensity as a uniform field as illustrated in Fig. 3.5. At any given time, we assume that any agent can either interact with the mass media message or with other agents in the system. Thus each agent in the network possesses a probability B of interacting with the message and a probability $(1 - B)$ of interacting with its neighbors. In our simulations we fix $M = 1$. The parameter μ defined in 3.1 is fixed as $\mu = \frac{1}{2}$.

3.3.1 Long range interaction networks

First we consider a fully connected network, and then we will extend the analysis for other kinds of interaction networks. As indicated in previous section, in the absence of an external field, $B = 0$, the system spontaneously reaches a homogeneous state $C_i = 0.5$, $\forall i$, for values $d < d_c \approx 0.23$; while for $d > d_c$ several domains are formed [10].

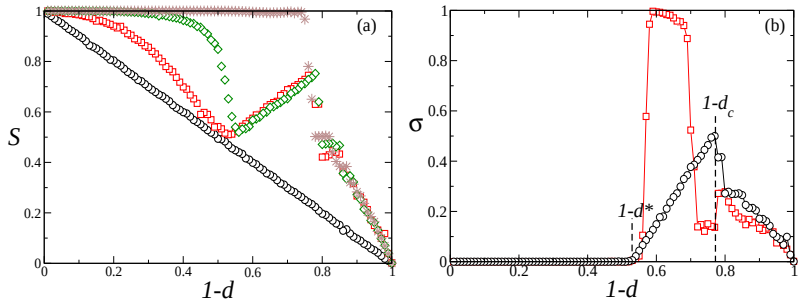

Figure 3.6: (a) S versus $1-d$ in the continuous model on a fully connected network for $B = 0$ (stars); $B = 0.5$ (diamonds); $B = 0.8$ (squares); $B = 1$ (circles). (b) σ versus d for $B = 0.8$ (circles) and $B = 0.1$ (squares). The values of $1 - d_c \simeq 0.77$ and $1 - d^* \simeq 0.5$ (for $B = 0.8$). System size $N = 2500$. Each data point is an average over 100 independent realizations.

To characterize the ordering properties of the system, we consider as order parameters the normalize average size of the largest domain S, and the largest domain displaying the state of the field S_M in the system. A *domain* is deffined as a set of connected agents with the same state.

For $B = 1$ agents only interact with the field. In this case the value of M is imposed on the largest domain whose normalized size increases with the threshold, i.e. $S = S_M = d$. For intermediate values of B, the spontaneous order emerging in the system for values of $1 - d < 1 - d_c$* due to the interactions between the particles competes with the order being induced by the field. The quantity S exhibits a sharp local minimum at a value $1 - d = 1 - d^* < 1 - d_c$, as shown in Fig. 3.6(a). To understand the nature of this minimum, we plot in Fig. 3.6(b) the quantity $\sigma = S - S_M$, as a function of $1 - d$, for different values of B. When the largest domain corresponds to the state of external field, $S = S_M$, then $\sigma = 0$, while when the largest domain no longer corresponds to the state of the external field M, $S > S_M$, and $\sigma > 0$. For $1 - d < 1 - d^*$ the largest domain is dominated by M, that is $S = S_M$, and thus $\sigma = 0$ (see Fig. 3.6b). At $1 - d = 1 - d^*$, the state of the field no longer corresponds to the largest domain, i.e., $S > S_M$, and σ starts to increase as $1 - d$ increases. For a small value of B, the quantity σ reaches a maximum close to one, indicating that the spontaneously formed largest domain almost occupies the entire system, i.e., the field is too weak to compete with the attracting homogeneous state $C_i = 0.5$, $\forall i$. However, when B is increased, the

*We use $1 - d$ as the control parameter to compare the results of this model with the Axelrod's model that we will introduce in the next chapter.

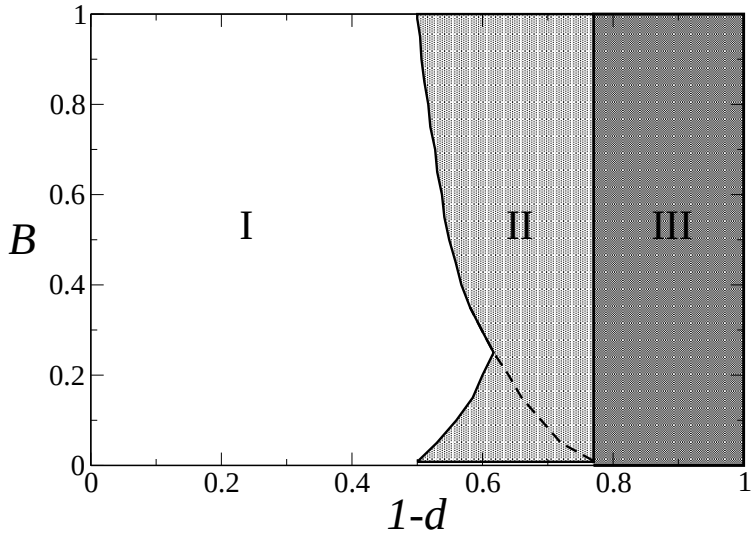

Figure 3.7: Phase space on the plane $(1-d, B)$ on a fully connected network subject to an external field. Regions where the phases I, II, and III occur are indicated. The dashed line in phase II separates two regions: one where the maximum of $\sigma \to 1$ (below this line), and another where $\sigma \leq 0.5$ (above this line).

maximum of σ is about 0.5, i.e., the attraction of the field $M = 1$ increases and the size of the domain with a state equal to M is not negligible in relation to the size of the largest domain.

The value of d^* depends on B and it can be estimated for $B \to 1$. In this case, $S_M \approx d$ and $S \approx 1 - d$; thus the condition $S = S_M$ yields $d^* \approx 0.5$ when $B \to 1$. The quantity σ reaches a maximum at the value $1 - d \approx 1 - d_c$, above which disorder increases in the system, and both S and S_M decrease. As a consequence, σ decreases for $1 - d > 1 - d_c$.

The collective behavior of the model on a fully connected network subject to an external field can be characterize by three phases

- Phase I: an ordered phase with a state of opinion fixed by the external field for $1 - d < 1 - d^*$, for which $\sigma = 0$ and $S = S_M \simeq 1$;

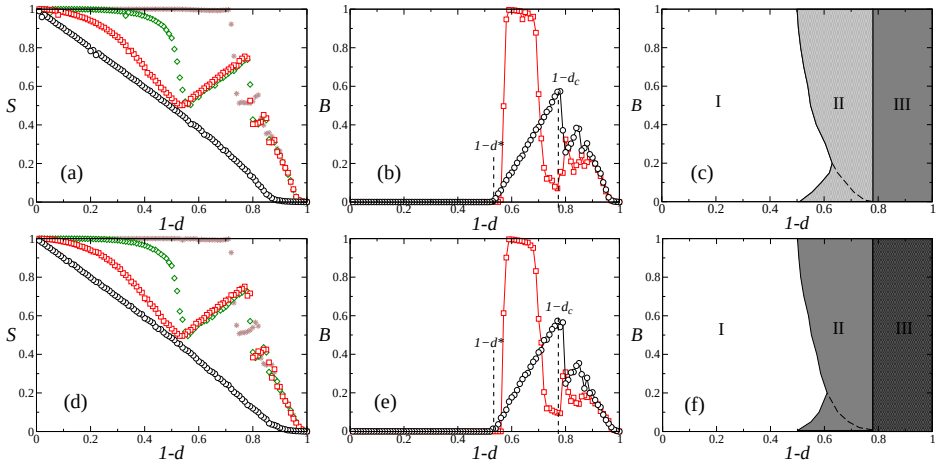

Figure 3.8: ***Top panels:*** Random networks with $\langle k \rangle = 8$, $N = 2500$. (a) S versus $1 - d$ for different values of the parameter B: $B = 0$ (stars); $B = 0.5$ (diamonds); $B = 0.8$ (squares); $B = 1$ (circles). (b) σ versus $1 - d$ for $B = 0.8$ (circles) and $B = 0.1$ (squares). (c) Parameter space on the plane $(1 - d, B)$. ***Bottom panels:*** Scale-free networks with $\langle k \rangle = 8$, $N = 2500$. (d) S versus $1 - d$ for different values of the parameter B: $B = 0$ (stars); $B = 0.5$ (diamonds); $B = 0.8$ (squares); $B = 1$ (circles). (e) σ versus $1 - d$ for $B = 0.8$ (circles) and $B = 0.1$ (squares). (f) Parameter space on the plane $(1 - d, B)$. For all simulations, each data point is an average over 100 independent realizations of the underlying network and the dynamics.

- Phase II: an ordered phase for $1 - q^* < 1 - d < 1 - d_c$, for which σ increases and $S > S_M$. In this phase local interactions dominate and the system reaches a consensus in an opinion different of the one gives the external field.

- Phase III: a disordered phase for $1 - d > 1 - d_c$, for which σ decreases and both S and S_M decrease.

Figure 3.7 shows the phase diagram on the plane $(1 - d, B)$ subject to an external field. The continuous curve separating phases I and II gives the dependence $d^*(B)$.

The emergence of an ordered phase with a state orthogonal to that of an applied field (Phase II) also occurs in complex networks with long range interactions. We have found these three phases on random and scale-free networks [73, 74, 89].

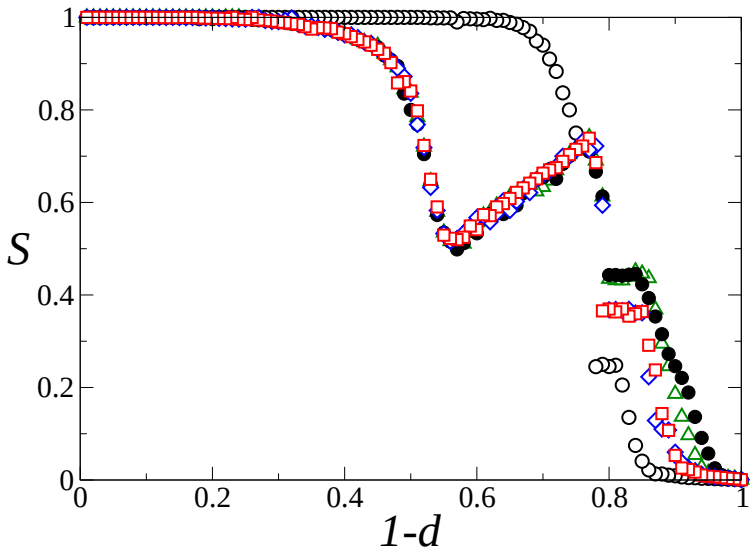

Figure 3.9: S versus $1-d$ on a small world network with $\langle k\rangle = 4$, $N = 10^4$, and $B = 0.5$, for different values of the probability p: $p = 0$ (empty circles), $p = 0.005$ (squares), $p = 0.05$ (diamonds), $p = 0.1$ (triangles), $p = 1$ (solid circles). Each data point is an average over 100 independent realizations of the underlying network and the dynamics.

Figure 3.8 shows the order parameter S as a function of $1-d$ for several values of B. Again, we observe that the quantity S exhibits a local minimum at a value $1-d = 1-d^* < 1-d_c$. The ordered phase with a state orthogonal to that of the field occurs for $1-d^* < 1-d < 1-d_c$, for which $S > S_M$.

3.3.2 Short and long range interactions

To analyze the role of the connectivity on the emergence of an ordered phase different to the one forced by the external field, we consider a small-world network [86], where the rewiring probability can be varied in order to introduce long-range interactions between the particles. We start from a two-dimensional lattice with nearest-neighbor interactions (degree $k = 4$). Each link is rewired at random with probability p. The value $p = 0$ corresponds to a two-dimensional

regular network with nearest neighbors interaction, while $p = 1$ corresponds to a random network with average degree $\langle k \rangle = 4$.

Figure 3.9 shows the order parameter S as a function of $1-d$ with an external field defined on this network for different values of the rewiring probability p and for a fixed value of the intensity of the field B. When the long-range interactions between particles are not present, i.e. $p = 0$, the external field is able to impose its state to the entire system for $d < 1 - d_c$. Spontaneous ordering different from the state of the external field appears as the probability of having long-range interactions increases. The size of this alternative largest domain increases with p, but it does not grow enough to cover the entire system (see inset in Fig. 3.9).

3.4 Conclusions

In this chapter, we have addressed the question of the competition between collective self organization and external forcing in the Deffuant's model with external field. In this systems whose dynamics is based on a bounded interaction, the presence of long-range connections allows the emergence of spontaneous ordering in a state different of the one selected by an external field. Studying this model on fully connected, random and scale-free networks, we have found three phases depending on parameter values: two ordered phases, one having the opinion imposed by the external field, and the other one consisting of a large domain on a opinion different to the one selected by the field; and a disordered phase. We have traced back the existence of a self-organized ordered phase in a state different to the external forcing to the presence of long range connections in the underlying networks considered. This claim is substantiated by considering the model in a small world network: We find that such phase does not exist in a regular network and emerges as long range interactions are included in a small world network.

We will show in section 4.2.3 that the same phenomena occurs in the Axelrod model of dissemination of culture with an external field. These two models share of the existence of non-interacting state in their dynamics Our results suggest that the emergence of an ordered phase with a state different from that of an external field should arise in other nonequilibrium systems provided they allow for non-interacting states. Potential candidates to show this phenomena are biological systems able to display clustering, aggregation and migration, whose dynamics usually possess a bound condition for interaction. This is the case for models including the presence of motile elements (such as swarms, fish schools,

bird flocks, and bacteria colony growth) and non-local interactions in population dynamics.

Chapter 4

Axelrod's model for the dissemination of culture

4.1 Introduction

In seminal paper, Robert Axelrod [150] addressed the question:

" if people tend to become more alike in their beliefs, attitudes, and behavior when they interact, why do not all differences eventually disappear ? "

To investigate this problem, Axelrod introduced an agent-based model to explore mechanisms of competition between the tendency towards globalization and the persistence of cultural diversity. These mechanisms seek to sketch how cultures are disseminated in the society. Culture in this model is defined as a set of individual attributes subject to social influence. Thus, the model assumes that an individual's culture can be described in terms of his or her attributes such as language, religion, technology, style of dress and so on. This definition describes a culture as a list of features or culture dimension. For each feature there is a set of traits, which are the alternative values the feature may have. For example, one feature of culture could be the religious belief, and the traits represent different choices for this feature, such as Buddhism, Atheism or Christianism. It is important to indicate that the emphasis of this work is not on the content of a specific culture, but rather on the way in which a culture is likely to emerge and spread.

Within this framework, the local interaction between neighboring agents follows two basic social principles that are believed to be fundamental in the understanding of the dynamics of cultural assimilation (and diversity): social influence and homophily. The first is the tendency of individuals to be more similar when they interact. The second is the tendency of likes to attract each other, so that they interact more frequently. In other words, these principles mean that the probability that two individuals interact is proportional to the cultural overlap between the agents, that is, to the amount of cultural similarities (number of features) that they share, and the similarity is enhanced when interaction occurs. With these two ingredients Axelrod show that the system can freeze in a multicultural state with coexisting spatial domains with different cultures, illustrating how a simple mechanism of local convergence can lead to global polarization.

The Axelrod model features a set of N agents located at the nodes of an interaction network. The state of an agent i is given by an F-component vector C_i^f ($f = 1, 2, \ldots, F$). In this model, the F components of vector C_i^f correspond to the culture features (language, religion, etc.) describing the F-dimensional culture of agent i. Each component of the cultural vector of i can take any of the q values in the set $\{0, 1, \ldots, q-1\}$ (called cultural traits in Axelrod's model). As an initial condition, each agent i is randomly and independently assigned on of the q^F possible state vectors with uniform probability. In the model, all q^F possible states are equivalent.

Starting from a random initial condintion, the discrete-time dynamics of the system is defined by iterating the following steps:

1. Select at random a pair of sites of the network connected by a bond (i, j).

2. Calculate the overlap (number of shared features) $d(i, j) = \sum_{f=1}^{F} \delta_{C_i^f, C_j^f}$.

3. If $0 < d(i, j) < F$, the bond is said to be active and sites i and j interact with probability $d(i, j)/F$. In case of interaction, choose g randomly such that $C_i^g \neq C_j^g$ and set $C_i^g = C_j^g$.

After N such update events, time is increased by 1.

From the view point of statistical physics, Axelrod's model is a simple and natural *vector* generalization of models of opinion dynamics that gives rise to a very rich and nontrivial phenomenology. In the next section, we will summarize the most important results of this model.

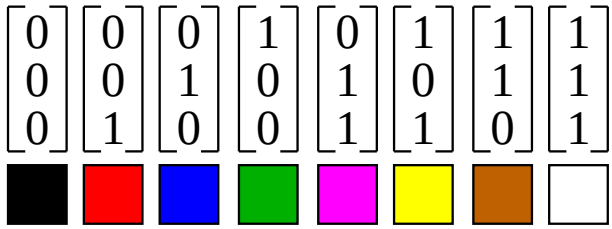

Figure 4.1: Color code for $F = 3$ and $q = 2$.

Summary of previous results

In the last years, systematic studies of Axelrod's model have identified a globalization -polarization transition depending on the value of q for a fixed F [41, 151–153]. These works have shown that the system reaches a stationary configuration in any finite network, where for any pair of neighbors i and j, $d(i,j) = 0$ or $d(i,j) = F$. Homogeneous or ordered states (globalization) correspond to $d(i,j) = F$, $\forall i,j$. This means that all the sites have the same value of cultural trait for each feature. Obviously there are q^F possible configurations of this state. Inhomogeneous or disordered states (global polarization) consists on the coexistence of several domains, where a domain is defined as a set of connected nodes with the same cultural vector state. The number of domains is taken as a measure of cultural diversity.

For the visualization of the state of the system, each cultural state is assigned a color (see figure 4.1). Thus we can identify a cultural domain with a given color. Figure 4.2, shows an example of a typical simulation of Axelrod's model in a two-dimensional network (see reference [154]). For a small value of q ($q = 5$) the system reaches a globalization state (see top right of figure 4.2) where all nodes form a single domain (blue color), indicating that all individuals have the same cultural state, while for $q = 60$, the system freezes in an absorbing multicultural state where different cultural domains coexist, illustrating how the local convergence can induce a global polarization.

In order to characterize the ordering properties of this system, the normalized average size of the largest domain $\langle S_{max}\rangle/N$ formed in the system is defined as order parameter. For any finite network the dynamics displays a critical point q_c that separates two phases: an ordered phase or monocultural state ($\langle S_{max}\rangle/N \simeq 1$) for $q < q_c$, and an disordered phase or multicultural state ($\langle S_{max}\rangle/N \ll 1$) for $q > q_c$ [12, 14, 151–153, 155–157].

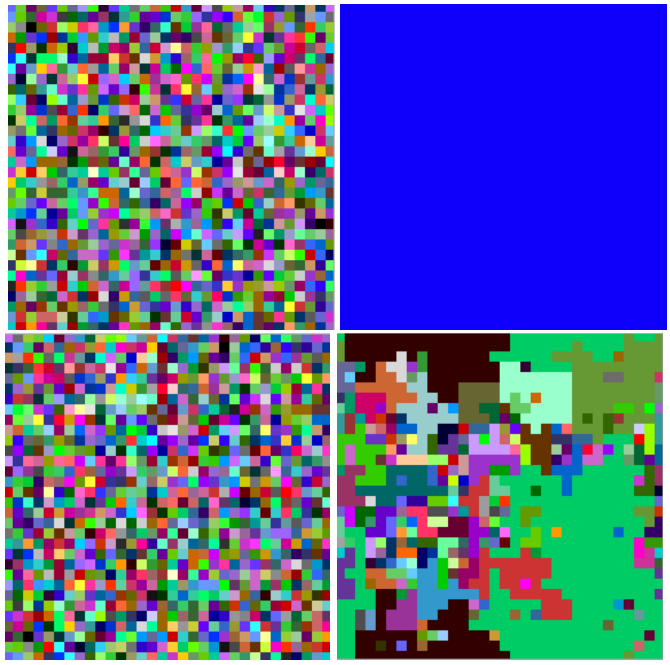

Figure 4.2: State of the system in $t = 0$ (left) and $t = \infty$ (right), $F = 10$, $q = 5$ (top), $F = 10$, $q = 60$ (bottom). System size $N = 1024$ [154].

In a regular two-dimensional lattice, the kind of the transition depends on the value of F [14, 151, 153, 156]. When $F > 2$ the transition is first order, with the size of the largest domain having a finite discontinuity as shown in figure 4.3. Here we identify a threshold $q = q_c \approx 55$ for order-disorder transition. When $q < q_c$ the order parameter $\langle S_{max} \rangle / N \simeq 1$ (see top right of figure 4.2), while for $q > q_c$, $\langle S_{max} \rangle / N \simeq \ll 1$ (see bottom right of figure 4.2). This figure also shows that the transition at the critical point ($q = q_c$) becomes sharper as the system size increases, so that in the thermodynamic limit the transition is well defined (see figure 4.3). However, the situation for $F = 2$ is different. In this case the order parameter $\langle S_{max} \rangle / N$ vanishes continuously as $q \longrightarrow q_c$ (see reference [151]). In one-dimension, the nature of the transition changes, becoming a second order transition for all values of F [153].

Analytical approaches have also been considered for this model. A mean field approach of this model has been discussed by Castellano et al. [151] and F. Vazquez & Redner [155]. This approach consists in writing down rate equations

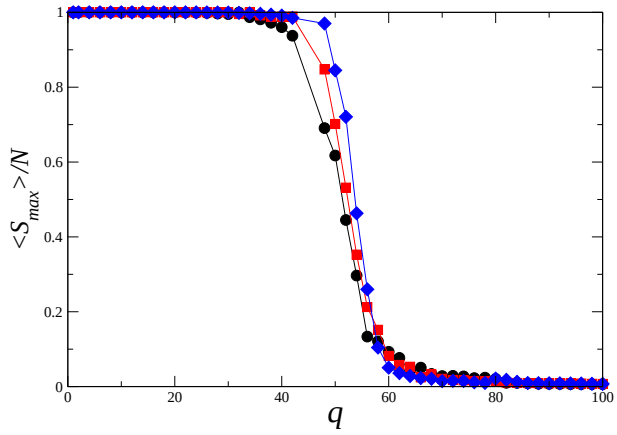

Figure 4.3: Average size of the largest cultural domain $\langle Smax \rangle / N$ vs q for $F = 10$ features and system sizes $N = 900$ (circles), $N = 1600$ (squares) and $N = 2500$ (diamonds). The transition at the critical point $q_c \simeq 55$ becomes sharper as the system size increases.

for the densities P_m of bonds of type m. These are bonds between interaction partners that have m common features. The natural order parameter in this case is the density of active links $n_a = \sum_{m=1}^{F-1} P_m$, where a link is active if $0 \leqslant m \leqslant F-1$. This order parameter is zero in the disordered phase, while it is finite in the ordered phase. This approach gives a discontinuous transition for any F. In the particular case of $F = 2$ the mean field equations was studied analytically in detail by Vazquez and Redner [155], providing insight into the non-monotonic dynamic behavior for $q \lesssim q_c$ and showing that the approach to the steady state is governed by a time scale diverging as $\mid q - q_c \mid^{-1/2}$.

A number of works have addressed the issue of the topology of the networks of interaction. The Axelrod model has been studied on small-world (SW)(Klemm et al., [156]) and scale-free networks Barabasi-Albert (AB)(Klemm et al., [156]) In the first case, the transition between consensus and a disordered multicultural phase is still observed, for values of the control parameter q_c that grow as a function of the rewiring parameter p. Therefore, this work shows that the non-local connectivity favors cultural globalization as described by the ordered state. This is shown in figure 4.4, where the order parameter $\langle S_{max} \rangle / N$ is plotted as function of q for different values of p. Since the SW network for $p = 1$ is a random network, this is consistent with the observation of the transition also in the mean field approach by Castellano et al. 2000 [151] and Vazquez and Redner

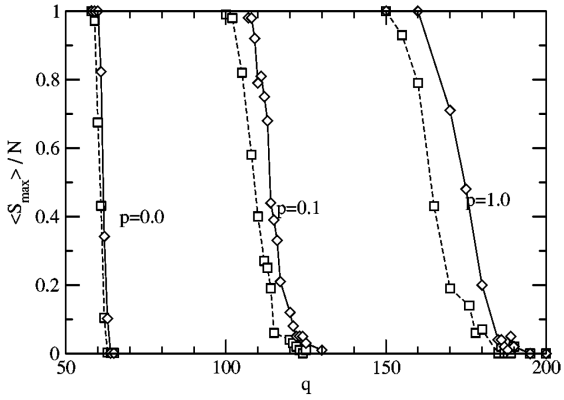

Figure 4.4: Average size of the fraction of the largest cultural domain $\langle Smax \rangle / N$ vs q for three different values of the small-world parameter p. System sizes $N = 500^2$ (squares) and $N = 1000^2$ (diamonds); number of features $F = 10$. From ([156])

2007 [155]. For a scale-free network, the behavior of the system dramatically changes the picture. For a given network size N, the system also displays a transition order-disorder for an effective value of $q = q_c$. However the critical point grows with N as $q_c \sim N^{0.39}$ (see figure 4.5), so that in the thermodynamic limit the transition disappears and only ordered states are possible.

Apart from of the study of the topology of interactions, other extensions of this model have been investigated. Some of them already suggested in Axelrod's paper, such as a the study of cultural drift. In references [152, 158], cultural drift is modeled as spontaneous change in a trait of one of the features of a node. These changes can be interpreted as a type of noise acting on the system. The perturbation consist in randomly choosing $i \in \{1, ..., N\}$, $f \in \{1, ..., F\}$ and $s \in \{1, ..., q\}$ and setting $C_i^f = s$. This rule is implemented by including a fourth step in the iterated loop of Axelrod's model.

4. With probability r, perform a single perturbation.

In these works, it is demostrated that noise (cultural drift) induces an order-disorder transition independently of the value of q, as shown in figure 4.6. In this figure, the effective noise rate $r' = r(1 - 1/q)$, is considered as control parameter. We observe that all curves collapse into a single curve, showing that independently of the values of the parameter q, the system displays the same

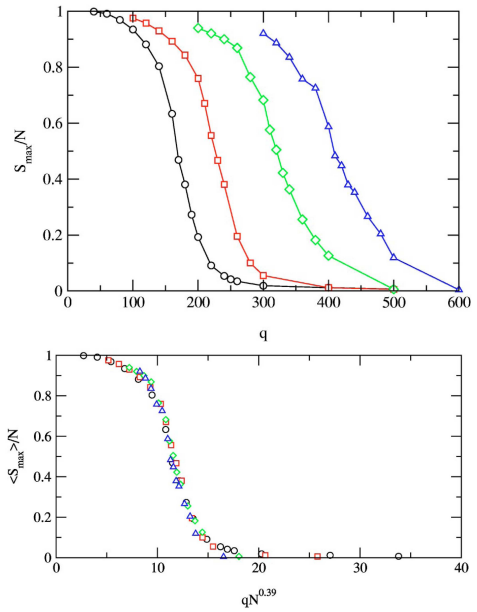

Figure 4.5: *Top*: The average order parameter $\langle S_{max} \rangle / N$ in scale free networks for $F = 10$. Different curves are for different system size: 1000 (circles), 2000 (squares), 5000 (diamonds) and 10,000 (triangles). *Bottom*: Rescales plot of the data shown in top of this figure for different system size. From ([156])

behavior. This curve identifies, for a fixed size of the system, a continuous order-disorder transition controlled by the noise rate r. For small noise rate the state of the system is monocultural. This occurs because disordered configurations are unstable with respect to the perturbation introduced by the noise. However, when the noise rate is large, the disappearance of domains is compensated by the rapid formation of new ones, so that the steady state is disordered. For a finite system, the ordered state of the system under the action of small perturbations, is not a fixed homogeneous configuration. During long time scales, the system visits a series of monocultural configuration. The threshold between the two behaviors is set by the inverse of the average relaxation time for a perturbation $T(N)$, so that the transition occurs for $r_c T(N) = O(1)$. An approximate evaluation of the relaxation time in $d = 2$ gives $T = Nln(N)$, in good agreement with simulations, while $T \sim N^2$ in $d = 1$ [152, 158], Therefore, no matter how small the

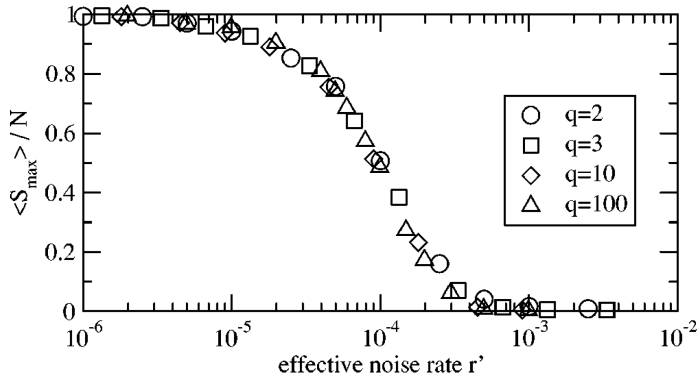

Figure 4.6: $\langle S_{max} \rangle / N$ as function of the effective noise rate $r' = r(1 - 1/q)$ for different values of q. System size $N = 50^2$ with $F = 10$. From [158]

rate of cultural drift is, in the thermodynamic limit the system remains always disordered for any q.

Other extensions of the Axelrod's model include the consideration of quantitative instead of qualitative values for the cultural traits [159], the extension to continuous values of the cultural traits and the inclusion of heterophobic interactions [160], the simulation of technology assimilation [161], and the consideration of specific historical contexts [162].

Within this general context of different forms of social interactions, the influence of mass media on the system has also been considered [12, 14, 15, 129–131]. In these works, mass media are modeled as different types of fields. A mass media cultural message is described as a vector M that can interact with each node in the system. The vector field M may be of different nature. For example, Shibanai et al. [129], study the effect of a global mass media influence, interpreted as a kind of global information feedback acting on the system. In this case, mass media is represented by a global field vector which contains the most predominant trait in each cultural feature present in a society. In this work [129] two mechanisms for the interaction with the global field have been considered. In the first one, the field has the same influential power as a real neighbor. In the second one, the neighbors are influential only when their traits are concordant with the trait of the global vector field to that. In this case the global information feedback acts as filter of local neighbor's influence. The intensity of the fields or the mass media influence is controlled by an additional parameter. The conclusion of this work, somehow counterintuitive, is that global information feedback facilitates

the maintenance of cultural diversity. However, Shibanai et al., restrict the study of global mass media interaction to a single value of q in the ordered phase.

Other recent related works deal with a version Axerlrod's model with both an external field and noise in a two-dimensional network and in social networks with community [130, 131]. Finally, in ref. [163], the authors incorporate into the model the possibility that agents living in a culturally dissimilar neighborhood can move to other place. The rule used here for the mobility of individuals, is based on the Schelling model for residential segregation. In this model, two new parameter are considered, the density of empty site and threshold T, that they called cultural intolerance. In the dynamics of the model, they incorporate the following rule: if the cultural overlap between the pair of agents selected to interact is zero or imitation has not ocurred, the mean overlap $\langle d \rangle$ (cultural overlap between the active agents and its neighborhood) is calculated. If $\langle d \rangle < T$, then the active agent moves to an empty site that is randomly chosen. They found that mobility favors the cultural globalization for small values of empty sites and the order parameter S_{max}/N scales with the system size. That is, the transition to multiculturalism only occurs for finite populations. For large values of empty sites and small values of T, a multicultural fragmented phase appears at low values of q, however, when the values of T are high enough, this regime is followed by a new transition to globalization for increasing values of q. Moreover, in the transition from global consensus to polarization, the size and the number of cultural domains are dynamically fluctuating by the competitive balance of consensus and fragmentation processes associated to the agent's mobility.

Outline

In the following sections of this chapter, we consider within the context of Axlerod's model the two general conceptual questions of the Ph.D thesis, namely the competition between global and local interactions (section 4.2) and coevolution dynamics (section 4.3). In section 4.2 we study Axelrod's model under the influence of different kind of fields. We consider interaction fields that originate either externally (an external forcing) or from the contribution of a set of elements in the system (an autonomous dynamics) such as global or partial coupling functions. Our study allows us to compare the effects that driving fields or autonomous fields of interaction have on the collective properties of systems with this type of nonequilibrium dynamics. In the context of social phenomena, our scheme can be considered as a model for a social system interacting with global or local mass media that represent endogenous cultural influences or information feedback, as well as a model for a social system subject to an external cultural influence. A usual equilibrium idea is that the application of a field

should enhance order in a system. Our results indicate that this is not always the case. On the contrary, disorder builds up by increasing the probability of interaction of the elements with the field. This occurs independently of the nature (either external or autonomous) of the field of interaction added to the system. Here also we show that an ordered state different from the one imposed by the external field is possible, when long-range interaction are considered. Moreover, we find that a spatially nonuniform field of interaction may actually produce less disorder in the system than a uniform field.

In section 4.3, we study the paradigm of co-evolution in Axelrod's model. We develop a model of cultural differentiation that combines the mechanisms of homophily and influence with a third mechanism of network homophily, in which network structure co-evolves with cultural interactions. We show that in certain regions of the parameter space of the system, these co-evolutionary dynamics can lead to patterns of cultural diversity that are stable in the presence of cultural drift is modeled as noise.

4.2 Global vs. local interaction in the Axelrod's model

4.2.1 Axelrod's model with global, local and external field interactions

In this Section we address the general question of the effects of different types of mass media influences on cultural dynamics in the context of Axelrod's model. Here the mass media is modeled as a field interaction applied on the system. This extension was referred to as "public education and broadcasting" [150]. Our aim is to identify the mechanisms, and their efficiency, by which mass media modifies processes of cultural dynamics based on local agent interactions. To answer these questions, we consider mass media influences that originate either externally or endogenously, and that the agent-agent interaction and interaction of the agents with the mass media is based on the same homophily and social influence principles of Axelrod model. For the case of an endogenous mass media interaction, our scheme is a model for social systems interacting with global or local mass media that represents plurality information feedback at different levels.

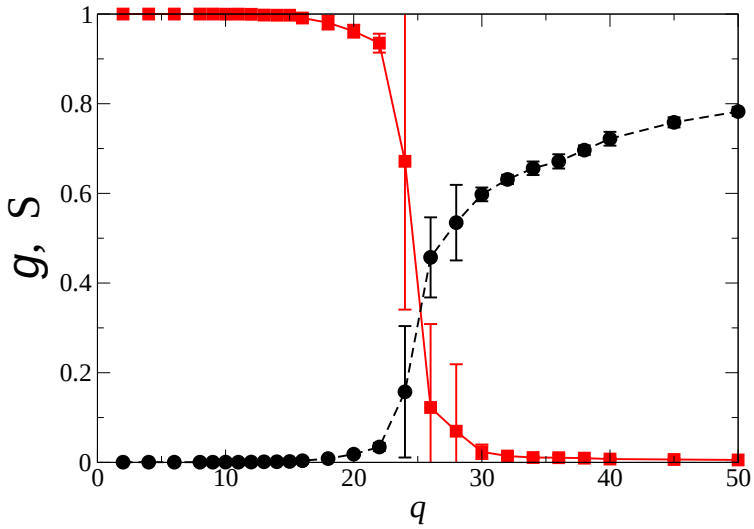

Figure 4.7: Order parameters g (circles) and S (squares) as a function of q, in the absence of a field $B = 0$ and $F = 5$.

The model

The system consists of N elements at the nodes of a square lattice. As discussed in 4.1 the state of an agent i is given by an F-component vector C_i^f ($f = 1, 2, \ldots, F$). In this model, the F components of vector C_i^f correspond to the culture features (language, religion, etc.) describing the F-dimensional culture of agent i. Each component of the cultural vector of i can take any of the q values in the set $\{0, 1, \ldots, q-1\}$ (called cultural traits in Axerlrod's model). As an initial condition, each agent i is randomly and independently assigned one of the q^F possible state vectors with uniform probability. We introduce a vector field M with components $(\mu_{i1}, \mu_{i2}, \ldots, \mu_{iF})$. Formally, we treat the field at each element i as an additional neighbor of i with whom an interaction is possible. The field is represented as an additional element $\phi(i)$ such that $C^f_{\phi(i)} = \mu_{if}$ in the definition given below of the dynamics. The strength of the field is given by a constant parameter $B \in [0, 1]$ that measures the probability of interaction with the field. The system evolves by iterating the following steps:

(1) Select at random an element i on the lattice (called active element).

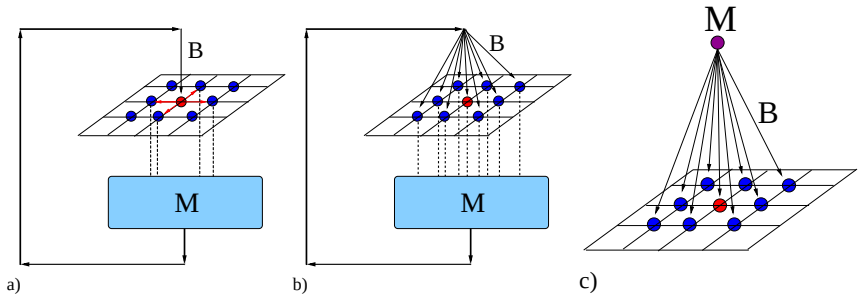

Figure 4.8: Diagrams representing the different types of mass media influences acting on the system. a) Global mass media. b) Local mass media. c) External mass media

(2) Select the source of interaction j. With probability B set $j = \phi(i)$ as an interaction with the field. Otherwise, choose element j at random among the four nearest neighbors (the von Neumann neighborhood) of i on the lattice.

(3) Calculate the overlap (number of shared components) $d(i,j) = \sum_{f=1}^{F} \delta_{C_i^f, C_j^f}$. If $0 < d(i,j) < F$, sites i and j interact with probability $l(i,j)/F$. In case of interaction, choose g randomly such that $C_i^g \neq C_j^g$ and set $C_i^g = C_j^g$.

(4) Update the field M if required (see definitions of fields below). Resume at (1).

Step (3) specifies the basic rule of a nonequilibrium dynamics which is at the basis of most of our results. It has two ingredients: i) A similarity rule for the probability of interaction, and ii) a mechanism of convergence to an homogeneous state.

The number of cultural groups has usually been employed by researchers in the Social Sciences as a measure of multiculturality in a social system [14, 129, 150]. Thus, in order to characterize the ordering properties of this system we will use this concept and we consider as an order parameter the average fraction of cultural domains $g =< N_g > /N$. Here N_g is the number of domains formed in the final state of the system for a given realization of initial conditions. The behavior of the quantity g as an order parameter in the presence of an external field for very large system size is discussed in the Appendix. Figure 4.7 shows the quantity g as a function of the number of options per component q, for $F = 5$, when no field acts on the system ($B = 0$). For values of $q < q_c \approx 25$, the system always reaches a homogeneous state characterized by values $g \to 0$. On the other hand, for values of $q > q_c$, the system settles into a disordered state, for which

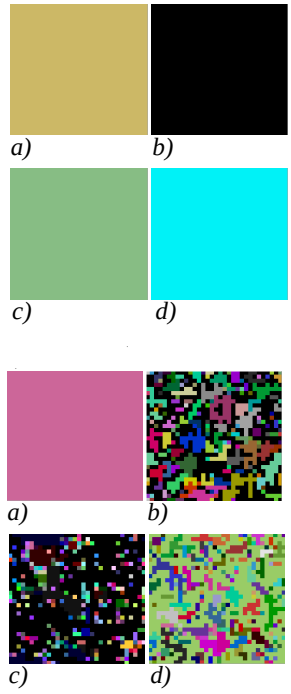

Figure 4.9: Asymptotic configurations of the Axelrod's model with mass media influence, for $F = 5$, $q = 10$, and $N = 32 \times 32$. *Top panel* corresponds the numerical simulation for $B = 0.0045 < B_c$. *Bottom panel* corresponds to the numerical simulation for $B = 0.5 > B_c$. *a*) Absence of field interaction, *b*) External field, *c*) Local field, *d*) Global field. The vector field in the case of external interaction is identified with the black color [154].

$\langle N_g \rangle \gg 1$. Another previously used order parameter, as described in Chapter 2 [151, 156], the average size of the largest domain size, S, is also shown in Fig. 4.7 for comparison. In this case, the ordered phase corresponds to $S = 1$, while complete disorder is given by $S \to 0$. Unless otherwise stated, our numerical results throughout this section are based on averages over 50 realizations for systems of size $N = 40 \times 40$, and $F = 5$.

Let us now consider the case where the elements on the lattice have a non-zero probability to interact with the field ($B > 0$). We distinguish three types of fields.

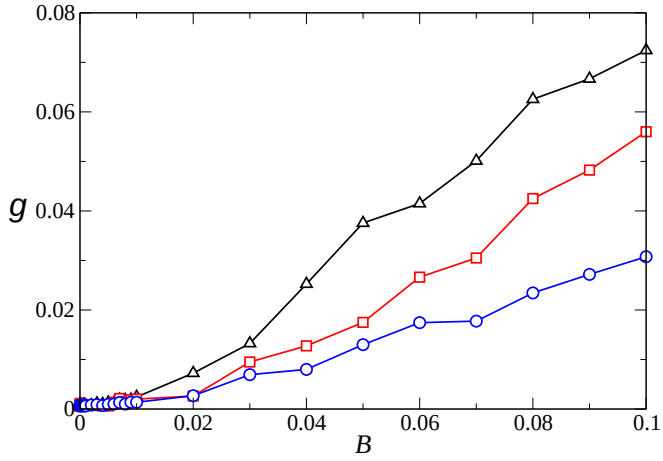

Figure 4.10: Order parameter g as a function of the coupling strength B of an *external* (squares), *global* (circles) and *local* (triangles) *field*. Parameter values $q = 10 < q_c \approx 25$ and $F = 5$.

1. The *external field* is spatially uniform and constant in time. Initially for each component f, a value $\epsilon_f \in \{1, \ldots, q\}$ is drawn at random and $\mu_{if} = \epsilon_f$ is set for all elements i and all components f. It corresponds to a constant, external driving field acting uniformly on the system. A constant *external field* can be interpreted as a specific cultural state (such as advertising or propaganda) being imposed by controlled mass media on all the elements of a social system [14].

2. The *global field* is spatially uniform and may vary in time. Here μ_{if} is assigned the most abundant value exhibited by the f-th component of all the state vectors in the system. If the maximally abundant value is not unique, one of the possibilities is chosen at random with equal probability. This type of field is a global coupling function of all the elements in the system. It provides the same global information feedback to each element at any given time but its components may change as the system evolves. In the context of cultural models [129], this field may represent a global mass media influence shared identically by all the agents and which contains the most predominant trait in each cultural feature present in a society (a "global cultural trend").

3. The *local field*, is spatially non-uniform and non-constant. Each component μ_{if} is assigned the most frequent value present in component f of the

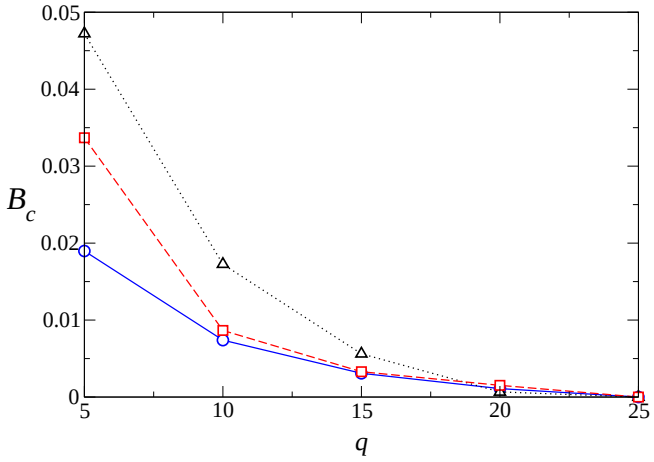

Figure 4.11: Threshold values B_c for $q < q_c \approx 25$ corresponding to the different fields. Each line separates the region of order (above the line) from the region of disorder (below the line) for an *external* (squares), *global* (circles), and *local* (triangles) *field*. Parameter value $F = 5$

state vectors of the elements belonging to the von Neumann neighborhood of element i. If there are two or more maximally abundant values of component f, one of these is chosen at random with equal probability. The *local field* can be interpreted as a local mass media conveying the "local cultural trend" of its neighborhood to each element in a social system.

Case (1) corresponds to a driven spatiotemporal dynamical system. On the other hand, cases (2) and (3) can be regarded as autonomous spatiotemporal dynamical systems. In particular, a system subject to a *global field* corresponds to a network of dynamical elements possessing both local and global interactions. Both the constant *external field* and the *global field* are uniform. The *local field* is spatially non-uniform; it depends on the site i. In the context of cultural models, systems subject to either *local* or *global fields* describe social systems with endogenous cultural influences, while the case of the *external field* represents and external cultural influence.

Cultural influences generated endogenously represent a plurality information feedback, which is one of the functions of mass media [129], but this can occur at a global ("broadcast") or at a local ("narrowcast") level.

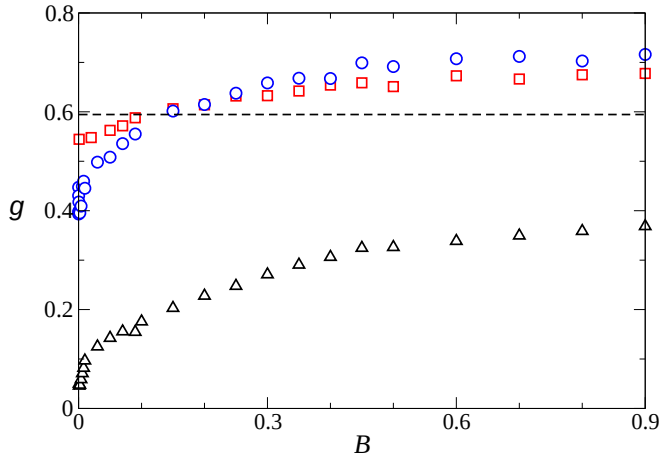

Figure 4.12: Order parameter g as a function of the coupling strength B of an *external* (squares), *global* (circles) and *local* (triangles) *field*. The horizontal dashed line indicates the value of g at $B = 0$. Parameter values, $F = 5$, $q = 30 > q_c \approx 25$.

The strength of the coupling to the interaction field is controlled by the parameter B. We assume that B is uniform, i.e., the field reaches all the elements with the same probability. The parameter B can be interpreted as the probability that the mass media vector has to attract the attention of the agents in the social system. The parameter B represents enhancing factors of the mass media influence that can be varied, such as its amplitude, frequency, attractiveness, etc. The different types of field or mass media influences are schematically shown in Fig. 4.8.

Simulations of the model described here for different values of parameters, can be accessed on-line (http://ifisc.uib-csic.es/research/APPLET_Axelrod/Culture.html) trough a Java Applet [154].

Effects of an interacting field for $q < q_c$

In the absence of any interaction field, the system settles into one of the possible q^F homogeneous states for $q < q_c$ (see Fig. 4.7). However, when the interaction with a field is added, the behavior is affected as shown in the numerical simulation of figure 4.9. This figure shows the asymptotic configurations of the system for the different fields and two values of B in the ordered phase ($q < q_c$). For the case $B = 0.0045$ the system reaches a homogeneous state, while for $B = 0.5$,

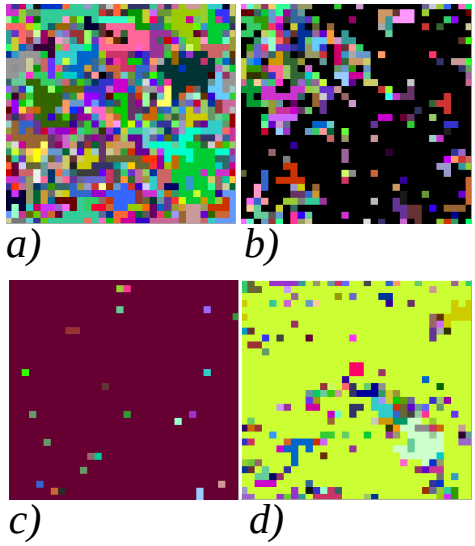

Figure 4.13: Asymptotic configurations of the Axelrod's model with mass media influence, for $F = 5$, $q = 30$ ($q_c \approx 25$), $N = 32 \times 32$ and $B = 0.0045$. *a*) Absence of field interaction, *b*) External field, *c*) Local field, *d*) Global field. The vector field in the case of external interaction is identify with the black color [154].

independently of the nature of the field, the system displays a disordered state. This results suggest that there is a threshold value of B for which the mass media induces disorder.

In a systematic study of this behavior, figure 4.10 shows the order parameter g as a function of the coupling strength B for the three types of fields. When the probability B is small enough, the system still reaches in its evolution a homogeneous state ($g \to 0$) under the action of any of these fields. In the case of an *external field*, the homogeneous state reached by the system is equal to the field vector [14]. Thus, for small values of B, a constant *external field* imposes its state over all the elements in the system, as one may expect. With a *global* or with a *local field*, however, for small B the system can reach any of the possible q^F homogeneous states, depending on the initial conditions. Regardless of the type of field, there is a transition at a threshold value of the probability B_c from a homogeneous state to a disordered state characterized by an increasing number of domains as B is increased. Thus, we find the counterintuitive result that, above

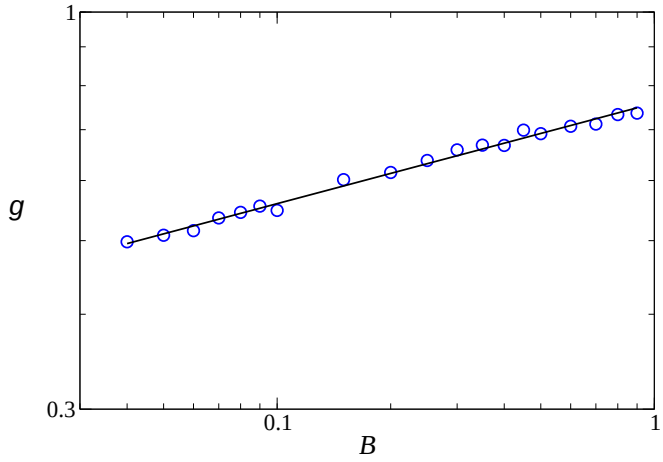

Figure 4.14: Scaling of the order parameter g with the coupling strength to the *global field* B. The slope of the fitting straight line is $\beta = 0.13 \pm 0.01$. Parameter values $q = 28 > q_c$ and $F = 5$.

some threshold value of the probability of interaction, a field induces disorder in a situation in which the system would order (homogeneous state) under the effect alone of local interactions among the elements. The same behavior is reported by Shebanai et al. for the case of a global field [129].

The threshold values of the probability B_c for each type of field, obtained by a regression fitting [14], are plotted as a function of q in the phase diagram of Fig. 4.11. The threshold value B_c for each field decreases with increasing q for $q < q_c$. The value $B_c = 0$ for the three fields is reached at $q = q_c \approx 25$, corresponding to the critical value in absence of interaction fields observed in Fig. 4.7. For each case, the threshold curve B_c versus q in Fig. 4.11 separates the region of disorder from the region where homogeneous states occur in the space of parameters (B, q). For $B > B_c$, the interaction with the field dominates over the local interactions among the individual elements in the system. Consequently, elements whose states exhibit a greater overlap with the state of the field have more probability to converge to that state. This process contributes to the differentiation of states between neighboring elements and to the formation of multiple domains in the system for large enough values of the probability B.

Note that the region of homogeneous ordered states in the (B, q) space in Fig. 4.11 is larger for the *local field* than for the *external* and the *global fields*. A nonuniform field provides different influences on the agents, while the interaction with uni-

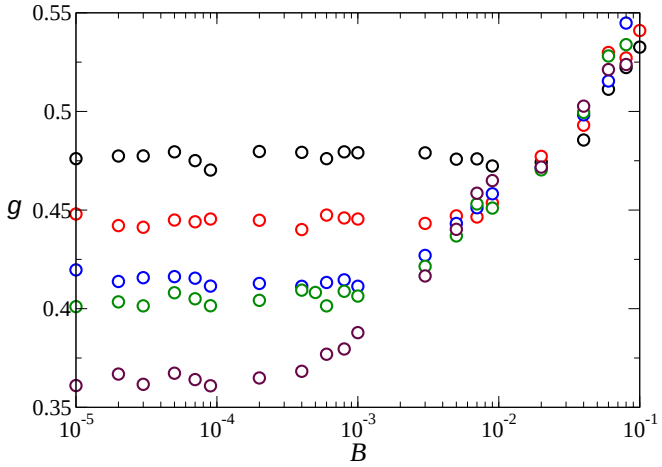

Figure 4.15: Finite size effects at small values of the strength B of a *global field*. Order parameter g as a function of B is shown for system sizes $N = 20^2$, 30^2, 40^2, 50^2, 70^2 (from top to bottom). Parameter values $q = 30$ and $F = 5$.

form fields is shared by all the elements in the system. The *local field* (spatially nonuniform) is less efficient than uniform fields in promoting the formation of multiple domains, and therefore order is maintained for a larger range of values of B when interacting with a *local field*.

Effects of an interacting field for $q > q_c$

When there are no additional interacting fields ($B = 0$), the system always freezes into disordered states for $q > q_c$ (see Fig. 4.7). Figure 4.12 shows the order parameter g as a function of the probability B for the three types of fields. The effect of a field for $q > q_c$ depends on the magnitude of B. In the three cases we see that for $B \to 0$, g drops to values below the reference line corresponding to its value when $B = 0$. Thus, the limit $B \to 0$ does not recover the behavior of the model with only local nearest-neighbor interactions. The fact that for $B \to 0$ the interaction with a field increases the degree of order in the system is related to the non-stable nature of the inhomogeneous states in Axelrod's model. When the probability of interaction B is very small, the action of a field can be seen as a sufficient perturbation that allows the system to escape from the inhomogeneous states with frozen dynamics. A example of this behavior is observed in figure 4.13, that shows the spatial configurations of the final states

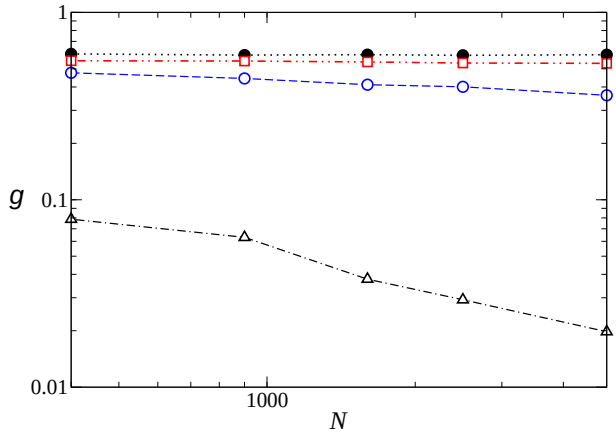

Figure 4.16: Mean value of the order parameter g as a function of the system size N without field ($B = 0$, solid circles), and with an *external* (squares), *global* (circles) and *local field* (triangles). Parameter value $q = 30$.

of the systems under the influence of a field in the disordered state ($q > q_c$). In the numerical simulation, we observe that a weak interaction with the field can induce order in the system. This effect is similar independently of the source of the field. However, the local field is more efficient to order the system, while the external field interaction is less efficient to induce order in the system. The role of a field in this situation is similar to that of noise applied to the system, in the limit of vanishingly small noise rate [158].

The drop in the value of g as $B \to 0$ from the reference value ($B = 0$) that takes place for the *local field* in Fig. 4.12 is more pronounced than the corresponding drops for uniform fields. This can be understood in terms of a greater efficiency of a nonuniform field as a perturbation that allows the system to escape from a frozen inhomogeneous configuration. Increasing the value of B results, in all three types of fields, in an enhancement of the degree of disorder in the system, but the *local field* always keeps the amount of disorder, as measured by g, below the value obtained for $B = 0$. Thus a *local field* has a greater ordering effect than both the global and the *external field*s for $q > q_c$.

The behavior of the order parameter g for larger values of B can be described by the scaling relation $g \sim B^{\beta}$, where the exponent β depends on the value of q. Figure 4.14 shows a log-log plot of g as a function of B, for the case of a *global field*, verifying this relation. This result suggests that g should drop to zero as $B \to 0$.

The partial drops observed in Fig. 4.12 seem to be due to finite size effects for $B \to 0$. A detailed investigation of such finite size effects is reported in Fig. 4.15 for the case of the *global field*. It is seen that, for very small values of B, the values of g decrease as the system size N increases. However, for values of $B \gtrsim 10^{-2}$, the variation of the size of the system does not affect g significantly.

Figure 4.16 displays the dependence of g on the size of the system N when $B \to 0$ for the three interaction fields being considered. For each size N, a value of g associated with each field was calculated by averaging over the plateau values shown in Fig. 4.15 in the interval $B \in [10^{-5}, 10^{-3}]$. The mean values of g obtained when $B = 0$ are also shown for reference. The order parameter g decreases for the three fields as the size of the system increases; in the limit $N \to \infty$ the values of g tend to zero and the system becomes homogeneous in the three cases. For small values of B, the system subject to the *local field* exhibits the greatest sensitivity to an increase of the system size, while the effect of the constant *external field* is less dependent on system size. The ordering effect of the interaction with a field as $B \to 0$ becomes more evident for a local (nonuniform) field. But, in any case, the system is driven to full order for $B \to 0$ in the limit of infinite size by any of the interacting fields considered here.

4.2.2 Global field and the filtering of local interactions

In this section we analyze a model of global information feedback where the global mass media acts as a moderator or filter of the local influence of neighbors, as proposed by Shibanai et al. [129]. In the original Axelrod's model one feature with different traits for two neighboring agents is chosen, and the trait of the active agent adopts the trait of the neighbor. This is modified in the model of indirect global mass media influence analyzed here, taking into account the agreement of the chosen trait of the neighbor and that of the global mass media or *the plurality* of the population. If the trait of the neighbor is concordant with the dominant one, that is, the same as that of the global mass media message M, the feature of the active agent will be changed to that of the neighbor. But if the feature of the neighbor is different from that of the global mass media message M, then, with probability R the active agent will not change. Thus, this model assumes that agents are more likely to adopt a trait from those neighbors that are concordant with the plurality. The conclusion in reference [129] is that the mass media, contrary to lay beliefs of their strong uniforming power, would rather contribute to creating differences in the long run. This conclusion is based on the analysis for a single value of parameter q and few values of the intensity of the influence of mass media. In this section we consider the full range of values of q when addressing the general question of the effects of different forms of

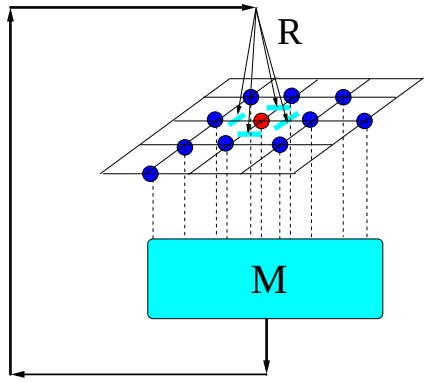

Figure 4.17: Diagram representing the filter model.

mass media effect on cultural dynamics in the Axelrod's model, finding different behaviours for $q < q_c$ and $q > q_c$.

We use the definition of a uniform global mass media as in Section 4.2.1.1, $M = (\mu_{i1}, \mu_{i2}, \ldots, \mu_{iF})$. The dynamical evolution of the filter model can be described in terms of the following iterative steps:

1. Select at random an agent i on the lattice (active agent).
2. Select at random one agent j among the four neighbors of i.
3. Calculate the overlap $d(i, j)$. If $0 < d(i, j) < F$, sites i and j interact with probability $p_{ij} = d(i, j)/F$. In case of interaction, choose g randomly such that $C_{i]g} \neq C_j^g$. If $C_j^g = \mu_g$, then set $C_i^g = C_j^g$; otherwise with probability R the state of agent i does not change and with probability $1 - R$ set $C_i^g = C_j^g$
4. (3) Calculate the overlap $d(i, j)$. If $0 < d(i, j) < F$, sites i and j interact with probability $p_{ij} = d(i, j)/F$. In case of interaction, choose g randomly such that $C_i^g \neq C_j^g$. If $C_j^g = \mu_g$, then set $C_i^g = C_j^g$; otherwise with probability R the state of agent i does not change and with probability $1 - R$ set $C_i^g = C_j^g$
5. Update the global mass media vector M if required. Resume at (1).

Figure 4.17 shows a diagram of the filter model. The parameter R describes the intensity of the filtering effect of the global mass media on the local interactions.

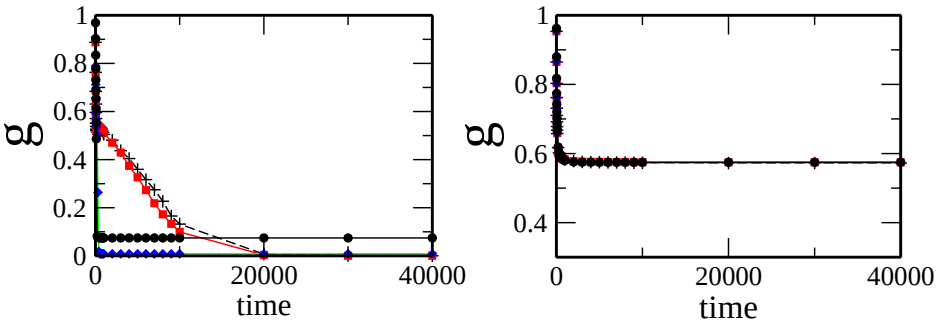

Figure 4.18: Time evolution of the average fraction of cultural domains g in the filter model for different values of the probability R, with fixed $F = 5$. Time is measured in number of events per site. System size $N = 50 \times 50$. Left: $q = 10$; $R = 0$ (crosses); $R = 0.0005$ (squares); $R = 0.15$ (diamonds); $R = 0.6$ (circles). Right: $q = 30$; $R = 0$ (crosses); $R = 0.0005$ (squares); $R = 0.005$ (circles); $R = 0.1$ (diamonds).

The case $R = 0$ corresponds to the original Axelrod's model, while $R = 1$ implies that cultural interaction only causes a change if the chosen trait of the neighbor was equal to that of the global mass media. The overall probability of interaction between an active agent i and a chosen neighbor j is $p_{ij}(1 - R)$ if the chosen trait of j is different from that corresponding to M, and p_{ij} if the chosen trait is equal to that corresponding to M.

Figure 4.18 shows the average fraction of cultural domains g (order parameter defined in section 4.2.1.1) as a function of time in the global mass media filter model, for two values of q with $F = 5$, and for different values of the filtering probability R. In Fig. 4.18 (left), when $q < q_c$ the system reaches a homogeneous state for $R = 0$ and also for small values of R. However, when the probability R increases, the filtering influence of the global mass media can induce cultural diversity. Our results for $q < q_c$ support the results obtained by Shibanai et al. [129] about the ability of the filtering process to induce cultural diversity in the same fashion as the model with direct global mass media influence. Comparison with Fig. 4.19, where we plot the average fraction of cultural domains g as a function of time under the direct action of global mass media, for $q < q_c$ with $F = 5$, and for different values of the probability B, shows that direct interaction with global mass media is more efficient in promoting cultural diversity than the filtering mechanism of agreement with the global plurality.

The analysis of reference [129] was restricted to a single value of $q < q_c$. We have also explored values of $q > q_c$, where the system would be in a heterogeneous cultural state in absence of any filtering ($R = 0$). For these values of q we find (Fig. 4.18, right) that the filtering mechanism has no appreciable effects for small R, in contrast with the case of direct global mass media influence where for small values of the probability B of interaction with the media message, the number of cultural groups is reduced as a consequence of this interaction.

A systematic analysis of the filtering effect for different values of q is summarized in Figure 4.20 which shows the asymptotic value for long times of the average fraction of cultural domains g as a function of q, with $F = 5$, for different values of the filtering probability R. When no filtering acts on the system ($R = 0$) the behavior is that of the original Axelrod's model and also coincides with the direct mass media models for $B = 0$.

The effects of the filtering process in the culturally homogeneous region, i.e., for parameter values $q < q_c$, is similar to that of a direct influence of endogenous mass media. When the probability R is increased, the threshold value of q decreases. There is a value $q_c(R)$ below which the system still reaches a homogeneous cultural state under the influence of the filter. An increase in R for parameters $q < q_c(R)$ leads to cultural diversity. Thus, both mechanisms of feedback information, either direct or indirect, promote multiculturality in the region of parameters where globalization prevails in the absence of any feedback. The similar behavior found for all types of mass media influences considered here suggests that the phenomenon of mass media-induced diversity should be robust in this region of parameters, regardless of the type of feedback mechanism at work.

However, in the region of parameters $q > q_c$ where multiculturality occurs for $R = 0$ or $B = 0$, the behavior of the filter model differs from those of the direct mass media influence. The filtering mechanism has little effect for values of the probability $R < 1$. As $R \to 1$ there is a small decrease in the number of cultural groups formed in the system. But at $R = 1$ a discontinuity appears: the fraction of cultural groups g jumps from a value close to the one for $R = 0$ to a value close to $g = 1$ corresponding to maximum multiculturality (number of cultural groups equal to the number of agents in the system). The case $R = 1$ corresponds to an extreme restriction on the dynamics, when no adoption of cultural features from neighbors is allowed unless the state of the neighbor coincides with the one of the global mass media. Since we are considering random initial conditions, when q is large enough, the probability that the features of any agent coincide with those of the global mass media message M is quite small, making the convergence to globalization, i.e., a common state with the media, very unlikely. As a consequence, the random multicultural state subsists in the system and manifests itself as a maximum value of g. The small probability of interaction

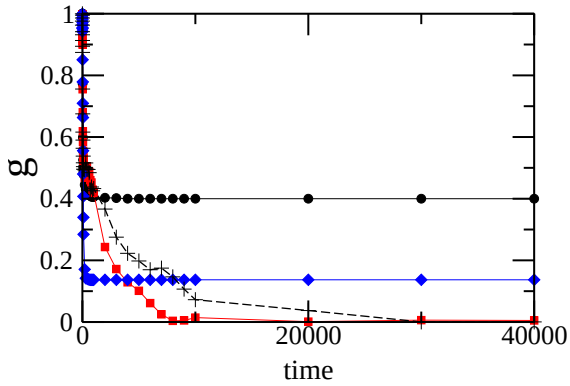

Figure 4.19: Evolution of g in a system subject to a global mass media message for different values of the probability B, with fixed $F = 5$. Time is measured in number of events per site. System size $N = 50 \times 50$, $q = 10$; $B = 0$ (crosses); $B = 0.0005$ (squares); $B = 0.15$ (diamonds); $B = 0.6$ (circles).

with the global mass media for large values of q when $R = 1$ is also reflected in the very long convergence time needed to reach the final multicultural state as compared with the convergence time for $R < 1$.

4.2.3 Spontaneous ordering against an external field

In this Section, we address the same general question considered in section 3.3 but now within the context of Axelrod's model. Namely, we consider the possibility that the system orders in an state different from the one selected by an external forcing field . Similarly, as we found in the Deffuant model with external field interaction, the system also displays three phases: two ordered phases, one in the state imposed by the external field and other in a state different to the one selected by the field, and one disordered phase. We show that also here this ordered phase in a state different from the one imposed by the external field is possible when long-range interactions exist.

The model that we use in this section, is the same studied in Section 4.2.1.1, for the case of external field interaction, but here, we have considered the system on a fully connected network and complex networks.

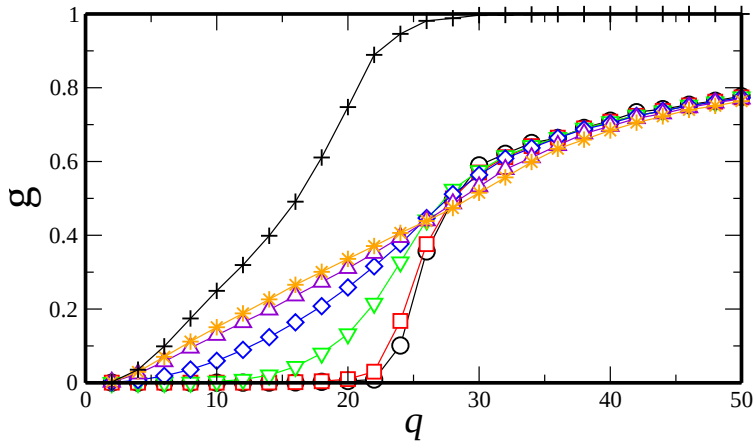

Figure 4.20: Average fraction of cultural domains g as a function of q, for different values of the probability R for the filter model. $R = 0$ (circles); $R = 0.01$ (squares); $R = 0.1$ (triangles down); $R = 0.5$ (diamonds); $R = 0.9$ (triangles up); $R = 0.99$ (stars); $R = 1.0$ (plus signs). Parameter value $F = 5$.

Long range interaction networks

To characterize the ordering properties of this system, we consider as order parameter the normalized average of the largest domain S disscussed in section 4.1.

First, we analyze the model in a fully connected network. In the absence of an external field, i.e. $B = 0$, the system spontaneously reaches an ordered phase for values $q < q_c$ (Fig. 4.21(a)). For $B \to 0$ and $q < q_c$, the external field M^f imposes its state in the system, as in Section 4.2 [14]. For $B = 1$, the particles only interact with the external field; in this case only those particles that initially share at least one component of their vector state with the components of M^f will converge to the field state M^f. The probability that a particle has feature f different from the external field is $(q-1)/q$; thus, the probability that all F features are different from the field is $(1-1/q)^F$. The fraction of particles that converge to M^f is the fraction of particles that initially share at least one feature with the external field

$$S_M(B=1) = 1 - (1-1/q)^F \,. \tag{4.1}$$

Figure 4.21(a) shows both the numerically calculated values of S as well as the analytical curve given by Eq. (4.1)for different values of q. Both quantities agree

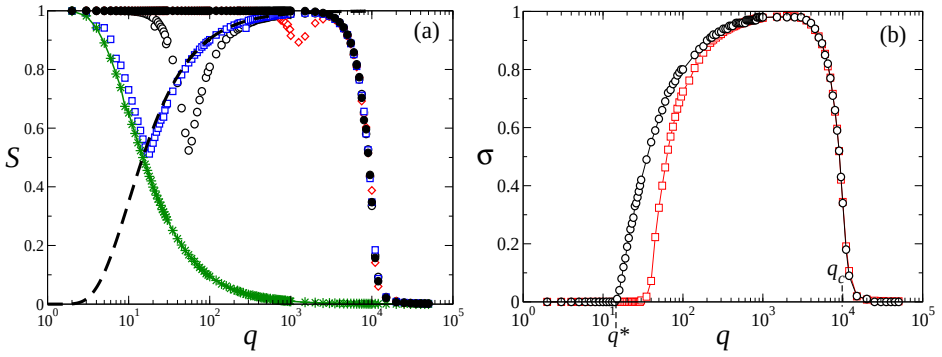

Figure 4.21: (a) S vs q on a fully connected network for $B = 0$ (solid circles); $B = 0.005$ (diamonds); $B = 0.05$ (empty circles); $B = 0.5$ (squares); $B = 1$ (stars). The continuous line is the analytical curve $1 - (1 - 1/q)^F$, while the dashed line corresponds to the curve $(1 - 1/q)^F$. (b) $\sigma = S - S_M$ versus q for $B = 0.8$ (circles) and $B = 0.1$ (squares). The values of $q_c \simeq 10^4$ and $q^* \simeq 14$ (for $B = 0.8$). Parameter values are $N = 2500$, $F = 10$. Each data point is an average over 100 independent realizations.

very well, indicating that the largest domain in the system has a vector state equal to that of the external field when $B = 1$.

For intermediate values of B, the spontaneous order emerging in the system for parameter values $q < q_c$ due to the particle-particle interactions competes with the order being imposed by the field. This competition is manifested in the behavior of the order parameter S which displays a sharp local minimum at a value $q^*(B) < q_c$ that depends on B, while the value of q_c is found to be independent of the intensity B, as shown in Fig. 4.21(a). To understand the nature of this minimum, we plot in Fig. 4.21(b) the quantity $\sigma = S - S_M$, as a function of q. For $q < q^*(B)$ the largest domain corresponds to the state of the external field, $S = S_M$, and thus $\sigma = 0$. For $q > q^*(B)$, the largest domain no longer corresponds to the state of the external field M^f but to other state non-interacting with the external field, i.e., $S > S_M$, and $\sigma > 0$. The value of $q^*(B)$ can be estimated for the limiting case $B \to 1$, for which $S_M \approx 1 - (1 - 1/q)^F$ and the largest domain different from the field is $S \approx 1 - S_M$. Therefore the condition $S = S_M$ yields

$$q^*(B \to 1) = \left[1 - (1/2)^{1/F}\right]^{-1} . \tag{4.2}$$

For $F = 10$ it gives $q^*(B \to 1) = 15$ in good agreement with the numerical results. The order parameter σ reaches a maximum at some value of q between q^* and q_c.

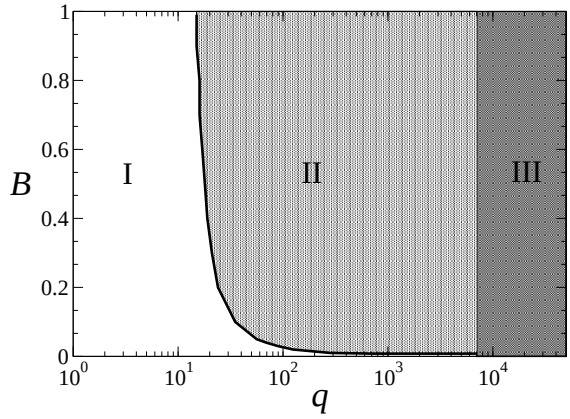

Figure 4.22: Phase space on the plane (q, B) on a fully connected network subject to an external field, with fixed $F = 10$. Regions where the phases I, II, and III occur are indicated.

For larger values of q the order decreases in the system and both $S \to 0$, $S_M \to 0$. As a consequence, σ starts to decrease.

The collective behavior on a fully connected network subject to an external field can be characterized by three phases on the space of parameters (q, B), as shown in Fig. 4.22:

- Phase I: an ordered phase induced by the field for $q < q^*$, for which $\sigma = 0$ and $S = S_M \sim 1$.
- Phase II: an ordered phase in a state *orthogonal* to the field (that is, the overlap between the ordered state and the external field is zero) for $q* < q < q_c$, for which σ increases and $S > S_M$, with $S \sim 1$;
- Phase III: a disordered phase for $q > q_c$, for which σ decreases and $S \to 0$, $S_M \to 0$.

For parameter values $q < q_c$ for which the system orders due to the interactions among the particles, a sufficiently weak external field is always able to impose its state to the entire system (phase I). However, for intermediate values of $q < q_c$ if the probability B of interaction with the field exceeds a critical value, the system spontaneously orders in a state orthogonal to the field (phase II).

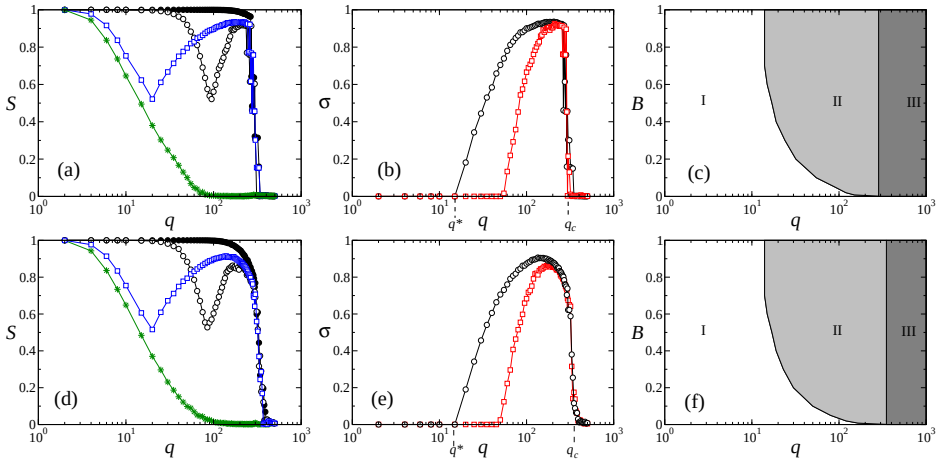

Figure 4.23: ***Top Panels:*** Vector model on random networks with $\langle k \rangle = 8$, $N = 5000$, $F = 10$. For these values, $q_c = 285$. (a) S versus q for different values of the parameter B: $B = 0$ (solid circles), $B = 0.05$ (empty circles), $B = 0.5$ (squares), $B = 1$ (stars). (b) σ versus q for $B = 0.8$ (circles) and $B = 0.1$ (squares). (c) Parameter space on the plane (q, B). ***Bottom Panels:*** Vector model on scale-free networks with $\langle k \rangle = 8$, $N = 5000$, $F = 10$. For these values, $q_c = 350$. (d) S versus q for different values of the parameter B: $B = 0$ (solid circles), $B = 0.05$ (empty circles), $B = 0.5$ (squares), $B = 1$ (stars). (e) σ versus q for $B = 0.8$ (circles) and $B = 0.1$ (squares). (f) Parameter space on the plane (q, B). For all simulations, each data point is an average over 100 independent realizations of the underlying network and the dynamics.

Like in the Deffuat's model under the influence of an external field studied in the previous chapter, this model also shows the emergence of an ordered phase with a state orthogonal to the external field in complex networks. Figure 4.23 shows the order parameter S as a function of q for different values of the intensity of the field B for the Axelrod's model defined on random and a scale-free networks with average degree $\langle k \rangle$ [74]. Again, we observe a local minimum in S at a value $q^*(B) < q_c$. For $q < q^*(B)$ the largest domain corresponds to the state of the external field, $S = S_M$. For $q > q^*(B)$, the largest domain no longer corresponds to the state of the external field but to other state orthogonal to that of the field, i.e., $S_M < S$. However, in contrast to the fully connected network, the size of this alternative largest domain is not big enough to cover the entire system, i.e., $S < 1$.

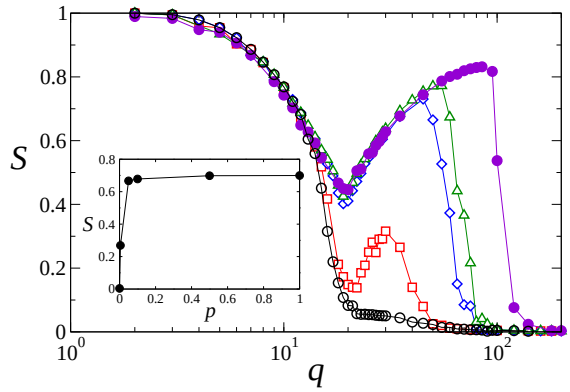

Figure 4.24: S versus q on a small world network with $\langle k \rangle = 4$, $N = 2500$, $B = 0.5, F = 3$, for different values of the probability p: $p = 0$ (empty circles), $p = 0.005$ (squares), $p = 0.05$ (diamonds), $p = 0.1$ (triangles), $p = 1$ (solid circles). Inset: S vs. p for fixed values $q = 40 > q^*$ and $B = 0.5$. Each data point is an average over 100 independent realizations of the underlying network and the dynamics.

Short-range interactions

As we already found with Deffuant's model (section 3.3) the presence of long-range connections allows the emergence of spontaneous ordering not associated with the state of an applied external field. To show this. we analyze the role of the network connectivity on the emergence of an ordered phase different to the one forced by the external field. We consider a small-world network [63], where the rewiring probability is varied in order to introduce long-range interactions between the particles. We start from a two-dimensional lattice with nearest-neighbor interactions (degree $k = 4$). Each link is rewired at random with probability p. The value $p = 0$ corresponds to a two-dimensional regular network with nearest neighbors interaction, while $p = 1$ corresponds to a random network with average degree $\langle k \rangle = 4$.

Figure 4.24 shows the order parameter S as a function of q on this network for different values of the rewiring probability p and for a fixed value of the intensity of the field B. The critical value q_c where the order-disorder transition takes place increases with p, which is compatible with the large value of q_c observed in a fully connected network. When the long-range interactions between particles

are not present, i.e. $p = 0$, the external field is able to impose its state to the entire system for $q < q_c$. Spontaneous ordering different from the state of the external field appears as the probability of having long-range interactions increases. The size of this alternative largest domain increases with p, but it does not grow enough to cover the entire system (see inset in Fig. 4.24).

4.2.4 External field and site percolation in consensus models

In this section we show that the the limiting case $B = 1$ in the models defined in section 3.3 (bounded confidence model with external field) and section 4.2.3 can be mapping exactly to site percolation. Site percolation refers to the dependence of the connected components of a network on the fraction of the occupied nodes [164, 165]: given a network, each node can be either occupied with probability p or empty with probability $1-p$. Following the traditional notation in percolation, a *cluster* is defined as a set of neighboring occupied nodes. In our notation this is what we have defined as a domain. Similarly, the order parameter is the (normalized) size of the largest domain (cluster). Percolation in a complex network typically displays a phase transition for a critical value of the occupancy parameter p [166, 167].

For both the Axelrod and bounded confidence models, the limiting case $B = 1$ corresponds to the situation in which the particles only interact with the external field. The particles that change their state are those with overlap different from zero in the Axelrod's model (that is, they share at least one feature with the external field) or with state in the range $[1 - d, 1]$ in the bounded confidence model. In these cases, the state of the particles becomes the same as the one of the external field. For zero overlap or states outside the range $[1 - d, 1]$ particles keep their original state. As a consequence, the ordered state in this limiting case $B = 1$ is the one determined by the field. The largest domain for random initial conditions has the state of the external field.

In the analogy with site percolation, an occupied node corresponds to a particle that has the state of the external field. In the Axelrod's model only those particles that initially share at least one component of their vector states with the external field will converge to the field state. The fraction of particles that converge to M^f is given by Eq. (4.1)

$$p = 1 - (1 - 1/q)^F \,. \tag{4.3}$$

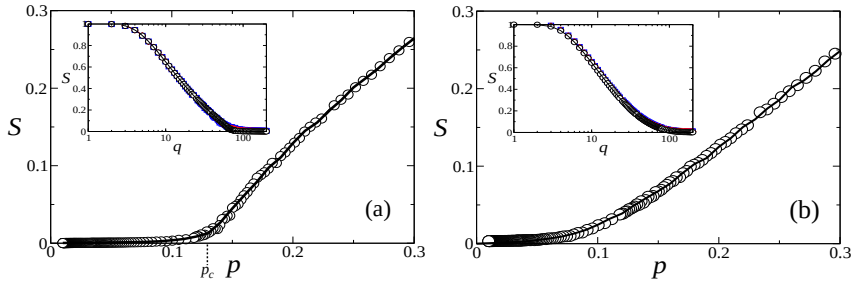

Figure 4.25: S vs. p for site percolation model (line) and the Axelrod's model with external field $B = 1$ (circles) on (a) a random and (b) a scale-free network with $\langle k \rangle = 8$. For the Axelrod model $p = 1 - (1 - 1/q)^F$, $F = 10$ and $B = 1$. System size $N = 104$. **Insets:** S vs. q in the site percolation model (line) and Axelrod's model (symbols) for different system size, $N = 10^4$ (circles), 10^3 (diamonds) and 500 (squares). The relation between q for the Axelrod's model and the occupancy probability p in site percolation is $q = [1 - (1 - p)^{(1/F)}]^{-1}$. Each data point is an average over 100 independent realizations.

Thus, the quantity p can be interpreted as a probability of interaction between the external field and any particle in the system. Similarly, the parameter $p = d$ in the bouded confidence model can be seen as the probability for particle-field interaction when $B = 1$. Therefore, the quantity p in either model measures the probability that any particle in the system reaches the state of the field, while the complementary probability $(1 - p)$ indicates the fraction of particles that do not converge to the state of field. The largest cluster in the site percolation problem can be viewed as the size of the largest domain S in both the Axelrod and the bounded confidence models when $B = 1$.

In order to illustrate the mapping of the bounded confidence and Axelrod mod els in an external field with $B = 1$ and site percolation, we have performed simulations of these models in several complex networks. Figure (8.2) [Figure (4.26)] shows the normalized size of the largest domain S as a function of the probability p of occupied sites for site percolation model, and as a function of the quantity $p = 1 - (1 - 1/q)^F$ [$p = d$] (Eq. (4.3)) for the Axelrod [bounded confidence] model subject to an external field with $B = 1$, on a random and in a scale-free network. The critical values for the onset of a spanning cluster (the ordered state) is $p_c = 1/\langle k \rangle = 0.125$ and $p_c = 0$, respectively, for the random and scale-free network [166, 167].

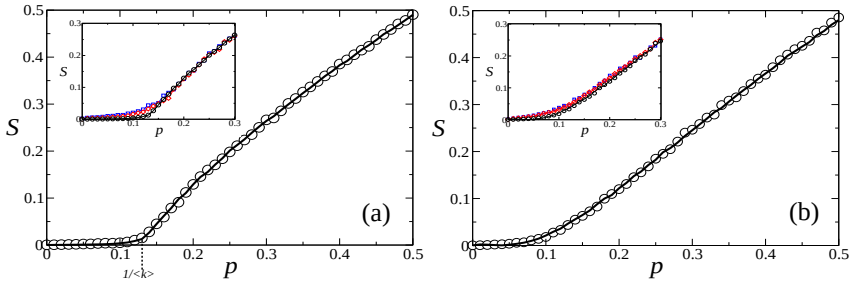

Figure 4.26: S vs. p for site percolation model (line) and the Bounded confidence model with external field $B = 1$ (circles) on a (a) random and a (b) scale-free network with $\langle k \rangle = 8$. System size $N = 10^4$. **Insets:** S vs. p for site percolation (line) and the scalar model (symbols) for system size $N = 10^4$ (circles), 10^3 (diamonds) and 500 (squares). The relation between d for the bounded confidence model and the occupancy probability p in site percolation is $d = p$. Each data point is an average over 100 independent realizations.

4.3 Co-evolution dynamics in Axelrod's model

In this section we address in the context of Axelrod's model, the question of co-evolution dynamics discussed generally in section 1.4. The network of interactions was kept fixed in section 4.2 while in this section it co-evolves in the same time scale that the dynamics of the state of nodes. This co-evolution dynamics it implemented allowing interaction links to be rewired depending on the state of the agents at their ends.

4.3.1 The model

The adaptation of the previously discussed Axelrod's model to a co-evolution dynamics is as follows:

A population of N agents are located at the nodes of a network. The state of an agent i is represented by an F-component vector C_i^f ($f = 1, 2, \ldots, F$) and $i = 1, 2, \ldots, N$, where each component represents an agent's attribute. There are q different choices or traits per feature, labelled with an integer $C_i^f \in \{0, \ldots, q-1\}$, giving rise to q^F possible different states.

Initially agents take one of the q^F states at random. In a time step an agent i and one of its neighbors j are randomly chosen:

1. If the agents share $m > 0$ features, they interact with probability equal to the fraction of shared features, i.e., the overlap (m/F). In case of interaction, an unshared feature is selected at random and i copies j's value for this feature.

2. If the agents do not share any feature, then i disconnects its link to j and connects it to a randomly chosen agent that i is not already connected to.

Step 1 defines the basic homophily and influence model discussed before, in which actors who are similar are more likely to interact. Interaction makes actors who are similar become even more similar, increasing the weight of their tie and the likelihood of future interaction. As some actors become more similar, others become less similar as the dynamics of cultural evolution create widening gaps between the emerging cultural communities. Some neighbors in the social network may become so different from one another that they no longer share any cultural traits in common. When this happens, the weight of the tie between them drops to zero and no longer functions as a means for cultural influence. Step 2, schematically explained in Figure 4.27 defines the co-evolution dynamics. It incorporates network dynamics into the specification of homophily by allowing actors to drop these zero-weight ties. Just like members of a social clique who have grown distant from one another by virtue of interacting with different social groups [160], or voluntary group members who share less and less in common as they derive more of their social and cultural influence from outside sources [168], as social differentiation reduces shared traits, the remaining ties become a vestigial feature of the actors' social histories and are ultimately broken [169]. This network homophily dynamics allow the structure of the social network to co-evolve with the dynamics of social influence. If an active individual tries to interact with a neighbor with whom there is zero overlap in cultural features, it drops the tie to this neighbor and randomly forms a new tie to another individual, preserving the overall density of the social network. In other words, the step 1 describes the original Axelrod dynamics: Alike agents become even more similar as they interact, increasing the probability of future interaction. Step 2 implements the network co-evolution: *incompatible agents*, i.e., agents with no features in common, tend to get disconnected.

We have performed extensive numerical simulations to study the behavior of the system as the control parameter q is varied, for different population sizes N, number of features $F = 3$, and starting from a random network with average degree $\langle k \rangle = 4$. The results do not depend on the initial network topology,

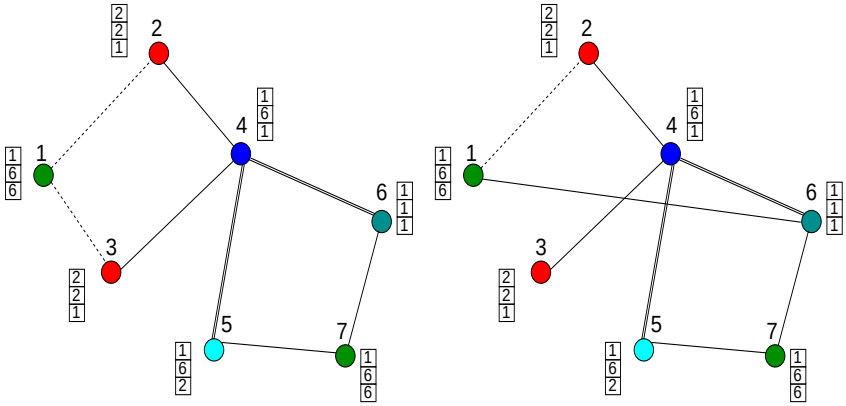

Figure 4.27: Network dynamics for a system with F =3 and q=7: The network on the left (at time t) shows each node with its corresponding vector of cultural features at time t. The network on the right shows the same population at time $t + 1$. The links between nodes are weighted according to their overlap: dashed line for zero overlap, continuous lines for overlap=1, and double line for overlap= 2. At time t, the overlap between nodes 1 and 2, O(1,2), is zero, as is O(1,3). At time t, node 1 has been selected as active and node 3 as its partner (step 1). Step 1 imply no changes of state given that O(1,3)=0. Following step 2, the link between 1 and 3 is removed, and node 1 is randomly linked to a different node. The new link between nodes 1 and 6 (shown in the network on the right) has overlap O(1,6)=1.

because the repeated rewiring dynamics leads to a random network with a Poisson degree distribution (see figure 4.28).

4.3.2 Phases and transitions

The co-evolution Axelrod's model displays two transitions, both very different in nature. The first one is an order-disorder transition at $q = q_c$ between two frozen phases, associated with the fragmentation of the network*. The dynamics leads to the formation of network components, where a component is a set of connected nodes. In a frozen configuration, agents that belong to the same component have the same state. For $q < q_c$ (ordered phase I), the system reaches

*Note that this critical value q_c is different from the one discussed in section 4.1 and 4.2 for the polarization-globalization transition in fixed networks.

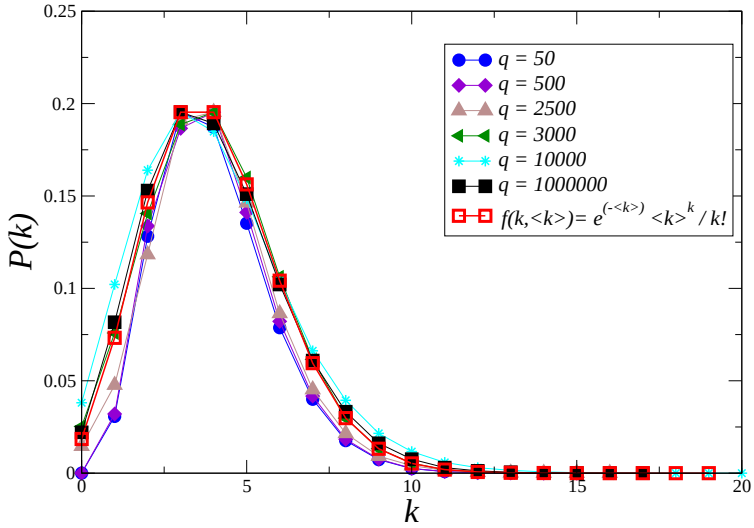

Figure 4.28: Node degree distribution $P(k)$ of the co-evolving network in the final frozen state for a system with $F = 3$, system size $N = 10^4$ and various values of q. The system starts from random network with average degree $\langle k \rangle = 4$. $P(k)$ is very similar to a Poissonian (sketched in empty squares for comparison) for all values of q.

a configuration composed by a giant component of the order of the system size, and a set of small components as illustrated in Figure 4.29a and Figure 4.29b; for $q > q_c$ (disordered phase II) the large component breaks into many small disconnected components (see Figure 4.29c). The second transition, related with network recombination, occurs at $q = q^*$ between the phase II and an active phase III, where the system reaches a dynamic configuration with links that are permanently rewired as is shown in Figure 4.29d.

For small values of q in phase I, the average size of the largest network component S in the final configuration is of the order of the system size N (Fig. 4.30), due to the high initial overlap between the states of neighboring agents. As q increases inside phase I, the initial overlap decreases and S also slowly decreases. For larger values of q (phase II), many distinct domains are formed initially inside the components which break into many small disconnected components and, as a result, S reaches a value much smaller than N (network fragmentation). During the evolution of the system, a network component can have more than one

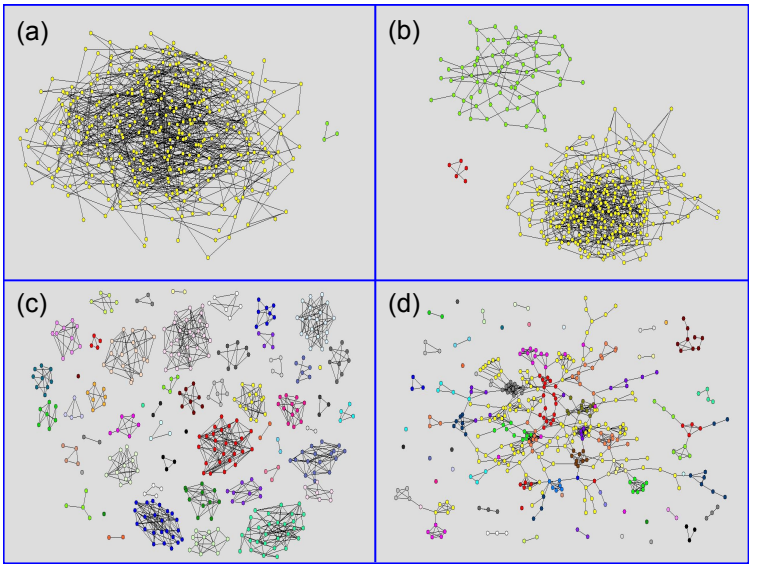

Figure 4.29: Network structure for $F = 3$ in the final frozen configuration in phase *I*: $q = 3$ (a), $q = 20$ (b) and in phase *II*: $q = 100$ (c) for $N = 400$. (d) Snapshot of the network in the stationary active configuration (phase *III*) for $q = 500$.

domain. However, in the final configuration of phases I and II, one component corresponds to one domain.

The transition point from phase I to phase II is defined by the value $q = q_c$ for which the fluctuations in S reach a maximum value. This value corresponds to the point where the order parameter S suffers a sudden drop. For $N = 2500$ we find $q_c = 85 \pm 2$ (see Fig. 4.30). To further investigate this transition point we calculated the size distribution of network components $P(s)$ (see Fig. 4.31). For small q, $P(s)$ shows a peak that corresponds to the average size of the largest component S, and has an exponential decay corresponding to the distribution of small disconnected components. The peak at S decreases as q increases, giving raise to a power law decay of $P(s)$ at $q_c \simeq 85$, a signature of a transition point [153, 165].

The behavior of the order parameter S/N depends on system size (Fig. 4.32). When both axis are rescaled by $N^{-\alpha}$ with $\alpha = 0.82 \pm 0.01$ the data collapses for q smaller than q_c. This implies that q_c increases with the system size N as $q_c \sim N^{\alpha}$,

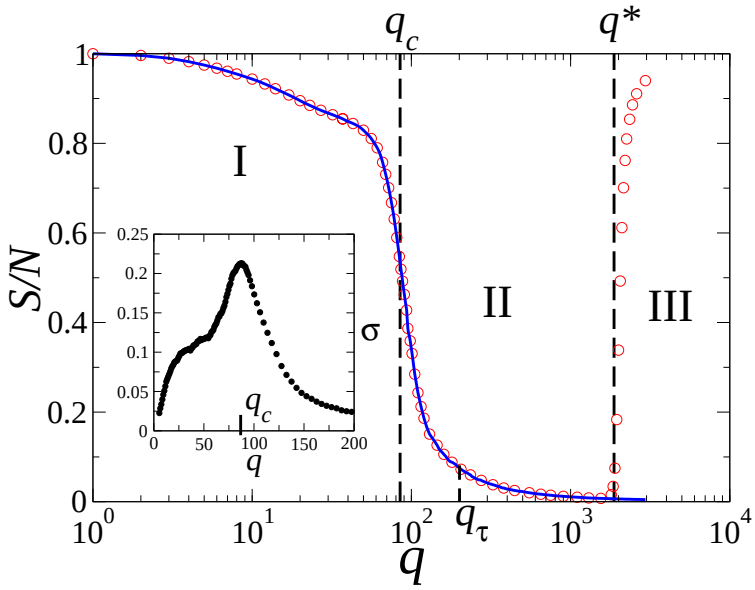

Figure 4.30: Average relative size of the largest network component (circles) and largest domain (solid line) in the stationary configuration vs q, for $N = 2500$, averaged over 400 realizations. The vertical lines at $q_c = 85$ and $q^* = 1875$ indicate the transition points between the different phases. Inset: fluctuations are maximum at the critical point q_c.

and suggests a scaling relation for S in the ordered phase $S = N^\alpha f(N^{-\alpha}q)$, where $f(\cdot)$ is a scaling function. The scaling relation implies that the discontinuity disappears in the large N limit. Thus, not only the transition point diverges as $q_c \sim N^{0.82}$ but also the amplitude of the order parameter $S/N \sim N^{-0.18}$ vanishes as N goes to infinity.

These results, maximum of the fluctuations, data collapse and distribution of component sizes, identify q_c as the critical point of the transition. The fact that the exponent of the size distribution is smaller than 2 and that the discontinuity of the order parameter tends to 0 as system size increases, suggest that in the large N limit the transition becomes continuous with $q_c \to \infty$.

We analyze the active phase (III) by looking at the rewiring dynamics. A link that connects a pair of incompatible agents is randomly rewired until it connects two compatible agents, i.e., agents with at least one feature in common. If the number of pairs of compatible agents L_c is larger than the total number of

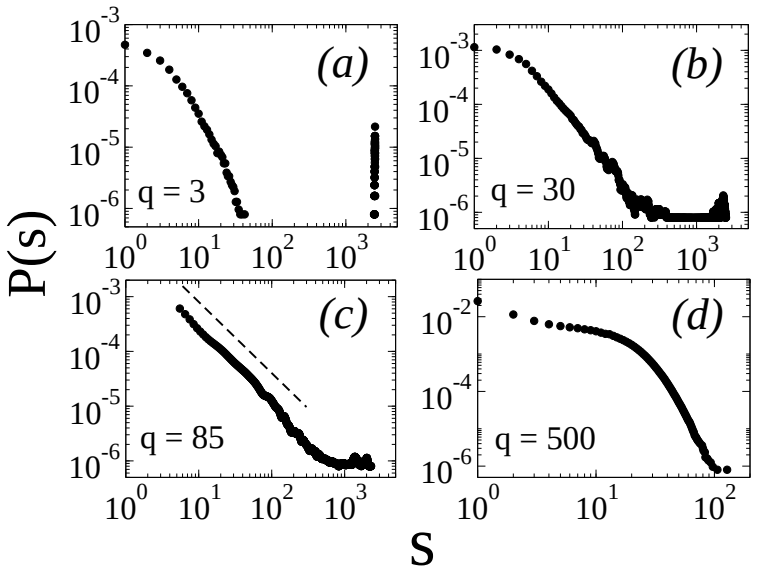

Figure 4.31: Size distribution of network components for $N = 2500$ and values of q (a,b) below, (c) at, and (d) above the transition point $q_c \simeq 85$. The dashed line represents a power law with exponent -1.3 ± 0.02.

links in the system $\langle k \rangle N/2$, this rewiring process continues until all links connect compatible agents. Later, the system evolves until each component constitutes a single domain, the frozen configurations reached in phases I and II. If, on the contrary, L_c gets smaller than $\langle k \rangle N/2$, the system evolves connecting first all L_c pairs by links. The state dynamics stops when no further change of state is possible, but the rewiring dynamics continues for ever with approximately $\langle k \rangle N/2 - L_c$ links that repeatedly fail to attach compatible agents. This is the active configuration observed in phase III. Thus, in contrast to phases I and II, in the stationary configurations of phase III there are typically more than one domain per component. The size of the largest component abruptly increases at q^* indicating that a giant component reappears (network recombination), while the size of the largest domain continues decreasing (see Fig. 4.30).

To estimate q^*, we will assume L_c constant during the evolution as for q large the state of the agents does not evolve much. Thus, with the ansatz $L_c \simeq L_c(t = 0) \simeq \frac{N(N-1)}{2}\left[1 - (1 - 1/q)^F\right] \simeq N^2 F/2q$, for $q \gg F$ and

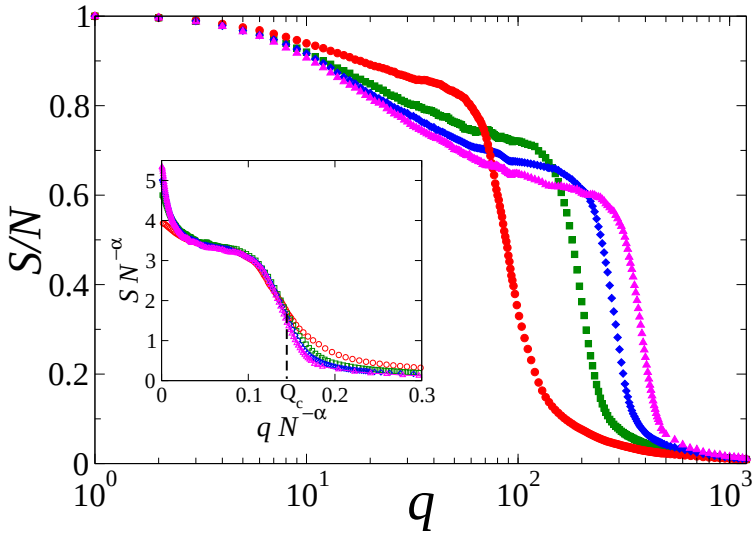

Figure 4.32: Average relative size of the largest network component S/N vs q for system sizes $N = 2500$, 6400, 10000 and 14400 (left to right), averaged over 400 realizations. Inset: Finite size scaling. The data collapses below the scaled transition point $Q_c = q_c N^{-\alpha}$, with $\alpha = 0.82$.

$N \gg 1$, the condition at the transition point is $N^2 F/2q^* \simeq \langle k \rangle N/2$, so that

$$q^* \simeq \frac{NF}{\langle k \rangle} \tag{4.4}$$

is the value of the recombination transition point. For the values considered here we obtain $q^* = 1875$ in good agreement with the numerical results (Fig. 4.30).

Changing the rewiring rate

In the previous section we assumed that when a pair of nodes with zero overlap is chosen, the link between them is always rewired. We now consider the case in which the rewiring happens with probability p. Varying p is equivalent to change the relative time scales at which the copy and the rewiring dynamics occur. In the limit of p going to zero we expect the system to behave as in the original Axelrod model, where the network is fixed. On the other limit, when p is one we recover the co-evolving model studied before. Thus, we should see that the transition point q_c shifts to higher values of q as p is increased from zero.

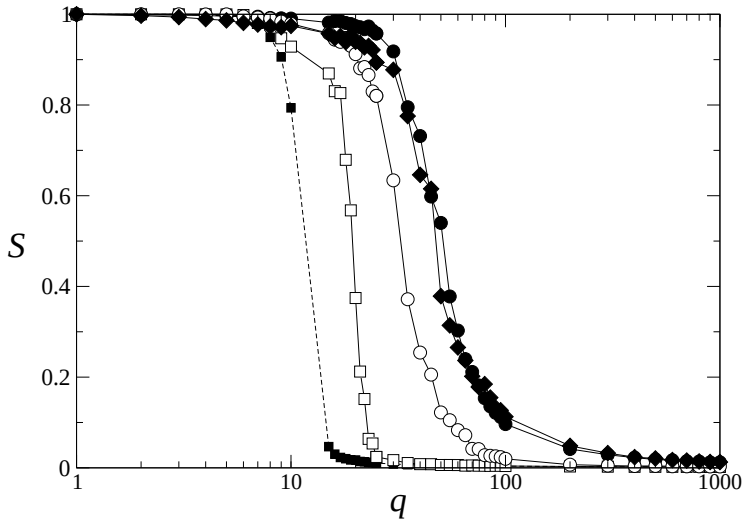

Figure 4.33: S vs q for values of the rewiring probability $p = 0, 10^{-6}, 5 \times 10^{-5}, 0.1$ and 1 from left to right, $N = 1000$ and $F = 3$. S was measured for every value of p at the same observation time $\tau = 10^8$.

Fig. 4.33 shows that the critical point for values of p above 0.1 is very close to the critical value $p_c \simeq 85$ for the $p = 1$ case, when S is measured at a fixed time $\tau = 10^8$.

To investigate this dependence, we calculated S for fixed $q = 20$ in the connected phase I, and for three different observation times. As we observe in fig. 4.34, for a fixed time, S/N is close to zero for very small values of p and it increases up to $S/N \simeq 0.9$ for larger values of p when the observation times are $\tau = 10^8$ and $\tau = 10^{11}$. However this transition in S seems to disappear when S is measured at longer times ($\tau = 10^{13}$). We expect that if we wait long enough the size of the largest component would reach the value $S/N \simeq 0.9$ for any value of p above zero. The last result means that there is a discontinuity in the critical value q_c at $p = 0$. For $p > 0$, the behavior of S as a function of q is essencially the same in the long time limit.

Beyond the statistical physics analysis of the transitions at $q = q_c$ and $q = q^*$, these transitions have an interesting in the interpretation and relevance in the context of social sciences: The transition between the phase I and phase II, responds to a process of group differentiation through which a large heterogeneous group fractures and then consolidates into multiple cliques or subgroups.

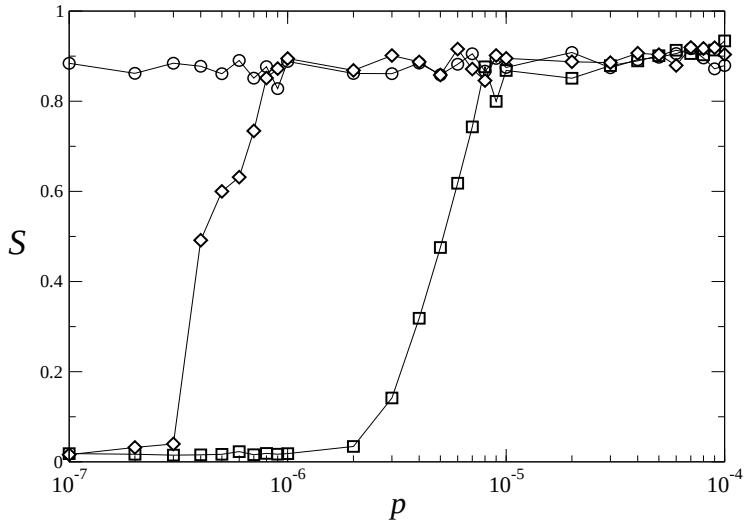

Figure 4.34: Relative size of the largest network component vs the rewiring probability p for $N = 1024$, $F = 3$, $q = 20$ and observation times $\tau = 10^8$ (squares), $\tau = 10^{11}$ (diamonds) and $\tau = 10^{13}$ (circles). For a long enough observation time, S/N approaches to the value $S/N \simeq 0.9$ independent on the value of p.

In phase I, the co-evolutionary model produces a global monoculture across a large range of q values. This is because actors in the dynamics networks are able to find paths around local borders by forming new ties. As actors create new links across the population, their ties form a large connected component (technically a giant network component) that allows cultural boundaries to break down and gives rise to a global monoculture. As q increases, we approach phase II, in which the dynamics network breaks into multiple component. In this case, there is sufficient heterogeneity to allow cultural diversity to emerge in the system.

This process has been documented in the formation of adolescent and adult friendship groups [170, 171], voluntary organizations [168, 172], social movements [173], class identity [174], and cultural norms more generally [175]. As the number of cultural options in a population increases, the average similarity among the members of large heterogeneous groups decreases. Furthermore, as individuals find others like them and grow more similar, emerging cleavages in the large group eventually result in a splintering process, whereby large groups disaggregate into smaller, more culturally specialized ones [168, 175]. The key

to these homophily dynamics is the changing nature of the social network. Cultural influence and social adaptation processes allow individuals to evolve in the space of cultural ideas and behaviors, changing the social landscape. As people grow apart, the reinforcing effects of reduced similarity and reduced interaction cause old ties to be dropped; reciprocally, new friendships are made with people who share one's current tastes and preferences. Eventually, this process of individual differentiation also creates group consolidation, as detachment from dissimilar people also gives rise to stronger bonds with more similar individuals [176]. This tendency for network relations to form between those who have similar social characteristics is known as the homophily principle. Since individuals close to one another on a dimension of social space are similar, homophily implies that ties are local in social space [172]. In phase II, the physical space of the social network is rearranged until all ties are local in social space. This process produces an emergent social landscape in which discrete social clusters (i.e., components) correspond to distinct trait groups. The more heterogeneity in the more exclusive these trait groups become [176].

In phase III, the abundance of cultural options overwhelms the population, creating anomic [177] actors, who develop unlikely combinations of cultural features that prevent them from interacting with anyone. While some actors are able to form into homophilous clusters, the anomic actors perpetually add and drop ties. When $q > q^*$, the largest component in the network consists of this disenfranchised group of actors who are unable to establish memberships in any of the homophilous social clusters. With increasing heterogeneity, the number of anomic actors increases, as does the size of this component, until the entire population forms a single network that is simply a buzz of adding and dropping ties with no mutual influence or lasting relationships. The overabundance of cultural options actually prevents the formation of cultural groups and thus eliminates the forms of social diversity that heterogeneity was thought to help create. This suggests that-in addition to previous findings that increased heterogeneity facilitates the maintenance of cultural diversity-under certain conditions, limiting cultural

4.3.3 Dynamic time scales

In order to understand the final structure of the network in phases I and II we analyzed the time evolution of the nodes' states and interaction links. In Fig. 4.35 we plot the time evolution of the density of network components, n_c = number of components/N, and domains, n_d =number of domains/N, averaged over 1000 realizations, and for three values of q. An interesting quantity is the average time to reach the final frozen configuration τ. If τ_d [τ_c] is the average time at which n_d

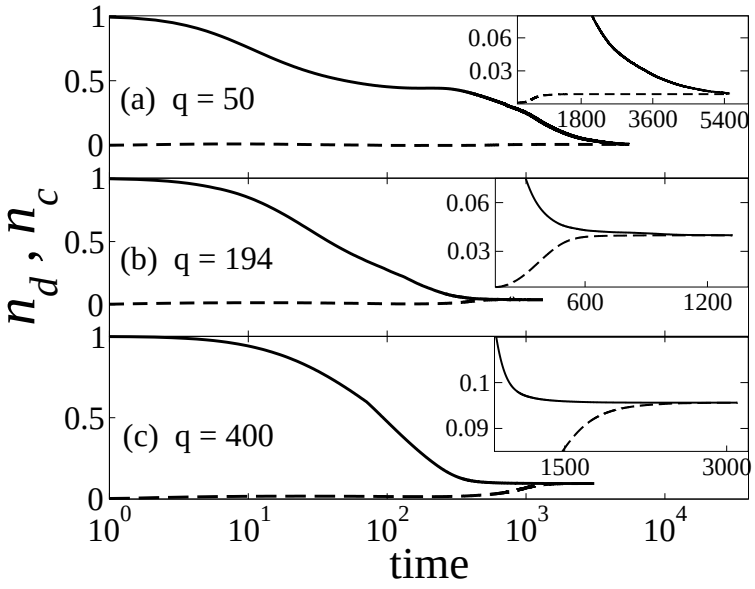

Figure 4.35: Time evolution of the density of domains n_d (solid line) and network components n_c (dashed line), for $N = 2500$ and values of q (a) below, (b) at, and (c) above the transition point $q_\tau = 194 \pm 10$. Each inset is a zoom of the region that shows the approach to the final configuration.

$[n_c]$ reaches its stationary value, then τ is largest between τ_d and τ_c (see Figs. 4.35 and 4.36). The curves for τ_d and τ_c as a function of q cross at a value q_τ (Fig. 4.36). As we shall see, q_τ identifies a transition between two different dynamic regimes for the formation of domains and network components, that lead to the frozen configurations observed in phases I and II (Figs. 4.35 and 4.36).

For $q < q_\tau$, the dynamics causes the network to break into a giant component and small components. Due to the initial overlap between the states of the agents inside each component, the network stops evolving at a time τ_c where n_c reaches its stationary maximum value (see Fig. 4.35a). After this stage, domains compete inside each component, until only one domain occupies each component. The approach to the frozen configuration is controlled by the coarsening process inside the largest component, whose structure is similar to a random network due to the random rewiring dynamics. Then, given that the dynamics of the last and longest stage before reaching consensus inside this component is governed

by interfacial noise as in the voter model [158], τ is expected to scale as the size of the largest component $\tau \sim S$ [69].

For $q > q_\tau$, there is a transient during which n_d decreases, indicating that, in average, domains grow in size (see Fig. 4.35c). At time τ_d, n_d reaches a stationary value when the overlap between distinct domains is zero. At this stage domains are still interconnected by links between incompatible agents. As domains progressively disconnect from each other n_c increases. When finally the links connecting incompatible agents disappear all domains get fragmented, n_c equals n_d and the system reaches its final configuration in a time $\tau = \tau_c$.

At q_τ, the time scale governing the state dynamics is the same as the time scale governing the network dynamics $\tau_d = \tau_c$ (Figs. 4.35b,4.36). Thus, it indicates that the ordered phase I is dominated by a slower state dynamics on a network that freezes on a fast time scale, while in the disordered phase II the state dynamics freezes before the network reaches a final frozen configuration. Even though q_τ is found to be larger than the critical point q_c, the relative difference between q_τ and q_c decreases with N (inset of Fig. 4.36), suggesting that both transition points become equivalent in the large N limit. Thus, the competition between the time scales τ_d and τ_c governs the fragmentation transition at q_c.

We have derived an approximate expression for τ in phase II by studying the decay of the number of links between incompatible agents N_0. We shall see that this approach unveils the transition from the frozen to the active phase, leading to the transition point q^*.

In the continuum time limit, and neglecting the creation of incompatible links, N_0 decays according to the equation:

$$\frac{dN_0}{dt} \simeq -\frac{1}{\frac{1}{N}} \frac{2N_0}{\langle k \rangle N} \frac{N_c}{N} = -\frac{2N_0 N_c}{\langle k \rangle N}. \tag{4.5}$$

In a time step $\Delta t = \frac{1}{N}$, an incompatible link (i, j) is chosen with probability $\frac{2N_0}{\langle k \rangle N}$. One of its ends j is moved to a random node k. The probability that k is compatible to i is $\frac{N_c}{N}$, where N_c is the number of compatible agents to i but still not connected to i. In a mean-field spirit, every node has $\langle k \rangle$ edges that need to be connected to $\langle k \rangle$ different compatible agents. We approximate N_c as the average number of compatible agents per agent. When i attaches an edge to a compatible agent, N_0 is reduced by one while N_c is reduced by $2/N$ given that both i and k loose a compatible partner. Assuming that the set of compatible agents to i remains the same we write $N_c \simeq \frac{2N_0}{N} + A$, where $A = N_c(0) - \frac{2N_0(0)}{N} \simeq \frac{NF}{q} - \langle k \rangle$

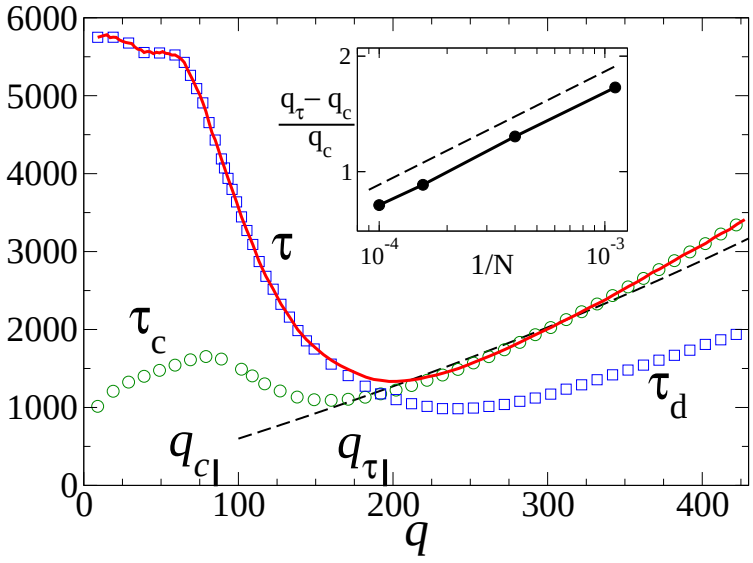

Figure 4.36: Convergence times τ_c (circles), τ_d (squares) and τ (solid line) vs q for $N = 2500$ and averaged over 500 configurations. The result from Eq. (4.8) (dashed line) is compared with τ and τ_c for $q > q_\tau = 194 \pm 10$. Inset: relative difference between the transition points q_τ and q_c vs $1/N$ in log-log scale. The dashed line has slope 0.30 ± 0.01.

for $N \gg 1$ and $q \gg F$. Substituting this last expression for N_c into Eq. (4.5) and rewriting it in terms of the transition point $q^* = NF/\langle k \rangle$ we obtain

$$\frac{dN_0}{dt} \simeq -\frac{2N_0}{\langle k \rangle N}\left(\frac{2N_0}{N} + \frac{\langle k \rangle}{q}(q^* - q)\right). \tag{4.6}$$

Equation (4.6) has two stationary solutions. For $q < q^*$, the steady configuration is $N_0^S = 0$, corresponding to the frozen phases I and II, while for $q > q^*$ the stationary solution $N_0^S = \frac{\langle k \rangle N}{2q}(q - q^*)$ corresponds to the active phase III. We recover our previous result that for $q > q^*$ the system reaches a stationary configuration with a constant fraction of links N_0 larger than zero, that are permanently rewired. Therefore, the system never freezes. Note that in the limit of very large q, all agents are initially incompatible, consequently N_0 approaches to the total number of links $\frac{1}{2}\langle k \rangle N$.

Integrating Eq. (4.6) by a partial fraction expansion gives

$$t = \frac{qN}{2(q^* - q)} \ln\left[\frac{q + \frac{\langle k\rangle N}{2N_0(t)}(q^* - q)}{q^*}\right]. \tag{4.7}$$

For $q < q^*$, the system freezes at a time τ at which $N_0 \simeq 1$, thus

$$\tau \simeq \frac{qN}{2(q^* - q)} \ln\left[\frac{q + \frac{1}{2}\langle k\rangle N(q^* - q)}{q^*}\right], \text{ for } q_\tau < q < q^*. \tag{4.8}$$

This result is in agreement with the numerical solution (Fig. 4.36).

For $q > q^*$, the system reaches a stationary configuration. Thus we define τ as the time at which $N_0 \simeq \frac{\langle k\rangle N}{2q}(q - q^*) + 1$, then

$$\tau \simeq \frac{qN}{2(q^* - q)} \ln\left[\frac{2q^2}{q^*(\langle k\rangle N(q - q^*) + 2q)}\right], \tag{4.9}$$

for $q^* < q < \frac{N^2F}{2}$. τ decreases with q and it vanishes for $q > N^2F/2$ where initially all pairs of nodes are incompatible, thus the system starts from a stationary configuration, giving $\tau = 0$ for $q > \frac{N^2F}{2}$.

From Eqs. (4.8) and (4.9) we obtain that τ reaches a maximum value equal to $\frac{1}{4}\langle k\rangle N^2$ at $q = q^*$; an indication of the transition.

4.3.4 Cultural Drift and Coevolution

In the review of previous results on the Axelrod's model in section 4.1 we discussed that cultural drift of small rate eventually orders the polarized configurations, therefore the globalization-polarization transition in a fixed networks is not robust against the introduction of cultural drift. Contrary of this feat, the analysis of the co-evolutionary dynamics suggests that in region II, where nontrivial multicultural states survive in a co-evolving network, the co-evolutionary cultural processes of homophily and influence may in fact stabilize the co-existence of distinct cultural regions even in the presence of continuous stochasticity. Following Klemm et al. [152, 158], we add cultural drift to the evolutionary dynamics by adding noise in the form of continuous random shocks, as defined by the following rule: With probability r, perform a single feature perturbation. A single feature perturbation is defined as randomly choosing an agent i from the population, $i \in \{1, ..., N\}$; randomly choosing one of i' s features, $f \in \{1, ..., F\}$; then randomly choosing a trait s from the list of possible traits, $s \in \{1, ..., q\}$, and setting

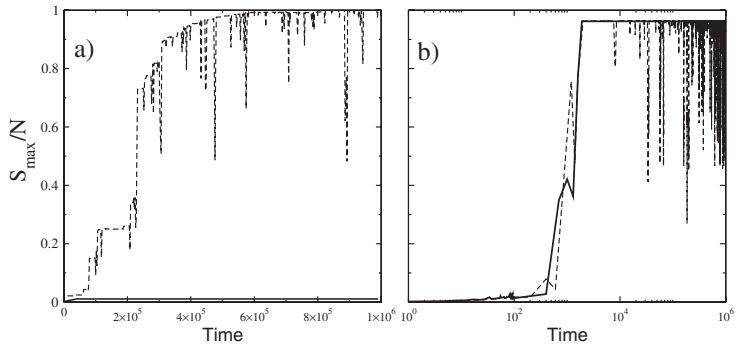

Figure 4.37: Panel (a) shows the numerical simulation of the model on $2D$ fixed network with no noise ($r = 0$, solid line) and cultural drift ($r = 10^{-5}$, dashed line) for $F = 3, N = 1024$ and $q = 20$. The solid line (at the bottom) shows very high cultural diversity, while the dotted line shows the emergence of a global monoculture. Panel (b) shows the dynamics for no noise ($r = 0$, solid line) and drift ($r = 10^{-5}$, dashed line) in a co-evolving network for the Phase I.

$\sigma_{if} = s$. Depending on whether the rate of perturbation r is less than or greater than the time scale on which the homophily and influence dynamics operate, the system will either be slightly perturbed on a regular basis (small noise rate), or the system will be constantly flooded with noise (large noise rate) and unable to reach any kind of equilibrium. In fixed networks, there is a critical value of the noise rate r_c above which noise dominates the behavior of the system [158]. We are here interested in the small noise rate limit ($r < r_c$),which tests the stability of cultural diversity in the presence of cultural drift.

As a benchmark for comparison, Figure 4.37 shows the effects of cultural drift for a fixed network with value of q in Phase I for which the system reaches a multicultural configuration and for a co-evolutionary model. For a fixed network (Figure 4.37a), we observe that without cultural drift ($r = 0$, solid line) the system stabilizes in a multicultural state $S_{max} \ll N$ for the whole duration of the simulation. The value of q chosen is larger that the critical value ($q = 12$) for the

globalization-polarization transition in a fixed network (section 4.1) However, cultural drift ($r = 10^{-5}$, dashed line) drives the system toward a monocultural state, where $S_{max} \sim N$ [152, 158]. It is worth noting that this monocultural state is not fixed, as perturbations take the system in random excursions away from and then back to any of the q^F equivalent monocultural states. As a new trait percolates through the network, the size of the largest cultural group drops as more people adopt the new trait. However, as even more people adopt the trait, the size of the largest group increases again until cultural uniformity is restored. For a co-evolving network (Figure 4.37b), we observe that after an initial transient, the system orders itself in a monocultural state. This happens in the same time scale with noise (dashed line) and without noise (solid line). As in the fixed network, cultural drift causes random excursions from the final monocultural state, only to return to another one.

A more interesting effect is shown in Figures 4.38a and 4.38b, which correspond to Phase II. For the fixed network (Figure 4.38a), the results are the same as the phase I: Without noise (solid line), the system stabilizes with high levels of heterogeneity, but with noise (dashed line), the system reaches a homogeneous state. As before, noise-induced excursions away from monoculture give rise to changes in the cultural makeup of the group, but the system always returns to a monocultural state. For the co-evolving network (Figure 4.38b), we observe that in the absence of cultural drift (solid line), the co-evolution model quickly finds a stable state and then remains in that state for the rest of the simulation. When cultural drift is added to the co-evolution model (dashed line), not much happens. The model with noise reaches a stable state in about the same time, and with S_{max}/N of about the same size, as it does without noise. Small perturbations occasionally propagate through the groups, causing shifts in their cultural identities. However, the network structure, the number of physical groups, and the composition of the groups remain unchanged.

Figure 4.39 shows the number of cultural groups corresponding to Figure 4.38. As expected, the fixed network without noise (solid line) stabilizes with a large number of cultural groups, but when noise is added (dashed line), the number of cultural groups drops to one. Conversely, for the co-evolving network both without noise (solid circles) and with noise (open circles), diverse cultural groups stabilize in about the same time and remain intact throughout the simulation. While cultural drift may cause slight changes in the internal culture of the groups-either through perturbations occurring, then dying out, or through perturbations successfully propagating through the cultural groups-the membership of the cultural groups remains distinct. Without cross-cutting [178] ties between these groups, there are no opportunities for new cultural exchanges to incite crossborder interaction between cultural groups. Their isolationism guar-

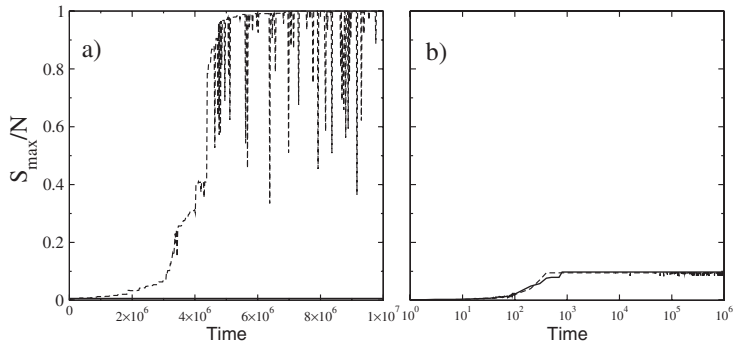

Figure 4.38: Panel (a) shows a fixed network in region II, with no noise ($r = 0$, solid line) and cultural drift ($r = 10^{-5}$, dashed line) for $F = 3$, $N = 1024$ and $q = 100$. Once again, the solid line (at the bottom) shows very high cultural diversity, while the dotted line shows the emergence of a global monoculture. Panel (b) shows the dynamics for no noise ($r = 0$, solid line) and drift ($r = 10^{-5}$, dashed line) in a co-evolving network in Phase II. The co-evolving model produces the same level of cultural diversity (and same number of groups), both without noise and in the presence of cultural drift.

antees that they can maintain their cultural distinctiveness-dynamic though it may be-even in the face of persistent cultural drift.

To understand why cultural drift does not cause cultural groups to break down, it is necessary to recall that groups will only break down if they form links to other groups. However, new links are only made when existing ties are dropped. Thus, the stability of groups in the dynamic model hinges on the low likelihood that an actor will drop a social tie, which is equivalent to the likelihood of having zero overlap with a fellow group member. Once groups have formed, the local processes of homophily and influence create cultural consensus within the group. Thus, for an actor to have zero overlap with one of its neighbors, a sequence of perturbations must occur such that an actor goes from complete overlap to zero overlap. A lone perturbation on one feature will leave the altered actor with

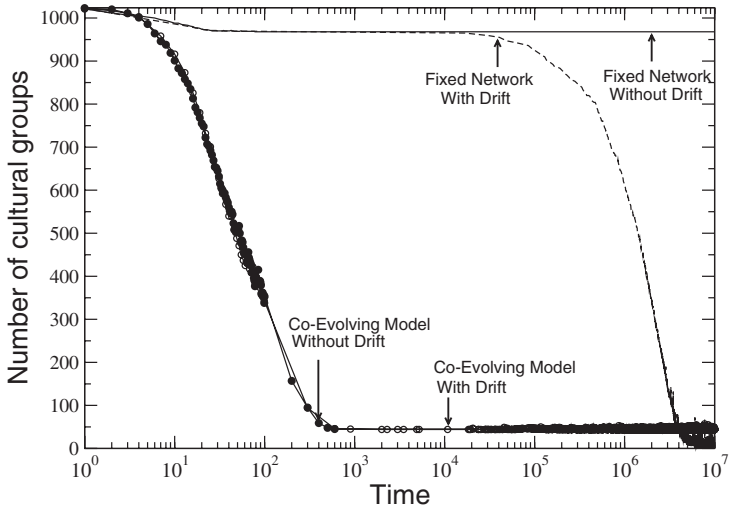

Figure 4.39: ($F = 3$, $N = 1024$, $q = 100$). The number of cultural groups in the fixed (no symbols) and co-evolving (circular symbols) networks are shown in the time series in Figure 4.38. For fixed networks without noise (solid line), the number of cultural groups remains high, while in the presence of cultural drift (dashed line), the number of cultural groups drops to 1. For co-evolving networks with cultural drift (empty circular symbols) and without it (solid circular symbols), the same number of cultural groups form and are maintained.

a very high level of similarity with its neighbors. Thus, a single perturbation will result in either the new cultural feature reverting to its original state (if the altered actor is influenced by its neighbor) or the new cultural feature being adopted by a neighbor (if the altered actor influences its neighbor). In both cases, the dynamics of homophily and influence guarantee that the local group will achieve cultural consensus on the newly introduced feature, either through its elimination or its adoption. For similarity between neighbors to decline, an actor with a new cultural feature must keep the cultural feature without it either being adopted or eliminated, while a second perturbation occurs, either to the originally altered actor or to one of its neighbors. This second perturbation must occur on a separate cultural feature and must lessen the overlap between the two neighbors. Once again, no influence can take place; otherwise, their similarity will increase, leading toward the absorption or elimination of the new traits. This sequence of perturbations must occur, without interruption by the processes of

local influence, F times for two culturally identical neighbors to develop zero overlap. The probability of this occurring is roughly $1/NF$, or the chance that a single agent will be perturbed F times in a row on a different feature each time. The probability is even lower if we consider that none of these perturbations can match any of the neighbors' current traits. For the systems we have been studying ($N = 104$) with $F = 10$, the chances of such an event are less than one in 1040. Furthermore, for the noise levels used here and elsewhere [152, 158] to represent cultural drift, the model dynamics operate at a much faster time scale than do the perturbations (on average, all actors are activated ten times between each global perturbation), making the probability that such a sequence of perturbations could occur before homophily and influence dynamics would recover cultural consensus infinitesimally small. Thus, at least during time scales that are quite large as compared with the time scale of cultural convergence (approximately 103), multicultural states in co-evolutionary systems are robust against cultural drift.

4.3.5 Discussion on co-evolution dynamics in Axelrod's model

We have studied the Axelrod model with co-evolution of the interaction network and state dynamics of the agents. The interplay between structure and dynamics gives rise to two different transitions. First, a recombination transition at $q = q^*$ between a frozen and an active phase. The characteristic time to reach a stationary configuration shows a maximum at the transition point between these two phases. Second, an order-disorder transition associated with network fragmentation that appears at a critical value q_c where the component size distribution follows a power-law. Finite size scaling analysis suggests that in the large N limit this transition becomes continuous with q_c going to infinity. The fragmentation is shown to be a consequence of the competition between two coupled mechanisms, network formation and state formation. These mechanisms are governed by two internal time scales, τ_c and τ_d respectively, which are not controlled by external parameters, but they emerge from the dynamics. For $q < q_c$ the network components, that are formed first, control the formation of states. For $q > q_c$ the fast formation of domains shape the final structure of the network.

From the perspective of social sciences, this co-evolutionary model formalizes the idea that patterns of social interaction change with processes of social influence. The co-evolution of network structure and cultural traits reveals a complex relationship between heterogeneity and the emergence of diverse cultural groups, indicating different qualitatively distinct regions or phases. In phase I, a large component of the network remains connected and co-evolutionary dynamics lead to a dominant monocultural state in the presence of noise. In phase II,

cultural groups can form in the dynamic network, and these groups are stable even in the presence of continuous stochastic shocks. Consistent with the results of Popielarz and McPherson [172], in region II, the interaction of homophily and influence produces a niche structure whereby peripheral members are either absorbed into the core beliefs of the social group (by influence) or are forced out of the social group (by zero overlap). It is significant, however, that these social niches are not produced through competition or selection pressure but through the mechanisms of homophily and influence in a co-evolutionary process. Thus, even in the absence of selection pressures, a population can self-organize into stable social niches that define its diverse cultural possibilities. We also found that as heterogeneity increases, q approaches the threshold at which it enters phase III. These very high levels of heterogeneity are empirically unrealistic in most cases; however, they warn of a danger that comes with increasing options for social and cultural differentiation, particularly when the population is small or there is modest cultural complexity. Unlike cultural drift, which causes cultural groups to disappear through growing cultural consensus, a sudden flood of cultural options can also cause cultural groups to disappear; but instead of being due to too few options limiting diversity, it is due to excessive cultural options creating the emergence of highly idiosyncratic individuals who cannot form group identifications or long-term social ties.

Moreover, recent studies of the behavior of participants in online communities suggest that group formation processes and the emergence of friendship cliques in online environments may exhibit the same co-evolutionary dynamics as those found in our model. Backstrom et al. [179] found that interactions in the dynamic social networks of online communities produced distinct social groups with densely knit strong ties [109] within social clusters. These emergent groups serve both to reinforce the existence of social ties within clusters and to maintain group identity and shared practices. These findings are particularly salient to our results, because the Backstrom et al. [179] study is one of the few studies of social interaction in which the dynamics of adding and dropping ties has been closely observed in the formation of communities. Their results show not only that distinct cultural clusters emerge through endogenous interaction but also that these groups are highly stable. This trend in online populations suggests that even in the virtual world, network homophily governs the dynamics of cultural co-evolution. People have a preference for interacting with others who share similar traits and practices [169, 180], which naturally diversifies the population into emergent social clusters. Our results thus reveal an optimistic implication of these preliminary findings from online communities: Despite the growing technological trends toward increased connectivity and globalization, social diversity can be maintained even in highly connected environments. For thousands of years of human history, the emergence and maintenance of group

boundaries has sustained the diversity of cultural practices across different populations [181–183]. In modern online communities, similar patterns of diversification emerge, and for a similar reason: The homophily principle actively constrains the communities to which we belong and the people with whom we choose to interact, share ideas, and adopt our patterns of life [169, 172]. The results from our model show that through the dynamics of network co-evolution, these patterns of preferential interaction of like with like produce cultural pockets whose identity and ideas, though flexible, are nonetheless stable from dissolution into a homogeneous global culture. While trends toward globalization provide more means of contact between more people, these same venues for interaction also demonstrate the strong tendency of people to self-organize into culturally defined groups, which can ultimately help to preserve overall diversity.

Chapter 5

Coeovolutionary Threshold Dynamics

5.1 Introduction

The relation between a cause and its effect is usually abrupt in complex systems, in the sense that a small change in the neighborhood of a subsystem may (or not) trigger its reaction. This mechanism is at the heart of many models of self-organized criticality [184] where a cascade starts when the system has been frustrated beyond some threshold, e.g. the angle of a sand pile, but also in models for the diffusion of ideas in social networks [9, 19, 185] where the adoption of a new idea requires simultaneous exposure to multiple active acquaintances, and in integrate-and-fire neuron dynamics [186] where the voltage on a single neuron increases until a specified threshold is reached and it suddenly fires by emitting an action potential, thereby quickly returning to its reference. These types of model consist in cascading propagations on a fixed topology, i.e., a network of some sort, until a frozen configuration is reached, but they do not incorporate the feed-back existing between network topology and dynamics [16, 33, 62, 122, 128, 187–190], namely that the topology itself may reorganize when it is not compatible with the state of the nodes. This coevolution dynamics was discussed in the introduction of this thesis (Chapter 1) and may originate from homophily and social balance in social networks or synaptic plasticity in neuron dynamics.

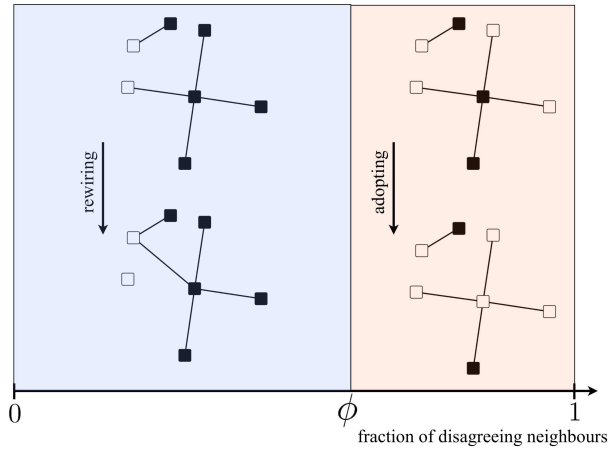

Figure 5.1: Update process of CTD for two different configurations of neighbors. When one out of four neighbors is in a different state, the central node breaks its links and creates a new link to a randomly chosen node. When three out of four neighbors are in a different state, the threshold ϕ is exceeded and the central node thus adopts the majority state.

In this chapter, we considered a model for coevolutionary threshold dynamics (CTD). Let us describe its ingredients in terms of diffusion of opinions in social networks [20, 191] while keeping in mind that the model is applicable to more general systems. The system is made of a social network of interaction, whose N nodes are endowed with a binary opinion s, + or −. The dynamics is driven by the threshold ϕ, such that $0 \leq \phi \leq 1$ and, in most cases of interest, $\phi > 1/2$. At each step, a randomly selected node i evaluates the opinion of its k_i neighbours. Let ϕ_i be the fraction of neighbours disagreeing with i. If $\phi_i \leq \phi$, node i breaks the links toward those disagreeing neighbours and rewires them to randomly selected nodes. If $\phi_i > \phi$, i adopts the state of the majority. In contrast with the model studied in Chapter 2, in this model the dynamic threshold is introduced as a dynamical rule for the evolution of the network, while in the case of the model for social learning the threshold is used as interaction rule for the consensus on a fixed network. By construction, the dynamics perdures until consensus, i.e., all agents having the same opinion, has been attainted in the whole system or in disconnected components. This absorbing state obviously depends on the threshold ϕ but also, as we will discuss below, on its initial condition.

A complete analysis of CTD requires extensive computer simulations, which is not the objective of our work. We will instead focus on a simplified version of the model that can be studied analytically and pinpoint the key mechanisms responsible for its behavior. In this simplified version, the network is directed and all the nodes have two incoming links, i.e. each is influenced by exactly two nodes, while their out-degree is initially Poisson distributed. Moreover, we will take $\phi = 1/2$, such that CTD now simplifies as follows. At each time step, a node i is selected at random. If i is surrounded by two nodes with different opinions, it switches its opinion, i.e., $s_i \to -s_i$. If the opinion of only one of its neighbors, say j is different, i cuts its link from j and reconnects to a randomly chosen node, i.e., its in-degree remains constant. It is interesting to stress that the choice $\phi = 1/2$ for a directed network with a constant in-degree of two corresponds to the unanimity rule [192] when no rewiring is implemented. This model is well-known to exhibit a non-trivial relation between initial and final densities of + nodes, denoted by $n_{+;0}$ and $n_{+;\infty}$ respectively. We will show that the addition of the rewiring mechanism leads to a transition from a connected phase with consensus where all the nodes asymptotically belong to the same cluster, to a fragmented phase where two disconnected clusters of different opinions survive. The critical parameter of this transition is shown to be the initial density $n_{+;0}$ of + nodes, i.e.,

$$\begin{aligned} n_{+;0} \langle n_c \ \ or \ \ n_{+;0} \rangle 1 - n_c \qquad & one \ \ single \ \ component, \\ n_c < n_{+;0} < 1 - n_c \quad & two \ \ disconnected \ \ components, \end{aligned} \tag{5.1}$$

where n_c is the critical density.

5.2 Fragmentation transition

In order to analyze the system dynamics, we follow the approach proposed in [192] and focus on the number $N_{s_0;s_1s_2}$ of configurations where a node in state s_0 receives its incoming links from a node in state s1 and another node in state s_2. Let us denote by $\{s_0; s_1s_2\}$ such a triplet of nodes. By construction, s_i may be +1 or 1 and $\sum_{s_0s_1s_2} N_{s_0;s_1s_2} = N$. Moreover, the order of the links is not important and therefore $N_{s_0;s_1s_2} = N_{s_0;s_2s_1}$. By neglecting higher order correlations than those included in $N_{s_0;s_1s_2}$, it is possible to derive the set of equations

$$
\begin{aligned}
N_{+;++}(t+1) &= N_{+;++} + \frac{1}{N}\left(N_{-;++} + n_+ N_{+;+-} + \pi_{-\to+} N_{+;+-} - 2\pi_{+\to-} N_{+;++}\right) \\
N_{+;--}(t+1) &= N_{+;--} + \frac{1}{N}(-N_{+;--} + \pi_{+\to-} N_{+;+-} - 2\pi_{-\to+} N_{+;--}) \\
N_{+;+-}(t+1) &= N_{+;+-} + \frac{1}{N}(-n_+ N_{+;+-} + 2\pi_{-\to+} N_{+;--} + 2\pi_{+\to-} N_{+;++} \\
&\quad -(\pi_{+\to-} + \pi_{-\to+}) N_{+;+-}) \\
N_{-;--}(t+1) &= N_{-;--} + \frac{1}{N}(N_{+;--} + n_- N_{-;+-} + \pi_{+\to-} N_{-;+-} - 2\pi_{-\to+} N_{-;--}) \\
N_{-;++}(t+1) &= N_{-;++} + \frac{1}{N}(-N_{-;++} + \pi_{-\to+} N_{-;+-} - 2\pi_{+\to-} N_{-;++}) \\
N_{-;+-}(t+1) &= N_{-;+-} + \frac{1}{N}(-n_- N_{-;+-} + 2\pi_{+\to-} N_{-;++} + 2\pi_{-\to+} N_{-;--} \\
&\quad -(\pi_{+\to-} + \pi_{-\to+}) N_{-;+-})
\end{aligned}
\tag{5.2}
$$

where n_+ and n are the density of + and − links respectively. $\pi_{+\to}(\pi_{\to_+})$ is the probability for a randomly selected +(−) node to switch its opinion to −(+). By construction, this quantity is the probability that a random +(−) node is connected to two −(+) nodes

$$
\begin{aligned}
\pi_{+\to-} &= \frac{N_{+;--}}{N_+}, \\
\pi_{-\to+} &= \frac{N_{-;++}}{N_-}
\end{aligned}
\tag{5.3}
$$

where $N_+ = \sum_{s_1,s_2} N_{+;s_1 s_2}$ and $N_- = N - N_+$ are the total number of + and − nodes respectively. Let us describe in detail the first equation for $N_{+;++}$, the other ones being obtained in a similar way. Its evolution is made of several contributions. The first term is the probability that a $\{-;++\}$ triplet is selected and transforms into $\{+;++\}$ by unanimity rule. The second term is the probability that a $\{+;+\}$ triplet is selected and the rewired link (originally from + to −) arrives on a + node (with probability n_+). The last two terms account for possible change of the state of one of the two neighbours in the triplet, as they may also switch their opinion because of a unanimity rule in another triplet, and are evaluated by using the aforementioned $\pi_{+\to-}$ and $\pi_{-\to+}$.

As discussed in [192], several initial conditions may in principle be chosen for the system of equations (5.2), each of them leading to its own trajectory in

the 6-dimensional dynamical space. Such initial conditions are subject to the normalization $\sum_{s_0,s_1,s_2} N_{s_0;s_1s_2} = N$, and to the conservation laws

$$T_+ = 2N_+, \quad T_- = 2N_- \tag{5.4}$$

where the quantities

$$\begin{aligned} T_+ &= 2N_{+;++} + 2N_{-;++} + N_{+;+-} + N_{-;+-} \\ T_- &= 2N_{+;--} + 2N_{-;--} + N_{+;+-} + N_{-;+-} \end{aligned} \tag{5.5}$$

are the total number of +(−) incoming neighbors in the triplets. Relations (4) simply mean that each node i that is a neighbor in a triplet $\left\{s_x; s_i s_y\right\}$ is also at the summit of another triplet $\left\{s_i; s_{x'} s_{y'}\right\}$ (as it also receives two incoming links by construction). In order to select one of the several configurations $N_{s_0;s_1s_2}$ that still satisfy the above constraints, we will further assume that the initial configuration is uncorrelated and therefore that each node has the same probability $n_{+;0}$ to be +. Among all the possible configurations for which $N_+ = Nn_{+;0}$, we therefore select the initial condition

$$\begin{aligned} N_{+;++} &= Nn_{+;0}^3 \\ N_{+;--} &= Nn_{+;0}(1-n_{+;0})^2 \\ N_{+;+-} &= 2Nn_{+;0}^2(1-n_{+;0}) \\ N_{-;--} &= N(1-n_{+;0})^3 \\ N_{-;++} &= N(1-n_{+;0})n_{+;0}^2 \\ N_{-;+-} &= 2N(1-n_{+;0})^2 n_{+;0} \end{aligned} \tag{5.6}$$

Before going further, it is instructive to look at the total number $N_+ = \sum_{s_1,s_2} N_{+;s_1s_2}$ of + nodes whose time evolution is obtained by summing over the first three equations of (5.2)

$$N_+(t+1) = N_+ + \frac{1}{N}(N_{-;++} - N_{+;--}) \tag{5.7}$$

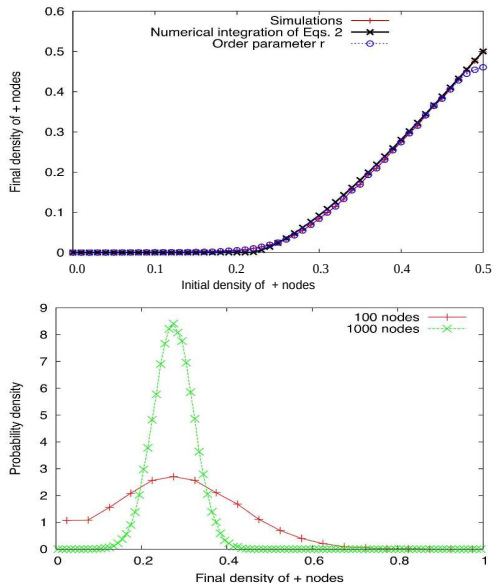

Figure 5.2: In the upper figure, we plot the relation (5.8) between the initial density and the final density of + nodes, evaluated by integrating the set of Eqs.(5.2) and by performing numerical simulations of a network made of 1000 nodes. We also plot the order parameter $r = \langle 1/2 - |1/2 - n_{+,\infty}| \rangle$ which confirms that the system actually breaks into disconnected components when $n_c < n_{+,0} < 1 - n_c$, i.e., we only plot (5.8) in the interval [0, 0.5] as the curves are symmetric around the point (0.5, 0.5). In the lower figure, we plot the probability density $\rho(n_{+;1})$ that the absorbing state has a density $n_{+;\infty}$ of + nodes for $N = 100$ and $N = 1000$ when $n_{+;0} = 0.4$.

This relation shows that $N_{-;++} = N_{+;--}$ at stationarity. A careful look at the second equation of (5.2) shows, however, that $N_{+;--}$ has to decay until it reaches zero. The third equation of (5.2) also shows that the only stationary solution of $N_{+;+-}$ is also zero when $N_{-;++} = N_{+;--} = 0$, thereby confirming that the dynamics asymptotically reaches a frozen configuration where consensus is reached among connected nodes. The dynamics is therefore driven by two types of triplets: the triplets $\{+;--\}$ and $\{-;++\}$ drive the system toward consensus, while the configurations $\{+;+-\}$ and $\{-;+-\}$ allow for a topological rearrangement of the network. This rearrangement implies that the only frozen states

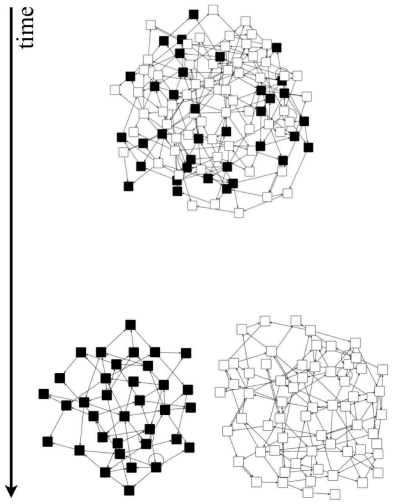

Figure 5.3: Visualisation of the initial and final states of one realization of the dynamics for a network made of $N = 100$ nodes. The initial density of + nodes $n_{+,0} = 0.4$. The asymptotic network is made of two clusters. The + cluster is now made of 35% of the nodes.

are those corresponding to consensus (in one or several clusters)* and drives the division of the system into disconnected clusters. The competition between these two types of mechanisms is crucial for the transition (5.1). One should also note that models for opinion dynamics are known to exhibit coexistence of different opinions when applied to a static underlying network with modular structure [194]. In the case of CTD, in contrast, it is the rewiring of the links that reorganizes the system into modules and thereby allows for coexistence. By integrating recursively the system of Eqs.(5.2) starting from the initial conditions (5.6), we obtain a non-trivial relation

$$n_{+,\infty}(n_{+,0}) \tag{5.8}$$

*This mechanism reminds of the social temperature defined in [193] where random rearrangements of the links drive the system toward consensus.

between the initial density and the final density of + nodes. This numerical integration confirms the above discussions, and clearly shows that a transition occurs at $n_c \approx 0.22$ (see Fig. 5.1). One should insist on the fact that this relation differs from the standard exit probability measured when the dynamics takes place on a static network [38, 195, 196]. In the latter models, $n_{+,\infty}(n_{+,0})$ would measure the probability to end in a + consensus (in the whole system) starting from some initial density of + nodes. Relation 5.8 is more reminiscent of the standard unanimity rule [193] without rewiring, where the system asymptotically reaches a frozen state different from consensus at each realization, and where $n_{+,\infty}$ is the average number of + nodes in this frozen state. Because of the rewiring process, however, a non-vanishing value of $n_{+,1}$ also implies that the system has split into two disconnected clusters and that a different consensus has been reached in each cluster.

We have verified the accuracy of our calculations by performing numerical simulations of the model (see Fig. 5.2). To do so, we have considered systems made of 1000 nodes and have averaged the asymptotic density of + nodes (evaluated when the dynamics is frozen) over 1000 realizations for each value of $n_{+,0}$. In order to check that the system actually breaks into two clusters when $n_c < n_{+,0} < 1 - n_c$ (see Fig. 5.3), we have also measured $r = \langle 1/2 - |1/2 - n_{+,\infty}| \rangle$. This order parameter would vanish if, for each realization, $n_{+,\infty}$ is either zero or one, while $r = \langle n_{+,\infty} \rangle$ if the system breaks into two clusters. The simulation results show an excellent agreement with the theoretical predictions and confirm the fragmentation of the network at the critical value n_c. Finally, we have also looked at the probability density $\rho(n_{+,\infty})$, i.e., $\int_0^1 \rho(x)dx = 1$, that the absorbing state is made of $n_{+,\infty}N$ nodes. This quantity is measured by performing 5×10^4 simulations starting from the same initial condition $n+;0 = 0.4$. The distribution is shown to be peaked around its average, in contrast with the two delta peaks at 0 and 1 that would be expected if full consensus had been the only absorbing state.

5.3 Conclusion and outlook

To conclude, we have focused on a model for coevolutionary threshold dynamics where the binary state of a node and its links coevolve. We have shown that the system may undergo fragmentation. Thus seen to be a general feature of coevolution network dynamics and we have also described this transition in section 4.3 for the Axelrod model. It has also been found in the voter model

[122], and also in the case of coupled maps with variable coupling strength [197]. In the case of CTD, the critical parameter is the initial condition, as a sufficient fraction of + nodes is necessary for such nodes to survive and to separate from the main cluster. In this chapter, we have focused on a simplified version of CTD where the underlying network is directed and regular, and where the in-degree has the smallest non-trivial value, i.e., two. Additional computer simulations are therefore required in order to explore the role of the threshold ϕ on the asymptotic state in more complex directed or undirected networks. Finally, let us point to an interesting generalization of CTD that would include two different threshold ϕ_r and ϕ_a for either rewiring links from disagreeing neighbours or adopting the state of the majority. Such a model would unify two seminal threshold models, namely the Granovetter model for the diffusion of cultural traits [9] and the Schelling model for social segregation [30, 198].

Chapter 6

Conclusions and summary

In this work, we have introduced and analyzed two important ingredients of the general problem of social consensus, including the specific cases of social learning, opinion formation and cultural globalization. These new ingredients are on the one hand, the competition between local and global interaction and on the other hand, the co-evolution dynamics. In this regard, we have explored different social models: threshold model of Granovetter [9] applied, in particular, to a situation of social learning, bounded confidence model of opinion formation introduce by Deffuant et al. [10] and the Axelrod's model for the dissemination of culture [11]. In summary, in Chapters 2, 3 and 4, we have studied the competition between local and global interactions, analyzing also the effect of the topology of the underlying network of interactions. The problem of co-evolution dynamics has been addressed in Chapters 4 (section 4.3) and 5.

General qualitative findings that can we identify in this work are the following: In systems with competition between local and global interactions, we have found that a strong interaction with a field can induce disorder in the system, while a weak interaction produces an alignment with the field, in contrast to the typical behavior observed in equilibrium systems. Our analysis shows that this behavior is generic independently of the local, global or external nature of the field. We have also found that systems interacting with an external field are able to order spontaneously in a state different to the one selected by the external field. This is possible when there are long range links in the network of interactions. For systems with co-evolutionary dynamics, we find a generic a fragmentation transition. We show that this fragmentation occurs when the time scales that govern the evolution of the interaction network and the evolution of the state of the nodes are of the same order.

In chapter 2, we have studied the problem of local versus global interactions in the context of social learning by mean-field analysis and numerical simulations. We have considered local interactions among the agents based on threshold dynamics [9]. These interactions compete with an external signal to be learnt by the agents. We show that depending on the intensity of the signal and the level of the threshold, complete social learning occurs (all nodes of the system adopt the same state of the signal) The system can reach three different stationary configurations: Two disordered phases, and one ordered phase in which the state of the nodes have the same state of the external signal. In the cases of the disordered phases, one phase corresponds to a disordered active phase, while the other one corresponds to a frozen disordered state. We have also analyzed the effect of the topology of the network of interactions, finding that local interactions are able to promote social learning.

Within the problem of global versus local interactions, we have studied in Chapters 3 and 4 (section 4.2.3) the competition between collective self-organization and external forcing in the Deffuant[10] and the Axelrod [11] models with an external field. We show that, for both models, the system displays three phases: two ordered phases, one equal to the state of the field and another different to the state imposed by the field, and one disordered phase. We show that the ordered phase in a state different from the one imposed by the external field is possible because of the long-range interactions that exist in fully connected, random and scale free networks. Our results challenge the expected effect of an external field: the field might break the symmetry in a given direction, but the system orders, breaking the symmetry in a different direction. There are two common ingredients in the two models in which we find this phenomenon: i)the agent-agent interaction rule is such that no interaction exists for some relative values characterizing the states of the agents in the system. ii)the presence of long-range links. Both features are typical of social systems: there is often some bound or restriction for the occurrence of interaction between agents, such as a similarity condition for the state variables, and also many real social networks posses long-range interactions.

In the context of Axlerod's model we have also considered in a regular $2d$ network interaction with global and local endogenous fields, besides the interaction with an external field. The fields represent different forms of mass media influences. We find two main effects that contradict intuition based on the effect of interacting fields in traditional equilibrium systems. First, we find that an interacting field might disorder the system: For parameter values for which the system orders due to the local interaction among the elements, there is a threshold value B_c of the probability of interaction with a field B. For $B > B_c$ the system becomes disordered. This happens because of the competition between a similarity rule

applied to the local interactions among elements, and applied to the interaction with the field. This leads to the formation of domains and to a disordered system. A second effect is that, for parameter values for which the dynamics based on the local interaction among the elements leads to a frozen disordered configuration, very weak interacting fields are able to order the system. However, increasing the strength of interaction with the field produces growing disorder in the system. The limit $B \to 0$ is discontinuous and the ordering effect for $B << 1$ occurs because the interaction with the field acts as a perturbation on the non stable disordered configurations with frozen dynamics appearing for $B = 0$. In this regard, the field behaves similarly to a random fluctuation acting on the system, which always induces order for small values of the noise rate [158].

Our results for Axelrod's model in a regular network are summarized in Fig. 6.1 which shows, for different values of B, the behavior of the order parameter S. In an effective way the nonequilibrium order-disorder transition is shifted to larger values of q when B is non-zero but very small. For larger values of B the transition shifts to smaller values of q and the system is always disordered in the limiting case $B \to 1$. This limiting behavior is useful to understand the differences with ordinary dynamics leading to thermal equilibrium in which a strong field would order the system. In our nonequilibrium case, the similarity rule of the dynamics excludes the interaction of the field with elements with zero overlap with the field. Since the local interaction among the elements is negligible in this limit, there is no mechanism left to change situations of zero overlap and the system remains disordered. We have calculated, for the three types of field considered, the corresponding boundary in the space of parameters (B, q) that separates the ordered phase from the disordered phase (see Fig. 4.11). In the case of a constant *external field*, the ordered state in this phase diagram always converges to the state prescribed by the constant field vector. The nonuniform *local field* has a greater ordering effect than the uniform (*global* and constant *external*) fields in the regime $q > q_c$ (see Figure 6.1). The range of values of B for which the system is ordered for $q < q_c$ is also larger for the nonuniform *local field*. In spite of the differences mentioned between uniform and nonuniform fields, it is remarkable that the collective behavior of the system displays analogous phenomenology for the three types of fields considered: external, endogenous global and local. At the local level, they act in the same manner, as a "fifth" effective neighbor whose specific source becomes irrelevant. In particular, both uniform fields, the *global* coupling and the *external field*, produce very similar behavior of the system.

In section 4.2.2 we have considered indirect mass media influence [129] in Axelrod's model. We implement a filtering process for the agent-field interaction. In the culturally homogeneous region, i.e., for $q < q_c$, the effect of this indirect influence is similar to that caused by direct influence of mass media. For small values

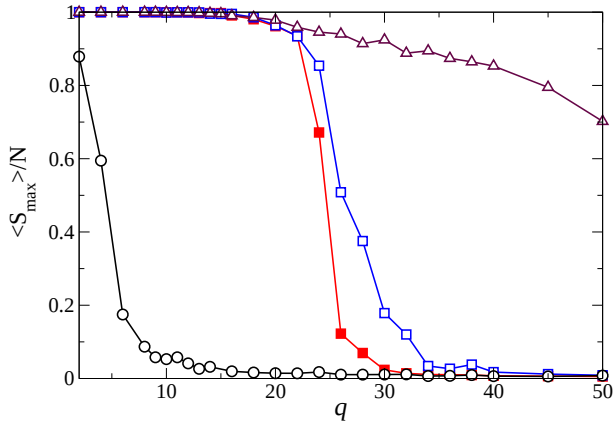

Figure 6.1: Influence of the interacting field on the nonequilibrium order-disorder transition as described by the order parameter S. Results are shown for $B = 0$ (solid squares), a *global* ($B = 10^{-5}$ (empty squares), $B = 0.3$ (circles)) and a *local* ($B = 10^{-5}$ (triangles)) *field*. Parameter value $F = 3$.

of the filtering probability R the system reaches a culturally homogeneous state. For values of R greater than a threshold value the system converges to a state of cultural diversity. Thus, both mechanisms of feedback information, either direct or indirect, promote multiculturality in a region of parameters where it would not be present in the absence of any feedback. In the region of parameters $q > q_c$ where multiculturality occurs for either $B = 0$ or $R = 0$, the filtering mechanism has, for values of the probability $R < 1$, a very weak effect in comparison to the one caused by a direct mass media influences: there is only a small decrease in the number of cultural groups formed.

Our results for direct and indirect mass media influences, substantiate previous findings by Shibanai et al.[129] showing that cultural diversity is favored by increasing the strength of the mass media influence. This effect occurs independently of the mechanisms of action of the mass media message. However, through an analysis of the full range of parameters measuring cultural diversity, we establish that the enhancement of cultural diversity produced by interaction with mass media only occurs for strong enough mass media messages. Strong media messages do not lead to cultural homogenization because agent-agent interaction becomes inefficient.

The interacting fields that we have considered can be interpreted as different kinds of mass media influences acting on a social system. Our results for Ax-

elrod model in a regular $2d$ network suggest that both, an externally controlled mass media or mass media that reflect the predominant cultural trends of the environment, have similar collective effects on a social system. We found the surprising result that, when the probability of interacting with the mass media is sufficiently large, mass media actually contribute to cultural diversity in a social system, independently of the nature of the media. Mass media is only efficient in producing cultural homogeneity in conditions of weak broadcast of a message, so that local interactions among individuals can be still effective in constructing some cultural overlap with the mass media message. These results identify the power of being subtle in mass media messages. In addition, local mass media appear to be more effective in promoting uniformity in comparison to global, uniform broadcasts, which identifies the importance of local media (feedback at regional levels) in the cultural globalization path.

In the last part of this thesis, we have analyzed in two different models, the problem of co-evolution dynamics. In Chapter 4 (Section 4.3) we have studied this problem in the context o the Axelrod's model, while in chapter 5 we have presented a threshold model for the co-evolution of the structure of the network and the state of its nodes. We have shown that both systems may undergo a fragmentation transition in spite of the different rules of local interaction and network evolution. Our results give a hint on the role of co-evolution dynamics in social group and community formation.

In the case of the Axelrod's model (Chapter 4) we show that the system displays two transitions, network recombination and fragmentation, governed by the time scale that emerges from the dynamics. The recombination formation separates a frozen configuration composed by disconnected network components whose nodes share the same state, from an active configuration with a fraction of links that are continuously being rewired. It is found that this fragmentation transition in the system is an anomalous order-disorder transition governed by crossover between the time scales that control the structure of the network and the state dynamics. Another interesting result that we have found in this system is that patterns of diversity are stable in presence of cultural drift (noise). In other words, we show that the system is robust in the presence of noise in contrast with the case of a fixed network, in which the system always reaches consensus.

From the point of view of Social Sciences, our co-evolution study of cultural differentiation introduces network homophily into the dynamics of cultural interaction. This co-evolutionary model formalizes the idea that networks of social interaction change with the processes of social influence. The co-evolution of network structure and cultural traits reveals a complex relationship between heterogeneity and the emergence of diverse cultural groups, indicating different qualitatively distinct regions of the parameter space. These qualitative results are

consistent with results of Popielarz and McPherson [199], in which the interaction of homophily and influence produces a niche structure whereby peripheral members are either absorbed into the core beliefs of the social group (by influence) or are forced out of the social group (by zero overlap). It is significant, however, that these social niches are not produced through competition or selection pressure but through the mechanisms of homophily and influence in a co-evolutionary process. Thus, even in the absence of selection pressures, a population can self-organize into stable social niches that define its diverse cultural possibilities.

In Chapter 5, we present a generic threshold model for the co-evolution of the structure of a network and the state of its nodes. In this model, we use a threshold dynamics for the evolution of the network. We have derived equations for the evolution of the system toward its absorbing state. We have shown that the system displays a transition from a connected phase to a fragmented phase as in the case of the Arelrod's model. This fragmetation transition depends on the initial configuration.

Chapter 7

List of publications

Publications related to this thesis:

- González-Avella J. C, Cosenza M. G,, Tucci K, "*Nonequilibrium transition induced by mass media in a model for social influence*", Physical Review E. **72**, 065102 (R)(1-4) (2005).

- González-Avella J. C, Eguíluz V. M, Cosenza M. G, Klemm K, Herrera J.L., San Miguel M, "*Local versus global interactions in nonequilibrium transitions: A model of social dynamics*", Physical Review E **73**, 046119 (1-7) (2006).

- González-Avella, J. C, Cosenza M.G, Klemm K, Eguíluz V. M, San Miguel M, "*Information Feedback and Mass Media Effects in Cultural Dynamics*", JOURNAL OF ARTIFICIAL SOCIETIES AND SOCIAL SIMULATION : http://jasss.soc.surrey.ac.uk/10/3/9.html 10, 1-17 (2007).

- Centola D, González-Avella J. C, Eguíluz V. M, San Miguel M, "*Homophily, Cultural Drift and the Co-Evolution of Cultural Group*", Journal of Conflict Resolution, **51**, 905-929 (2007).

- Vazquez F, González-Avella J. C, Eguíluz V. M, San Miguel M, "*Time scale competition leading to fragmentation and recombination transitions in the co-evolution of network and states.*", Physical Review E **76**, 046120 (1-5) (2007).

- González-Avella J. C, Cosenza M. G, Klemm K, Eguíluz V. M., San Miguel M, "*Information feedback and mass media effects in cultural dynamics*", In Proceedings of the 4th Conference of the European Social Simulation Association ESSA 2007, F. Amblard , IRIT Editions, 467-481 (2007).

- Vazquez F, González-Avella, J. C, Eguíluz V. M, San Miguel M, in "*Collective Phenomena in Complex Social Networks*", pp. 189-200 (Visarath; Longhini, Patrick; Palacios, Antonio, eds), Springer Verlag (2009).
- González-Avella J. C, Cosenza Mario G, Eguíluz V. M, San Miguel M, "*Spontaneous ordering against an external field in nonequilibrium systems*", New Journal of Physics, **12**, 013010 (2010).
- Lambiotte, R and González-Avella J. C, "*Coeovolutionary Threshold Dynamics*", pre print (2010) (version avialable at *arXiv:0906.3389*)
- González-Avella J. C, Eguíluz V. M, Marsili M. Vega-Redondo, F. and San Miguel, M "*Threshold learning dynamics in social networks*", pre print (2010)

Chapter 8

Appendix

In this Appendix we compare the two parameters, the average fraction of cultural domain g and the normalize average size of the largest domain S that we have used to characterize the ordering properties in Axelrod's model of cultural dynamics in Chapter 4. We will consider $2d$ lattice with an external field interaction.

Researchers in the Social Sciences have usually employed the number of cultural groups as a measure of multiculturality in a social system [11, 129, 150]. Following these studies, and in order to characterize the transition from the ordered (monocultural) state imposed by a field M to a disordered (multicultural) state when the intensity of the external field B is varied, we have considered in Sec. 4.2 the average fraction of cultural domains respect to the system size, g, as an order parameter. Figure (8.1) shows the parameter g as a function of q for different sizes of the system N and with a fixed intensity of the external field $B = 0.035$. A change of behavior from an ordered phase to a disordered one takes place at given transition value q_c that can be determined by a regression fitting [14] ($N = 40000$, it yields $q_c = 5$). The slope of the curve $g(q)$ changes at the value q_c. Figure (8.1)(b), in log-log scale, allows us to appreciate the effect of the system size on the transition value q_c in the presence of an external field. For the given values of N, the transition value q_c decreases as N increases. This points to the existence of finite size effects in the order-disorder transition as described by g. The behavior of the parameter g in the presence of an external field for very large values of the system size N has been recently investigated numerically in reference [200]. These authors show that, for square lattices of sizes $N > 500 \times 500$, the behavior of g in a system subject to an external field with intensity B can be

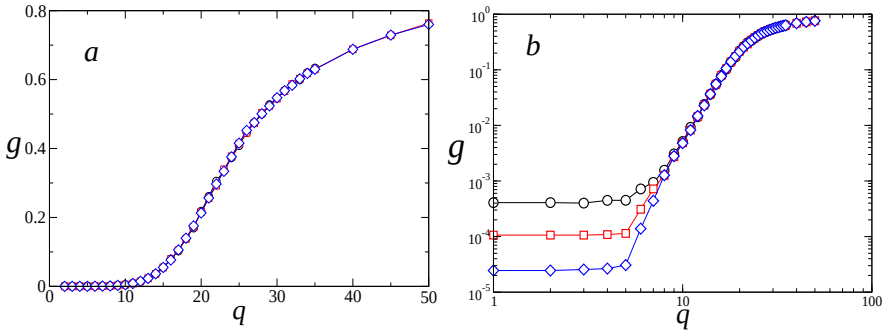

Figure 8.1: The average fraction of cultural domain g vs. q for $B = 0.035$, $F = 5$ and different system size in $2d$ lattice. $N = 2500$ (circles), $N = 10000$ (squares) and $N = 40000$ (diamonds). a: lineal scale, b: log-log scale.

fitted by the relation

$$g(B) = a(B) + \frac{b}{N} \tag{8.1}$$

where $a(B)$ is a function such that $a(B) \to 0$ as $B \to 0$. In the thermodynamical limit $N \to \infty$ with a finite value of B, the parameter g does not vanish [200]. As a consequence, no transition order-disorder can be observed in the limit $N \to \infty$ when the quantity g is used as an order parameter.

In the Physics community the tradition is to use S a order parameter. However, the order-disorder transition induced by an external field when its intensity is varied can also be characterized by the parameter S that measures the mean value of the relative size of the larger domain in the system. Figure (8.2)(a) shows S as a function of q for different system sizes N, and with a fixed intensity $B = 0.035$ of an external field. An order-disorder transition is observed at a critical value q_c, which becomes better defined as N increases.

The lower inset in Fig. (8.2)(a) plots the standard deviation σ of S showing an maximum at q_c characteristic of an order-disorder transition, occurs at the critical value $q_c = 21$. In addition, the upper inset in Fig. (8.2)(a) shows that the distribution of domain sizes $P(s)$ for the value $q_c = 21$ follows a power law $P(s) \sim S^{-\gamma}$ with $\gamma = 2.31 \pm 0.02$, a typical behavior at an order-disorder transition point. Figure (8.2)(b) shows the parameter S as a function of $q_c - q$ for different system sizes. The disordered phase here corresponds to values $q_c - q < 0$, while the ordered phase occurs for $q_c - q > 0$. The transition at $q_c - q = 0$ becomes better defined as N increases. The curve $S \sim (q_c - q)^{\alpha}$, with $\alpha \approx 0.45 \pm 0.02$ fits the behavior of S in the ordered phase for different system sizes. Thus,

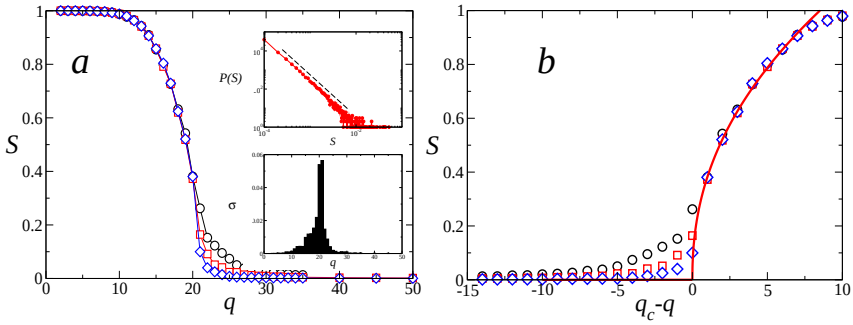

Figure 8.2: (a) S vs. q for different system sizes N, with fixed values $B = 0.035$, $F = 5$. Top inset: Size distributions of groups for $N = 2500$ at the transition point $q \approx 21$. The dashed line represents a power law with exponent -2.34 ± 0.02. Bottom inset: fluctuations are maximum at the critical point q_c. (b) S vs. $q_c - q$ for different system sizes, with fixed values $B = 0.035$, $F = 5$. The red line corresponds to the curve $S \sim (q_c - q)^{\alpha}$, with $\alpha \approx 0.45 \pm 0.02$. In both (a) and (b), sizes are $N = 2500$ (circles), $N = 10000$ (squares), and $N = 40000$ (diamonds).

the parameter S exhibits the expected properties of an order parameter that characterizes a phase transition.

The parameters g and S express different statistical order-disorder properties of the system. The critical value of q for the order-disorder transition in the presence of a field characterized through S does not coincide with that for this transition as described by g. The maximum fluctuation of this order parameter, the power law distribution of S and the scaling around to the critical point, together with mapping of percolation reported in Section 4.2.4 suggest that S is a order parameter in the usual sense, while g does not these properties.

List of Figures

References

[1] R. Badii and A. Politi, *Complexity*, Cambridge University Press, Cambridge, 1997.

[2] V. Mikhailov, *From swarms to Societies: Models of Complex behavior*, Springer, 2002.

[3] P. Ball, *Critical Mass: how one things leads to another*, Arrows Books, 2005.

[4] H. Meinhardt, *Models of Biological Pattern Formation*, Academic Press, New York, 1982.

[5] D. Lima, D. Battogtokh, A. S. Mikhailov, G. Dewel, and P. Borkmans *Europhys. Lett.* **42**, p. 631, 1998.

[6] K. Kaneko and I. Tsuda, *Complex systems: Chaos and Beyond*, Springer, 2000.

[7] S. Strogatz, *Sync: The Emerging Science of Spontaneous Order*, Hyperion Press, 2003.

[8] A. Pikovsky, M. Rosenblum, and J. Kurths, *Synchronization: A universal concept in nonlinear sciences*, Cambridge University Press, 2002.

[9] M. Granovetter *The American Journal of Sociology* **83**(6), pp. 1420–1443, 1978.

[10] G. Deffuant, D. Neau, F. Amblard, and G. Weisbuch *Advances in Complex Systems* **3**, p. 87, 2000.

[11] R. Axelrod *The Journal of Conflict Resolution* **41**(2), pp. 203–226, 1997.

[12] J. C. González-Avella, V. M. Eguíluz, M. G. Cosenza, K. Klemm, J. L. Herrera, and M. San Miguel *Physical Review E* **73**(4), p. 046119, 2006.

[13] J. C. González-Avella, M. G. Cosenza, V. M. Eguíluz, and M. San Miguel *New Journal of Physics* **12**, pp. 1–14, January 2010.

[14] J. C. González-Avella, M. Coenza, and K. Tucci *Physical Review E* **72**(065102(R)), 2005.

[15] J. C. González-Avella, M. G. Cosenza, K. Klemm, V. M. Eguíluz, and M. S. Miguel *Journal of Artificial Societies and Social Simulation* **10**, 2007.

[16] D. Centola, J. C. González-Avella, V. Eguíluz, and M. San Miguel *Journal of Conflict Resolution* **51**, p. 905, 2007.

[17] F. Vazquez, J. C. González-Avella, V. M. Eguíluz, and M. San Miguel *Physical Review E* **76**(046120), 2007.

[18] M. Marsili, F. Vega-Redondo, and F. Slanina *Proc. Natl. Acad. Sci. USA* **101**, pp. 1439–1442, 2004.

[19] D. Centola, V. Eguíluz, and M. Macy *Physica A* **374**, pp. 449–456, 2007.

[20] C. Castellano, S. Fortunato, and V. Loreto *Reviews of Modern Physics* **81**, p. 591, 2009.

[21] S. Boccaletti, V. Latora, Y. Moreno, M. Chavez, and D. Hwang *Physics Reports* **424**, pp. 175–308, February 2006.

[22] K. B. Chakrabarti, A. Chakraborti, and A. Chatterjee, *Econophysics and Sociophysics*, Wiley-VCH, Berlin, 2006.

[23] "Red temática española: Socioeconofisica." http://sites.google.com/site/socioeconofisica/.

[24] "International workshop on challenges and vissions in the social sciences." Eidgenössische Technische Hochschule (ETH), Zürich, Switzerland., 2008.

[25] "Complex systems society." http://cssociety.org/tiki-index.php.

[26] F. Schweitzer, G. Fagiolo, D. Sornette, F. Vega-Redondo, A. Vespignani, and D. R. White *Science* **325**, pp. 422–425, 2009.

[27] P. Umbanhowar, F. Melo, and H. Swinney *Nature* **382**, p. 793, 1996.

[28] W. Wang, I. Kiss, and J. Hudson *Physical Review Letters* **86**, p. 4954, 2001.

[29] A. Lin, A. Hegberg, A. Ardelea, M. Bertram, H. Swinney, and E. Meron *Physical Review E* **62**, p. 3790, 2000.

[30] T. C. Schelling, *Micromotives and Macrobehavior*, New York: Norton, 1978.

[31] D. Stauffer and S. Solomon *European Physical Journal B* **57**, pp. 473–479, June 2007.

[32] D. Stauffer, S. Moss de Oliveira, P. de Oliveira, and J. Sá Martin, *Biology, sociology, geology by computational physicsts*, Elsevier Amsterdam, Amsterdam, 2006.

[33] P. Holme and M. E. Newman *Physical Review E* **74**(056108), 2006.

[34] A. Lloyd and R. M. May *Science* **292**, pp. 1316–1317, 2001.

[35] W. Weidlich, *Sociodymanics: A systematic approach to mathematical modeling in social saciences*, Taylor & Francis, London, 2002.

[36] D. Stauffer *Computer in Science and Engineering* **5**, p. 71, 2003.

[37] M. Marsili, D. Challet, and Y.-C. Zhang, *Minority Games: Interacting Agents in Financial Markets*, Oxford University Press, Oxford, 2004.

[38] P. L. Krapivsky and S. Redner *Physical Review Letters* **90**, p. 238701, 2003.

[39] C. Tessone, R. Toral, P. Amengual, H. Wio, and M. San Miguel *European Physical Journal "B"* **39**, p. 535, 2004.

[40] S. Galam *Physical Review E* **71**, p. 046123, 2005.

[41] M. San Miguel, V. Eguíluz, R. Toral, and K. Klemm *Computer in Science and Engineering* **7**, pp. 67–73, 2005.

[42] A. Comte, *Course de Philosophie Positive, 6 tomos*, París, 1830-1842.

[43] P. L. Garrido, J. Marro, and M. A. Munoz, *Eight Granada Lectures on Modeling cooperative behavior in the Social Sciences; AIP Conference proceedings 779*, Melville, NY: AIP, 2005.

[44] R. Holley and T. Liggett *Annals of Probability* **3**, p. 643, 1975.

[45] R. J. Glauber *Journal of Mathematical Physics* **4**, pp. 294–307, Feb. 1963.

[46] K. S. Weron and J. Sznajd *International Journal of Modern Physics C* **11**(6), pp. 1157–1165, 2000.

[47] D. Centola and M. Macy *American Journal of Sociology* **113**, pp. 702–34, 2007.

[48] R. Hegselmann and U. Krause *Journal of Artificial Societies and Social Simulation* **5**(3), p. 2, 2002.

[49] L. Steels *Artificial Life* **2**, p. 319, 1995.

[50] X. Castelló, R. Toivonen, V. M. Eguíluz, L. Loureiro-Porto, J. Saramäki, K. Kaski, and M. San Miguel, *The evolution of language; Proceedings of the 7th International Conference (EVOLANG7)*, ch. Modelling language competition: bilingualism and complex social networks, pp. 59–66. World Scientific Publishing Co., 2008.

[51] X. Castelló, A. Baronchelli, and V. Loreto *European Physical Journal B* **71**, pp. 557–564, Oct 2009.

[52] S. Galam *The European Physical Journal B* **25**, p. 403, 2002.

[53] F. Vega-Redondo, *Economics and the Theory of Games*, Cambridge University Press, Cambridge, 2003.

[54] C. P. Roca, J. A. Cuesta, and A. Sánchez *Physical Review Letters* **97**, p. 158701, 2006.

[55] M. Zimmermann, V. Eguíluz, M. San Miguel, and A. Spadaro, *Cooperation in an Adaptive Network*, Application of Simulations to Social Sciences., Hermes Science Publications, 2000.

[56] R. Jiménez, H. Lugo, and M. San Miguel *The European Physical Journal B* **71**, pp. 273–280, 2009.

[57] D. Stauffer, X. Castelló, V. M. Eguíluz, and M. San Miguel *Physica A* **374**, pp. 835–842, 2007.

[58] X. Castelló, V. M. Eguíluz, and M. San Miguel *New Journal of Physics* **8**, pp. 308–322, 2006.

[59] F. Vazquez, X. Castelló, and M. San Miguel *Journal of Statistical Mechanics: Theory and Experiment* , p. P04007, 2010.

[60] X. Castelló, R. Toivonen, V. M. Eguíluz, J. Saramäki, K. Kaski, and M. San Miguel *Europhysics Letters* **79**, pp. 66006 (1–6), 2007.

[61] R. Toivonen, X. Castelló, V. M. Eguíluz, J. Saramäki, K. Kaski, and M. San Miguel *Physical Review E* **79**(016109), pp. 1–8, 2009.

[62] M. Zimmermann, V. Eguíluz, and M. San Miguel *Physical Review E* **69**, p. 065102(R), 2004.

[63] D. J. Watts and S. H. Strogatz *Nature* **393**, pp. 440–442, 1998.

[64] A. L. Barabasi, *Linked: The New Science of Networks.*, Perseus Publishing Co., 2002.

[65] M. E. J. Newman *SIAM Review* **45**, p. 167, 2003.

[66] V. M. Eguíluz, M. G. Zimmermann, C. J. Cela-Conde, and M. San Miguel *American Journal of Sociology* (110), pp. 977–1008, 2005.

[67] R. Albert and A. L. Barabasi *Reviews of Modern Physics* **74**, p. 47, 2002.

[68] C. Castellano, V. Loreto, A. Barrat, F. Cecconi, and D. Parisi *Phys. Rev. E* **71**, p. 066107, 2005.

[69] V. Sood and S. Redner *Physical Review Letters* **94**, p. 178701, 2005.

[70] K. Suchecki, V. M. Eguíluz, and M. San Miguel *Physical Review E* **72**, p. 036132, 2005.

[71] P. Flory *Journal of American Chemical Society* **63**, pp. 3083–3090, 1941.

[72] A. Rapoport *Bulletin of Mathematical Biophysics* **19**, pp. 257–277, 1957.

[73] P. Erdős and A. Rényi *Publ.Math. (Debrecen)* **6**, pp. 290–297, 1959.

[74] A.-L. Barabási and R. Albert *Science* **286**, p. 509, 1999.

[75] M. Girvan and M. E. Newman *Proc Natl Acad Sci U S A* **99**, pp. 7821–7826, June 2002.

[76] D. J. Watts, *Six Degrees: The Science of a Connected Age*, Norton, New York, 2003.

[77] M. Faloutsos, R. Pankaj, and K. C. Sevcik, "Multicasting in directed graphs," in *18th Biennial Symposium on Communications*, pp. 2–5, 1996.

[78] N. Schwartz, R. Cohen, D. Ben-Avraham, A. L. Barabási, and S. Havlin *Physical Review E* **66**(1), p. 015104, 2002.

[79] M. E. J. Newman *Phys. Rev. E* **64**, p. 016132, Jun 2001.

[80] M. A. Serrano, M. Boguña, and A. Vespignani *Proc. Natl. Acad. Sci. USA* **106**, p. 6483, 2009.

[81] P. Holland and S. Leinhardt *Comparative Group Studies* **2**, pp. 107–124, 1971.

[82] M. E. J. Newman and M. Girvan *Phys. Rev. E* **69**, p. 026113, Feb 2004.

[83] S. Wasserman and K. Faust, *Social Network Analysis: Methods and Applications*, Cambridge University Press, 1 ed., 11 1994.

[84] L. da F. Costa, F. A. Rodrigues, G. Travieso, and P. R. Villas Boas *Adv. Phys.* **56**(1), pp. 167–242, 2007.

[85] S. Milgram *Psychology Today* **1**, p. 60, 1967.

[86] D. J. Watts, *Small-worlds: The Dynamics of Networks between Order and Randomness*, Princeton University Press, Princeton, NJ (USA), 1999.

[87] M. E. J. Newman and D. J. Watts *Physics Letters A* **263**(4-6), pp. 341–346, 1999.

[88] R. Monasson *European Physical Journal B* **12**(555), 1999.

[89] A.-L. Barabási, R. Albert, and J. H. *Physica A* **272**, p. 173, 1999.

[90] S. N. Dorogovtsev, J. F. F. Mendes, and A. N. Samukhin *Phys. Rev. Lett.* **85**, pp. 4633–4636, Nov 2000.

[91] P. L. Krapivsky, S. Redner, and F. Leyvraz *Phys. Rev. Lett.* **85**, pp. 4629–4632, Nov 2000.

[92] S. P. Borgatti, A. Mehra, D. J. Brass, and G. Labianca *Science* **323**, pp. 892–895, February 2009.

[93] J. L. Moreno, *Who shall survive?*, Mental Disease Publishing Company, Washington DC, 1934.

[94] A. Davis, B. B. Gardner, and M. Gardner, *Depp South*, University of Chicago Press, Chicago, 1941.

[95] F. J. Roethlisberger and W. J. Dickson, *Management and the Worker*, Harvard University Press, Cambridge, M.A., 1939.

[96] T. J. Fararo and M. H. Sunshine, *A Study of a Biased Friendship Net*, Syracuse Univ. Press: Syracuse, NY, 1964.

[97] A. Rapoport and W. J. Horvath *Behavioral Science* **6**, pp. 279–291, 1964.

[98] J. Galaskiewicz, *Social Organization of an Urban Grants Economy*, Academic Press, New York, 1985.

[99] J. Galaskiewicz and P. V. Marsden *Social Science Research* **7**, pp. 89–107, 1978.

[100] P. Mariolis *Social Science Quarterly* **56**, pp. 425–439, 1975.

[101] P. S. Bearman, J. Moody, and K. Stovel, *Chains of affection: The structure of adolescent romantic and sexual networks.*, Preprint, Department of Sociology., Columbia University.

[102] J. H. Jones and M. S. Handcock *Proc. R. Soc. Lond. B* **270**, pp. 1123–1128, 2003.

[103] F. Liljeros, C. R. Edling, L. A. N. Amaral, H. E. Stanley, and Y. Aaberg *Nature* **411**(6840), pp. 907–908, 2001.

[104] J. Travers and S. Milgram *Sociometry* **32**, p. 425, 1969.

[105] J. Guare, *Six Degrees of Separetion: A play*, Vintage, New York, 1990.

[106] E. Garfield *Current Contents* **43**, pp. 5–10, 1979.

[107] S. H. Strogatz *Nature* **410**, pp. 268–276, 2001.

[108] J. P. Onnela, J. Saramaki, J. Hyvonen, G. Szabo, D. Lazer, K. Kaski, J. Kertesz, and A. L. Barabasi *PNAS* **104**, pp. 7332–7336, 2007.

[109] M. S. Granovetter *The American Journal of Sociology* **78**(6), pp. 1360–1380, 1973.

[110] J. Leskovec and E. Horvitz, "Planetary-scale views on a large instant-messaging network," in *WWW '08: Proceeding of the 17th international conference on World Wide Web*, pp. 915–924, ACM, (New York, NY, USA), 2008.

[111] M. E. J. Newman *PNAS* **98**(2), pp. 404–409, 2001.

[112] M. E. J. Newman *Phys. Rev. E* **74**, p. 036104, 2006.

[113] A. M. Turing *Philos. Trans. R. Soc. London B* **237**, p. 37, 1952.

[114] G. Veser, F. Mertens, A. S. Mikhailov, and R. Imbihl *Physical Review Letters* **71**(935), 1993.

[115] H. Nishimori and N. Ouchi *Physical Review Letters* **71**(197), 1993.

[116] I. Kiss, Y. Zhai, and J. Hudson *Physical Review Letters* **88**(238301), 2002.

[117] M. G. Cosenza, M. Pineda, and A. Parravano *Physical Review E* **67**(066217), 2003.

[118] M. Pineda and M. G. Cosenza *Physical Review E* **67**(057201), 2005.

[119] O. Alvarez-Llamoza and M. G. Cosenza *Physical Review E* **78**, p. 046216, 2008.

[120] R. Montagne, E. Hernández-García, and M. San Miguel *Physica D* **96**(46), 1996.

[121] G. Ehrhardt, M. Marsili, and F. Vega-Redondo *Int. J. Game Theory* **34**(383), 2006.

[122] F. Vazquez, V. M. Eguiluz, and M. S. Miguel *Phys. Rev. Lett.* **100**(108702), 2008.

[123] S. Gil and D. H. Zanette *Physica D* **224**(156), 2006.

[124] T. Gross and B. Blasius *J. R. Soc. Interface* **5**(20), pp. 259–271, 2008.

[125] M. Zimmermann, V. M. Eguíluz, and M. San Miguel, *Cooperation, adaptation and the emergence of leadership*. Proc. of Workshop on Economics with Heterogeneous Interacting Agents Springer Verlag, 2001.

[126] J. Poncela, J. Gómez-Gardeñes, L. M. Floría, A. Sánchez, and Y. Moreno *PLoS ONE* **3**(6), 2008.

[127] J. Poncela, J. Gómez-Gardeñes, L. M. Floría, Y. Moreno, and A. Sánchez *Europhys. Lett.* **88**, 2009.

[128] G. Ehrhardt, M. Marsili, and F. Vega-Redondo *Physical Review E* **74**(036106), 2006.

[129] Y. Shibanai, S. Yasuno, and I. Ishiguro *Journal Conflict of Resolution* **45**(80), 2001.

[130] K. Mazzitello, J. Candia, and V. Dosseti *Int. Journal of Modern Physics C* **18**(1475), 2007.

[131] J. Candia and K. Mazzitello *J. Stat.Mech.* (PO7007), 2008.

[132] V. Bala and S. Goyal *Review of Economic Studies* **65**, pp. 595–621, 1998.

[133] D. Fundenberg and D. K. Levine, *The theory of learning in games*, Cambridge MIT Press, 1998.

[134] B. Golub and M. Jackson *American Economic Journal: Microecnomics* **2**, pp. 112–149, 2009.

[135] F. Schweitzer and J. Holyst *Eur. Phys. J. B* **15**(4), pp. 723–732, 2000.

[136] D. Stauffer *Advances in Complex Systems* **5**(1), pp. 97–100, 2002.

[137] D. Stauffer *Int. Journal of Modern Physics C* **13**(3), pp. 315–317, 2002.

[138] E. Ben-Naim, P. L. Krapivsky, and S. Redner *Physica D* **183**, pp. 190–204, May 2003.

[139] J. Lorenz *Int. Journal of Modern Physics C* **18**(12), pp. 1819–1838, 2007.

[140] G. Weisbuch, G. Deffuant, F. Amblard, and N. J.P. *Complexity* **7**, pp. 55–63, March 2002.

[141] D. Neau, "Revisions des croyances dans un systeme d'agents en interaction," tech. rep., 2000.

[142] T. Carletti, D. Fanelli, S. Grolli, and A. Guarino *Europhys. Lett.* **74**, pp. 222–228, April 2006.

[143] J. Lorenz, *Modeling, analysis and simulation of continous opinion dynamics.* PhD thesis, 2007.

[144] G. Weisbuch *Eur. Phys. J. B* **38**, pp. 339–343, May 2004.

[145] M. Pineda, R. Toral, and E. Hernández-García *Journal of Statistical Mechanics: Theory and Experiment* **2009**(08), p. P08001, 2009.

[146] S. Fortunato *International Journal of Modern Physics C* **15**(9), pp. 1301–1307, 2004.

[147] J. Lorenz and D. Urbig *Advances in Complex Systems* **10**(2), pp. 251–269, 2004.

[148] D. Stauffer and H. Meyer-Ortmanns *Int. Journal of Modern Physics C* **15**(2), pp. 241–246, 2004.

[149] G. Deffuant, F. Amblard, G. Weisbuch, and T. Faure *Journal of Artificial Societies and Social Simulation* **5**(4), p. 1, 2002.

[150] R. Axelrod, *The Complexity of Cooperation*, Princeton University Press, 1997.

[151] C. Castellano, M. Marsili, and A. Vespignani *Phys. Rev. Lett.* **85**, pp. 3536–3539, Oct 2000.

[152] K. Klemm, V. M. Eguí luz, R. Toral, and M. San Miguel *Journal of Economic Dynamics and Control* **29**(1-2), p. 321, 2005.

[153] K. Klemm, V. M. Eguíluz, R. Toral, and M. San Miguel *Physica A* **327**(1), 2003.

[154] J. C. González-Avella, "Axelrod's model for dissemination of cutural." From IFISC website: http://ifisc.uib.es/research/APPLET_Axelrod/Culture.html, 2007.

[155] F. Vazquez and S. Redner *Europhysics Letters* **78**, p. 18002, 2007.

[156] K. Klemm, V. M. Eguíluz, R. Toral, and M. San Miguel *Phys. Rev. E* **67**, p. 026120, Feb 2003.

[157] J. C. González-Avella, M. G. Cosenza, K. Klemm, V. M. Eguíluz, and M. San Miguel *Journal of Artificial Societies and Social Simulation* **10**(3), p. 9, 2007.

[158] K. Klemm, V. Eguíluz, R. Toral, and M. San Miguel *Physical Review E* **67**((R)), p. 045101, 2003.

[159] A. Flache and M. Macy *http://arxiv.org/abs/physics/0604201* , 2006.

[160] M. Macy, J. Kitts, A. Flache, and S. Bernard *National Academies Press* , pp. 162–173, 2003.

[161] Leydesdorf *Journal of Artificial Societies and Social Simulation* **4**(3), 2001.

[162] R. Bhavnani *Journal of Artificial Societies and Social Simulation* **6**(4), 2003.

[163] C. Garcia-Lázaro, L. Lafuerza, L. Floría, and Y. Moreno *Physical Review E* **80**(046123), 2009.

[164] D. Stauffer *Phys. Rep.* , 1979.

[165] D. Stauffer and A. Aharony, *Introduction to Percolation Theory*, London, taylor and francis ed., 1992.

[166] C. Moore and M. E. Newman *Physical Review Letters* **85**(5468), 2000.

[167] S. N. Dorogovtsev, A. V. Goltsev, and J. F. F. Mendes *Reviews of Modern Physics* **80**(4), p. 1275, 2008.

[168] J. M. McPherson, P. A. Popielarz, and S. Drobnic *American Sociological Review* **57**(2), pp. 153–170, 1992.

[169] M. McPherson, L. Smith-Lovin, and J. M. Cook *Annual Review of Sociology* **27**(1), pp. 415–444, 2001.

[170] J. Cohen *Sociology of Education* **50**, 1997.

[171] L. Verbrugge *Social Forces* **62**, pp. 78–83, 1997.

[172] P. Propielarz and J. M. McPherson *American Journal of Sociology* **101**, pp. 698–720, 1995.

[173] D. Heckathorn *American Journal of Sociology Review* **61**, 1996.

[174] K. A. Weeden and D. Grusky *American Journal of Sociology* **111**, pp. 141–212, 2005.

[175] B. Latané, *Pressure to uniformity and the evolution of culture norms*, American Psychological Association, Washington, D.C., 2000.

[176] P. Bourdieu, *Distinction*, Harvard University Press, Cambridge, M.A.

[177] E. Durkheim, *Suicide*, Reprint: Free Press, 1997, New York, 1897.

[178] P. Blau and J. Schwartz *Academic Press* , 1984.

[179] L. Backstrom, D. Huttenlocher, X. Lan, and J. Kleinberg, "Group formation in large social networks: Membership, growth, and evolution," ACM Press, (New York), 2006.

[180] G. C. Homans, *Sentiments and activities*, Free Press, New York, 1962.

[181] F. Barth, *Ethnic and groups boundaries*, Reprint: Long Grove, IL, Waveland, 1998.

[182] E. Durkheim, *The elemntary forms of religious life*, Reprint: Oxford University Press, 2001, New York, 1912.

[183] R. Boyd and P. Richerson, *The origin and evolution of cultures*, Oxford University Press, New York, 2005.

[184] H. J. Jensen, *Self-Organized Criticality*, Cambridge University Press, Cambridge, England, 1998.

[185] D. J. Watts *Proc. Natl. Acad. of Sci. USA* **99**(5766), 2002.

[186] A. Holden, *Models of the stochastic activity of neurons*, Springer-Verlag, Berlin, Germany, 1974.

[187] S. Gil and D. H. Zanette *Physics Letters A* **356**(89), 2006.

[188] D. Garlaschelli, A. Capocci, and G. Caldarelli *Nature Physics* **3**, pp. 813–817, 2007.

[189] C. Nardini, B. Kozma, and A. Barrat *Physical Review Letters* **100**(158701), 2008.

[190] I. Benczik, NewAuthor1, B. Schmittmann, and R. K. P. Zia *Europhysics Letters* **82**(48006), 2008.

[191] S. Galam *Journal of Mathematical Physics* **30**, pp. 426–434, 1986.

[192] R. Lambiotte, S. Thurner, and R. Hanel *Physical Review E* **76**(046101), 2007.

[193] P. Klimek, R. Lambiotte, and S. Thurner *Europhys. Lett.* **82**(28008), 2008.

[194] R. Lambiotte, M. Ausloos, and J. Holyst *Physical Review E* **75**, p. 030101, 2007.

[195] M. Mobilia and S. Redner *Physical Review E* **68**(046106), 2003.

[196] R. Lambiotte and S. Redner *Europhys. Lett.* **82**(18007), 2008.

[197] J. Ito and K. Kaneko *Physical Review E* **67**(046226), 2003.

[198] T. C. Schelling *J. of Math. Soc.* **1**, pp. 143–186, 1971.

[199] P. A. Popielarz and J. M. McPherson *American Journal of Sociology* **101**, pp. 698–720, 1995.

[200] L. R. Peres and J. F. Fontanari *Journal of Physics A: Mathematical and General* **43**(055003), pp. 1–8, 2009.